

ปฏิกิริยาकार์บอนไดออกไซด์เมเทนเนสบนตัวเร่งปฏิกิริยาฐานนิกเกิลสปีเนล



นางสาวชญญา ธรรมมา

บทคัดย่อและแฟ้มข้อมูลฉบับเต็มของวิทยานิพนธ์ตั้งแต่ปีการศึกษา 2554 ที่ให้บริการในคลังปัญญาจุฬาฯ (CUIR)
เป็นแฟ้มข้อมูลของนิสิตเจ้าของวิทยานิพนธ์ ที่ส่งผ่านทางบัณฑิตวิทยาลัย

The abstract and full text of theses from the academic year 2011 in Chulalongkorn University Intellectual Repository (CUIR)
are the thesis authors' files submitted through the University Graduate School.

วิทยานิพนธ์นี้เป็นส่วนหนึ่งของการศึกษาตามหลักสูตรปริญญาวิศวกรรมศาสตรมหาบัณฑิต

สาขาวิชาวิศวกรรมเคมี ภาควิชาวิศวกรรมเคมี

คณะวิศวกรรมศาสตร์ จุฬาลงกรณ์มหาวิทยาลัย

ปีการศึกษา 2560

ลิขสิทธิ์ของจุฬาลงกรณ์มหาวิทยาลัย

CO₂ methanation over NiAl₂O₄ spinel - based catalysts



A Thesis Submitted in Partial Fulfillment of the Requirements
for the Degree of Master of Engineering Program in Chemical Engineering

Department of Chemical Engineering

Faculty of Engineering

Chulalongkorn University

Academic Year 2017

Copyright of Chulalongkorn University

Thesis Title CO₂ methanation over NiAl₂O₄ spinel - based catalysts
By Miss Chanya Thamma
Field of Study Chemical Engineering
Thesis Advisor Professor Joongjai Panpranot, Ph.D.

Accepted by the Faculty of Engineering, Chulalongkorn University in Partial Fulfillment of the Requirements for the Master's Degree

.....Dean of the Faculty of Engineering
(Associate Professor Supot Teachavorasinskun, D.Eng.)

THESIS COMMITTEE

.....Chairman
(Professor Bunjerd Jongsomjit, Ph.D.)

.....Thesis Advisor
(Professor Joongjai Panpranot, Ph.D.)

.....Examiner
(Associate Professor Anongnat Somwangthanaroj, Ph.D.)

.....External Examiner
(Assistant Professor Okorn Mekasuwandumrong, D.Eng.)

ชัญญา ธรรมมา : ปฏิริยาकार์บอนไดออกไซด์เมเทนเนชันบนตัวเร่งปฏิริยาฐานนิกเกิลสปีเนล (CO₂ methanation over NiAl₂O₄ spinel - based catalysts) อ.ที่ปริกาษาวิทธานิพนธ์หลัก: ศ. ดร. จุงใจ ปั้นประณต, 101 หน้า.

ในงานวิจัยนี้ศึกษาการเตรียมตัวเร่งปฏิริยาฐานนิกเกิลออกไซด์/นิกเกิลสปีเนล ที่มีอัตราส่วนโมล Ni/Al = 1/2 ด้วยวิธีตกตะกอนร่วม ที่อุณหภูมิการตกตะกอน 30 และ 80 องศาเซลเซียส และอุณหภูมิการเผา 500, 700, 900 และ 1200 องศาเซลเซียส วิเคราะห์คุณลักษณะของตัวเร่งปฏิริยาด้วยเทคนิค เช่น การดูดซับด้วยแก๊สไนโตรเจน การเลี้ยวเบนของรังสีเอ็กซ์ การรีดักชันแบบโปรแกรมอุณหภูมิด้วยไฮโดรเจน กล้องจุลทรรศน์อิเล็กตรอนแบบส่องกราด พบว่าตัวเร่งปฏิริยานิกเกิลออกไซด์บนตัวรองรับนิกเกิลสปีเนลที่เตรียมด้วยอุณหภูมิตกตะกอน และเผา ที่อุณหภูมิ 80 และ 900 องศาเซลเซียส ตามลำดับ แสดงประสิทธิภาพที่ดีที่สุด ในการทดสอบในปฏิริยาเมเทนเนชันที่อุณหภูมิ 350 องศาเซลเซียส เป็นเวลา 3 ชั่วโมง โดยให้ค่าการเปลี่ยนของคาร์บอนไดออกไซด์เป็นมีเทน 92 เปอร์เซ็นต์ โดยปราศจากการเกิดคาร์บอนมอนอกไซด์ ปริมาณสัดส่วนที่เหมาะสมของนิกเกิลออกไซด์และนิกเกิลอะลูมิเนท ที่ 24.7 และ 75.3 เปอร์เซ็นต์โดยน้ำหนัก ส่งผลต่อการลดการรวมตัวกันของโลหะกัมมันต์ เพิ่มความเสถียรของตัวเร่งปฏิริยา อีกทั้งยังส่งผลให้อุณหภูมิในการรีดิวซ์ของนิกเกิลออกไซด์ลดลง นอกจากนี้การเผาตัวเร่งปฏิริยาที่อุณหภูมิสูง ส่งผลให้ปริมาตรรูพรุนใหญ่ขึ้น ซึ่งช่วยให้แก๊สตั้งต้นเข้าถึงตำแหน่งกัมมันต์ได้ดีในระหว่างการทำปฏิริยา เมื่อเปรียบเทียบกับตัวเร่งปฏิริยาที่ไม่ได้เติมโลหะมีค่าพบว่า ตัวเร่งปฏิริยาที่สนับสนุนด้วยรูเทเนียมบนตัวเร่งปฏิริยานิกเกิลออกไซด์บนตัวรองรับนิกเกิลอะลูมิเนท แสดงประสิทธิภาพที่สูงกว่าตัวเร่งปฏิริยาที่ไม่สนับสนุนด้วยโลหะมีค่า ในการทดสอบในปฏิริยาเมเทนเนชัน ที่อุณหภูมิต่ำ ประมาณ 250-300 องศาเซลเซียส โดยปราศจากการเกิดคาร์บอนมอนอกไซด์ ซึ่งผลจากการเติมรูเทเนียม ทำให้ผลึกของโลหะนิกเกิลมีขนาดลดลง การกระจายตัวบนตัวรองรับดีขึ้น และช่วยเพิ่มความสามารถในการรีดิวซ์ ซึ่งเป็นผลดีต่อความว่องไวของตัวเร่งปฏิริยา

ภาควิชา วิศวกรรมเคมี

ลายมือชื่อนิสิต

สาขาวิชา วิศวกรรมเคมี

ลายมือชื่อ อ.ที่ปริกาษาหลัก

ปีการศึกษา 2560

5970141521 : MAJOR CHEMICAL ENGINEERING

KEYWORDS: CO₂ METHANATION , NiO/NiAl₂O₄ , CO-PRECIPIATION

CHANYA THAMMA: CO₂ methanation over NiAl₂O₄ spinel - based catalysts.

ADVISOR: PROF. JOONGJAI PANPRANOT, Ph.D., 101 pp.

In the present work, a series of NiO/NiAl₂O₄ catalysts were prepared by co-precipitation method with molar ratio of Ni/Al equal 1/2 at different precipitation temperatures (30 and 80°C) and calcination temperatures (500, 700, 900, and 1200°C). The catalyst properties were characterized by using N₂ physisorption, X-ray diffraction, H₂ – TPR, SEM, and TEM. The NiO/NiAl₂O₄ precipitated at 80°C and calcined at 900°C showed the best activity in CO₂ methanation at 350°C with conversion 92% and 100% methane selectivity without CO formation. The optimal of NiO and NiAl₂O₄ composition at 24.7% and 75.3%wt could provide a stabilizing effect preventing the metal aggregation and to lowering the reduction temperature of NiO. Moreover, the higher calcination temperature led to larger total pore volume was good to provide sufficient exposed metallic active sites for gas reactants. Compared the unpromoted catalyst, the Ru promoted NiO/NiAl₈₀ – 900 catalyst exhibited higher activity at low temperature (250-300°C) without CO formation due to the decrease of crystallite size of Ni metal resulting in high dispersion and enhanced reducibility of catalyst, which had a positive effect for catalytic activity.

CHULALONGKORN UNIVERSITY

Department: Chemical Engineering Student's Signature

Field of Study: Chemical Engineering Advisor's Signature

Academic Year: 2017

ACKNOWLEDGEMENTS

I would like to acknowledge to my thesis advisor, Prof. Dr. Joongjai Panpranot for the best counsel and research fund supported. I am very impressed appreciation for everything that I received from her and this thesis would not have been complete without her supported to me.

In addition, we would like to thank Prof. Dr. Bunjerd Jongsomjit, as chairman, Assoc. Prof. Dr. Anongnat Somwangthanaroj and Asst. Prof. Dr. Okorn Mekasuwandamrong as a member of thesis committee for our dissertation and special thanks our center of excellence on catalysis and catalytic reaction engineering research group, Chemical Engineering, Faculty of engineering Chulalongkorn University for supporting laboratory and equipment that be necessary for my project.

Finally, I most gratefully acknowledge my parents and my friends for their helping, supporting and encouraging during the period of this research.

CONTENTS

	Page
THAI ABSTRACT	iv
ENGLISH ABSTRACT	v
ACKNOWLEDGEMENTS	vi
CONTENTS	vii
LIST OF TABLES	1
LIST OF FIGURES	3
CHAPTER I.....	6
INTRODUCTION.....	6
1.1 Motivation.....	6
1.2 Objective of research	8
1.3 Scope of research	8
1.4 Contribution of Research.....	9
CHAPTER II.....	10
THEORY AND LITERATURE REVIEW	10
2.1 The CO ₂ methanation reaction mechanism	10
2.2 Characterisation of methanation catalysts	14
2.3 The Ni based catalysts	16
2.3.1 The effect of Ni loading.....	17
2.3.2 The effect of supported catalysts	23
2.3.3. The effect of promoters on Ni based catalysts.....	28
2.3.3.1 Ruthenium (Ru), Rhodium (Rh), Palladium (Pd), Platinum (Pt).....	29
2.3.3.2 Other metal promoter.....	34

	Page
2.4 The NiAl ₂ O ₄ spinel catalyst on steam reforming reaction	37
CHAPTER III	39
MATERIALS AND METHODOLOGY	39
Part I: Catalysts preparation.....	39
3.1 Materials.....	39
3.2 Catalysts preparation by co-precipitation method.....	40
3.2.1 NiAl ₂ O ₄ spinel catalysts preparation	40
3.2.2 Ni/Al ₂ O ₃ catalyst preparation	40
3.2.3 Promoted catalysts preparation	41
Part II: Catalysts characterization.....	41
3.3 Catalysts characterization.....	41
3.3.1 N ₂ physisorption (BET)	41
3.3.2 X-ray diffraction (XRD).....	41
3.3.3 Temperature program reduction (TPR)	41
3.3.4 Scanning Electron Microscopy (SEM)	42
3.3.5 Transmission Electron Microscopy (TEM).....	42
Part III: Catalytic activity.....	42
3.4 Catalytic activity	42
3.4.1 Materials	42
3.4.2 Apparatus	42
CHAPTER IV	44
RESEARCH METHODOLOGY AND RESEARCH PLAN	44
4.1 Research methodology.....	44

	Page
4.1.1 The effect of preparation and calcination temperatures of NiO/NiAl ₂ O ₄ spinel catalyst during CO ₂ methanation reaction.....	44
4.1.1.1 The effect of spinel phase formation compared Ni support on commercial Al ₂ O ₃	45
4.1.2 The effect of noble metal loading support on NiO/NiAl ₂ O ₄ spinel catalyst during CO ₂	46
4.1.2.1 The effect of reaction temperature over Ru-NiO/NiAl ₂ O ₄ catalyst during CO ₂ methanation.....	47
CHAPTER V	48
RESULTS AND DISCUSSION	48
Part I: The effect of preparation and calcination temperatures of NiO/NiAl ₂ O ₄ spinel catalysts during CO ₂ methanation reaction.....	48
5.1 Characterization of NiO/NiAl ₂ O ₄ spinel catalysts.....	48
5.1.1 N ₂ - physisorption (BET)	48
5.1.2 X-ray diffraction (XRD).....	51
5.1.3 Temperature programmed reduction (H ₂ - TPR).....	58
5.1.5 Scanning Electron Microscopy (SEM).....	63
5.1.6 Transmission Electron Microscopy (TEM).....	65
5.2. Catalytic activity of NiO/NiAl ₂ O ₄ catalysts.....	68
Part II : The effect of noble metal loading on the NiO/NiAl ₂ O ₄ spinel catalyst during CO ₂ methanation.....	72
5.3 Characterization of metal-NiO/NiAl ₂ O ₄ spinel catalysts.....	72
5.3.1 N ₂ - physisorption (BET).....	72
5.2.2 X-ray diffraction (XRD).....	73

	Page
5.2.3 Temperature programmed reduction (H ₂ -TPR)	75
5.2.5 Scanning Electron Microscopy (SEM)	77
5.4. Catalytic activity of noble metal doping on NiO/NiAl ₂ O ₄ catalysts	78
CHARTER VI	81
CONCLUSION	81
6.1 Conclusion	81
6.2 Recommendations	81
REFERENCES	82
APPENDIX	93
APPENDIX A	93
CALCULATION FOR CATALYST PREPARATION	93
Preparation of NiO/NiAl ₂ O ₄ catalysts by using Co-precipitation method	93
Preparation of Ni/Al ₂ O ₃ catalysts by using impregnation method	94
Preparation of metal dope onto NiAl ₂ O ₄ catalysts by using impregnation method	96
APPENDIX B	98
CALCULATION OF THE CRYSTALLITE SIZE	98
Calculation of the crystallite size by Debye – Scherrer’s equation	98
APPENDIX C	100
CALCULATON OF CO ₂ CONVERSION AND SELECTIVITY	100
VITA	101

LIST OF TABLES

	Page
Table 2.1 Calculated activation energies for methanation of carbon dioxide on the Ni ₂₅ cluster surface [1].....	12
Table 2.2 Characteristics of methanation catalysts.....	14
Table 2.3 Summary of research on the effect of Ni content in CO ₂ hydrogenation.....	17
Table 2.4 Summary of research of supported on Ni catalysts	23
Table 2.5 Physicochemical properties of Ni/CeO ₂ catalysts with different surface areas[2].....	25
Table 2.6 Summary of research of noble metal promoter.....	29
Table 2.7 Summary of research of other metal promoters.....	34
Table 3.1 List of chemicals prepared catalysts by co-precipitation method.....	39
Table 3.2 Co-precipitation and calcination conditions of the prepared catalysts.....	40
Table 3.3 The operating conditions of TCD gas chromatographs for the catalytic activity test	43
Table 5.1. The BET surface area, total pore volume and average pore size diameter of all NiO/NiAl ₂ O ₄ – spinel based catalysts.....	50
Table 5.2 The average crystallite size and phase amount of NiO/NiAl ₂ O ₄ - spinel based catalysts.....	53
Table 5.3 The average crystallite size of spent NiO/NiAl ₂ O ₄ - spinel based catalysts.....	55

Table 5.4 The average crystallite size of fresh and spent Ni/Al ₂ O ₃ catalysts.....	57
Table 5.5 The summary of H ₂ – TPR results.....	62
Table 5.6 The BET surface area, total pore volume and average pore size diameter of metal doped onto NiO/NiAl ₂ O ₄ – spinel based catalysts.....	73
Table 5.7 The average crystallite size and phase amount of metal doping (Ru,Rh,Pd) on NiAl ₈₀ – 900 catalysts.....	75



LIST OF FIGURES

	Page
Figure 2.1 Proposed reaction pathway for CO ₂ methanation on a Ni/Ce _{0.5} Zr _{0.5} O ₂ catalyst [3, 4].....	13
Figure 2.2 Plausible mechanism of CO ₂ methanation on Ni/MSN; (i) bridged carbonyl, (ii) linear carbonyl and (iii) bidentate formate.....	13
Figure 2.3 Proposed mechanism for CO ₂ hydrogenation on Ni/SiO ₂	21
Figure 2.4 (a) Effect of Ni content on CO ₂ conversion and (b) CH ₄ selectivity [52]	22
Figure 2.5 (a) CO ₂ conversion and (b) CH ₄ selectivity vs. temperature [51].....	22
Figure 2.6 Catalytic performance of supported Ni catalysts for CO ₂ methanation [48].....	25
Figure 2.7 Catalytic performance of Ni/CeO ₂ with different surface areas for CO ₂ methanation [48]	26
Figure 2.8 (a) CO ₂ conversion, and (b) CH ₄ and (c) CO yields in CO ₂ methanation over 10 wt. % Ni/metal oxide catalysts (Al ₂ O ₃ , Y ₂ O ₃ , ZrO ₂ , La ₂ O ₃ , CeO ₂ , and Sm ₂ O ₃) [53].....	27
Figure 2.10 Time courses of (a) CO ₂ conversion, and (b) CH ₄ and CO yields in CO ₂ methanation over 10 wt.% Ni/Al ₂ O ₃ , Ni/Y ₂ O ₃ , and Ni/Sm ₂ O ₃ [53].....	28
Figure 2.11 (a) CO ₂ conversion, and (b) CH ₄ selectivity profiles obtained on Ni/ γ -Al ₂ O ₃ , Ni-Pt/ γ -Al ₂ O ₃ , Ni-Pd/ γ -Al ₂ O ₃ , and Ni-Rh/ γ -Al ₂ O ₃ [12].....	32
Figure 2.12 Effect of time on stream on the (a) conversion of CO ₂ , and (b) CH ₄ selectivity in the methanation reaction over Ni/ γ -Al ₂ O ₃ , Ni-Pt/ γ -Al ₂ O ₃ , Ni-Pd/ γ -Al ₂ O ₃ , and Ni-Rh/ γ -Al ₂ O ₃ at 250°C [12].....	32

Figure 3.1 Schematic diagram of the reaction line for testing the CO ₂ methanation analyzed by GC – TCD equipped with molecular sieve and Porapack Q columns.....	43
Figure 5.1 Adsorption-Desorption Isotherm of all NiO/NiAl ₂ O ₄ – spinel based catalysts.....	49
Figure 5.2 The XRD patterns of fresh NiO/NiAl ₂ O ₄ spinel – based catalysts.....	52
Figure 5.3 The XRD patterns spent NiO/NiAl ₂ O ₄ spinel – based catalysts.....	54
Figure 5.4 The XRD patterns of (a) fresh Ni/Al ₂ O ₃ catalysts (b) spent Ni/Al ₂ O ₃ catalysts.....	57
Figure 5.5 The H ₂ – TPR profiled of NiO commercial catalysts plot against time.....	58
Figure 5.6 The H ₂ – TPR profiled of NiO/NiAl ₂ O ₄ – spinel catalysts plot against time.....	60
Figure 5.7 The H ₂ – TPR profiled of 36.5Ni/Al ₂ O ₃ and 20Ni/Al ₂ O ₃ catalysts plot against time.....	61
Figure 5.8 The SEM images of NiO/NiAl ₂ O ₄ spinel – based catalysts.....	65
Figure 5.9 The TEM images of NiAl ₈₀ – 900 catalyst.....	66
Figure 5.10 The TEM images of 20Ni/Al ₂ O ₃ catalyst.....	67
Figure 5.11 The TEM images of 36.5Ni/Al ₂ O ₃ catalyst.....	68
Figure 5.12 The activity of NiO/NiAl ₂ O ₄ -spinel based catalysts during CO ₂ methanation reaction under atmospheric (1 atm) at 350°C for 180 min.....	71

Figure 5.13 Adsorption-Desorption Isotherm of metal doped (Ru,Pd and Rh) into NiO/NiAl ₂ O ₄ - spinel based catalysts.....	72
Figure 5.14. The XRD patterns of (a) fresh and (b) reduced metal doping (Ru,Rh,Pd) on NiAl ₈₀ – 900 catalysts.....	74
Figure 5.15 The H ₂ – TPR profiled of metal doping onto NiAl ₈₀ – 900 catalysts plot against time.....	76
Figure 5.16 The SEM images of metal doping onto NiAl ₈₀ – 900 catalysts.....	77
Figure 5.17 The activity of 1 wt% metal (Ru,Rh,Pd) doping into NiO/NiAl ₂ O ₄ -spinel based catalysts during CO ₂ methanation reaction under atmospheric (1 atm) at 350°C for 180 min.....	79
Figure 5.18 The activity of comparison of 1.0Ru-NiO/NiAl ₂ O ₄ and NiAl ₈₀ – 900 catalysts during CO ₂ methanation reaction under atmospheric and temperature profile (250,275 and 300°C) condition.....	80
Figure B1 Derivation of Bragg’s Law for X-ray diffraction.....	97
Figure B2 The plot indicating the value of line broadening due to the equipment The data were obtained by using α -alumina as a standard.....	98

CHAPTER I

INTRODUCTION

1.1 Motivation

In recent years, the increasing energy demand required for our society development, the usage of carbon-based sources fossil fuel has increased enormously. However, many renewable and environmentally friendly sources of energy pose challenge. Solar energy can be successfully harnessed only in regions which have a highly amount of sunshine, wind turbines can be used to generate electricity only in area with sufficient amount and power of the wind. On the other hand, the biogas upgrading to biomethane can be produced just about everywhere. However, the biogas produced from anaerobic digesters contains 40-75% methane, 25-55% carbon dioxide and other traces gas (N_2 , O_2 , H_2S and H_2) 0.1-3% [5]. The biomethane has many environment benefits to the natural gas replacement for sustainable and environmentally friendly sources of energy including compressed natural gas (CNG), liquid natural gas (LNG), and diesel replacement (bio-CNG and bio-LNG for transport fuel usage).

At the present, CO_2 methanation is a practical way to convert biogas into high methane concentration. The CO_2 hydrogenation to methane has many several positive effects due to very simple reaction that can be operated under atmospheric pressure. However, the formation of methane from CO_2 at low temperature has become an interesting topic to study in many studies, although the conversion was still very low [3].

Ni based catalyst is the most widely studied materials because of their low cost, easily availability with reducible oxide material and possible practical application for this reaction [3]. However, Ni catalyst may be easily deactivated even at low temperature due to the sintering of Ni particle [6].

Many supported Ni catalyst has been investigated on various oxide supports (TiO_2 , CeO_2 , SiO_2 , and ZrO_2). $Ni/\gamma-Al_2O_3$ shows high catalytic activity but is the easily deactivates at high temperature due to carbon deposition, sintering of Ni metal active site resulting to poor stability [7, 8]. Moreover, nickel and alumina easily form the

strong interaction between NiO and γ -Al₂O₃ to NiAl₂O₄ spinel phase catalyst resulting to low catalytic activity in CO methanation reaction [9, 10]. In the same way, in the study about Mn-promoted Ni/Al₂O₃ catalysts for CO₂ methanation, it was found that the formation of NiAl₂O₄ inhibited and decreased the catalytic activity [11]. On the other hand, Mahesh M. Nair et.al reported that in dry reforming of methane the formation of NiAl₂O₄ may improve coke resistance and enhance stability [12]. In the same way, in the hydrogenation of acetylene over Ni/NiAl₂O₄ catalyst, the formation of NiAl₂O₄ can provide a stabilizing effect resulting in the inhibition of metal aggregation and enhance control over sintering or lowering coking rate formation [13].

Thus, there are some contradiction about effect of NiAl₂O₄ spinel phase in CO₂ methanation and steam reforming of methane. CO₂ methanation is the highly exothermic reaction that the deactivation occurs due to sintering or carbon deposition on surface of catalyst during operating at high temperature corresponding to low stability and very poor of catalytic activity. Also, the catalysts used in CO₂ methanation reaction, coke or sintering resistance properties is needed. Meanwhile, in a previous work that studied about steam reforming reaction over NiAl₂O₄ based catalyst, the formation of NiAl₂O₄ can improve the coke formation rate, inhibit the deactivation cause of sintering, and enhance the stability resulting in high catalytic performance.

Although, Ni based catalyst may be easily deactivation due to sintering. Many strategies have been investigated to enhance the stability and catalytic activity of Ni based catalyst. The effect of promoted catalyst is interesting to study. In a previous work, Ru/ γ -Al₂O₃ showed high stability and high activity for CO₂ methanation (96% methane yield at 300°C) [14]. Furthermore, Maria Mihet and Mihaela D. Lazar reported about the effect of noble metal promotion over Ni/ γ -Al₂O₃. The enhancement of CO₂ conversion and CH₄ selectivity were found in the Pt and Pd promoted of Ni/ γ -Al₂O₃ at the 180-270°C and all the catalysts exhibited high stability over the investigated time range (240 min) [15].

Therefore, this work aims to investigate a series of NiAl₂O₄ based catalysts prepared by co-precipitation method in the CO₂ methanation. The effects of precipitation temperature and calcination temperatures on the characteristics and catalytic performances of the NiAl₂O₄ spinel were focused in part I. Furthermore, in part II the effect of promotion by Ru, Rh and Pd over NiAl₂O₄ based catalysts were investigated. The prepared catalysts were characterized by multi-techniques such N₂

physisorption (BET), X-ray Diffraction (XRD), temperature program reduction (TPR), thermogravimetric analysis (TGA), and transmission electron microscopy (TEM).

1.2 Objective of research

The objectives of this research are to investigate

(i) The effect of preparation and calcination temperatures of NiAl_2O_4 spinel based catalysts in CO_2 methanation.

(ii) The effect of spinel phase formation compared with Ni supported commercial Al_2O_3 in CO_2 methanation.

(iii) The effect of noble metal (Ru,Rh,Pd) promotion on NiAl_2O_4 catalyst in CO_2 methanation.

1.3 Scope of research

(i) The NiAl_2O_4 catalysts were prepared by co-precipitation method with molar ratio of Ni/Al is 1/2. The temperatures of precipitation was 30°C and 80°C and the calcination temperature was $500, 700$ and 900°C .

(ii) The activity comparison of $\text{NiAl}_{80} - 900$ catalyst with 20 and 36.5% wt Ni loading onto Al_2O_3 commercial supported catalysts that prepared by impregnation method.

(iii) The noble metal (Ru,Rh,Pd) loading was 1%wt as promoter on Ni- $\text{Al}_2\text{O}_3 - 900$ catalyst.

(iv) The catalysts were characterized by using N_2 physisorption (BET), X-ray diffraction (XRD), temperature program reduction (TPR), temperature program desorption (TPD), thermogravimetric analysis (TGA) and transmission electron microscopy (TEM).

(v) The catalytic performances were tested in CO_2 methanation reaction. Prior to catalytic testing the catalysts were pretreated in H_2 at 450°C for 2.30 h with H_2 at flow rate of $30 \text{ cm}^3/\text{min}$. The reaction temperature was 350°C under atmospheric pressure with gas mixed ratio of $\text{CO}_2:\text{H}_2:\text{N}_2$ are 10:1:4 with total flow rate $40 \text{ cm}^3/\text{min}$.

The composition of outlet gas was analyzed by pulse inlet to GC-TCD with molecular sieve and Porapak Q columns. .

(vi) Both NiAl_2O_4 and 1wt%Ru/ NiAl_2O_4 catalysts were tested in temperature profiles at 250-350°C and each temperature was kept for 1 h.

1.4 Contribution of Research

1.4.1 Knowledge of preparation and properties of NiAl_2O_4 based catalyst by using co-precipitation method.

1.4.2 Knowledge about the best reaction conditions for CO_2 methanation reaction and the effect of catalyst properties on the catalytic performance.

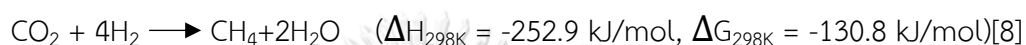


CHAPTER II

THEORY AND LITERATURE REVIEW

2.1 The CO₂ methanation reaction mechanism

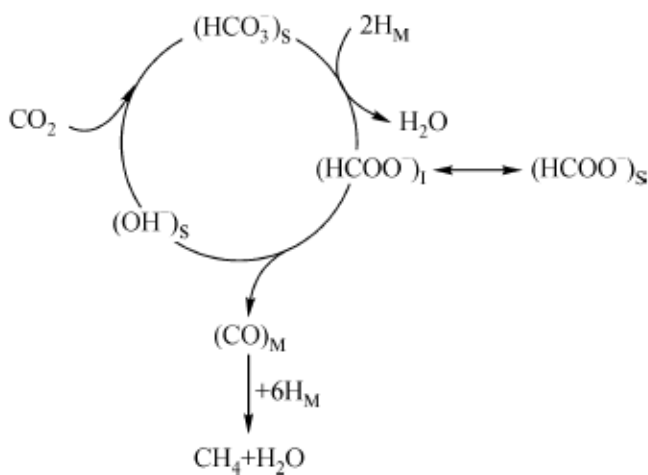
Catalytic hydrogenation of carbon dioxide to methane, also called the Sabatier reaction, is an important catalytic process.



The mechanism of CO₂ methanation is difficult to establish. There are arguments of opinion on the nature of the intermediate compound involved the rate determining step of the process and on the formation of methane scheme. The mechanism of CO₂ methanation have been classified into two main categories. The first step is the CO₂ convert to CO as the intermediate prior to formation of methane as the same CO methanation reaction. And the second one is the direct hydrogenation of CO₂ to methane without CO formation as the intermediate. It has been proposed that the rate-limiting step is either the formation of the intermediate CH_xO and its interaction with hydrogen or the formation of surface carbon in CO dissociation and its hydrogenation [3, 8]. Similarly, Wu, H.C. et.al [16] revealed the reaction path way of CO₂ methanation over Ni/SiO₂ catalyst. The reaction path way may be classified into two pathways. The first pathway is the consecutive, the conversion of CO₂ to CO as intermediate prior methane formation. The other one is the parallel path way, the mixed of both consecutive pathway and the direct CO₂ hydrogenation to methane without CO formation.

The reaction mechanism shown in scheme 2.1 includes to the formation step of formate through carbonate species. The intermediates of reaction involved carbon monoxide and formate were the key intermediate formed and its hydrogenation led to methane formation. In addition, the bounding more strongly on the support and in equilibrium with the active formate species on the metal-support interface. The hydrogenation of the adsorbed carbon monoxide involved six adsorbed hydrogens. A pathway involving hydrogen carbonate was presented for the formation of the interfacial formate because DRIFTS experiments indicated that this species was formed

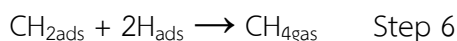
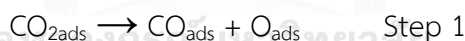
on the support during the reaction and its transient response was consistent with the response of a carbon monoxide precursor [17].



S: the support, M: the metal, l: the metal-support interface

Scheme 2.1 The proposed reaction mechanism of CO₂ methanation [17]

Choe et al. [1] investigated the elementary reaction step and activation energies for CO₂ methanation on Ni (111) surface. The elementary reaction steps considered are:



This elementary steps considered to two mechanisms that are carbon formation and carbon methanation. Step 1 assumed CO as the intermediate on the surface in the CO₂ methanation proceed. Step 2 for the CO dissociation is irreversible owing to rapid removal of surface O by hydrogenation, while step 3 for CO dissociation is attributed

to the disproportion, and lastly step 6 for desorption of methane is irreversible. Step 4 and step 5 are steps occurring after the rate-determining steps.

Table 2.1 shows the calculated activation energies. The dissociation reactions of carbon dioxide and carbon monoxide shown in step 1, step 2, and step 3, and calculated activation energies are 1.27 eV, 2.97 eV and 1.93 eV, respectively. The calculated carbon hydrogenation is shown in step 4, step 5, and step 6, with activated energies of 0.72 eV, 0.52 eV, and 0.50 eV, respectively. Although, the rate-limiting step is the CO dissociation elementary step as step 2 and the calculated activation energy is 2.97eV.

Table 2.1 Calculated activation energies for methanation of carbon dioxide on the Ni₂₅ cluster surface [1].

Activation Energies (E _a (eV))		
$\text{CO}_{2\text{ads}} \rightarrow \text{CO}_{\text{ads}} + \text{O}_{\text{ads}}$	Step 1	1.27 eV
$\text{CO}_{\text{ads}} \rightarrow \text{C}_{\text{ads}} + \text{O}_{\text{ads}}$	Step 2	2.97 eV
$2\text{CO}_{\text{ads}} \rightarrow \text{C}_{\text{ads}} + \text{CO}_{2\text{gas}}$	Step 3	1.93 eV
$\text{C}_{\text{ads}} + \text{H}_{\text{ads}} \rightarrow \text{CH}_{\text{ads}}$	Step 4	0.72 eV
$\text{CH}_{\text{ads}} + \text{H}_{\text{ads}} \rightarrow \text{CH}_{2\text{ads}}$	Step 5	0.52 eV
$\text{CH}_{2\text{ads}} + 2\text{H}_{\text{ads}} \rightarrow \text{CH}_{4\text{gas}}$	Step 6	0.50 eV

Qiushi Pan et al. [4] has investigated the in situ FTIR spectroscopic of CO₂ methanation mechanism on Ni/Ce_{0.5}Zr_{0.5}O₂ to identify the adsorption species and any intermediate species. They found that CO₂ prefers to adsorb on surface oxygen sites adjacent to Ce (III) more than those one that adjacent to Ce (IV)/Zr or hydroxyl surface sites. There are five adsorption species for CO₂ adsorption on catalyst surface and monodentate carbonates formed on Ce (III) are easier to be hydrogenated than those on Ce (IV). Formate species is the main intermediate species and Ce (III) sites were proposed to be active sites for the hydrogenation. The identification confirms that the adsorption and hydrogenation of formic acid as the intermediate species during reaction and for the first time found the CH₂OH species and further to the intermediates in the reaction. The mechanism presented in Fig.2.1.

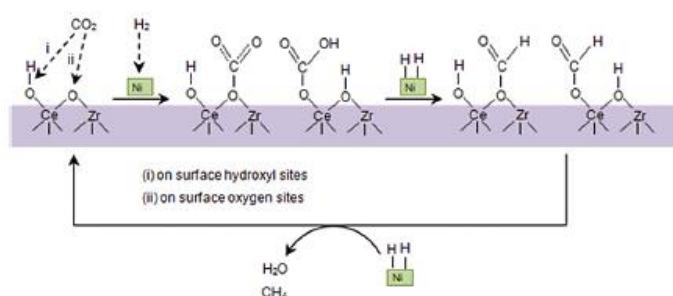


Figure 2.1 Proposed reaction pathway for CO₂ methanation on a Ni/Ce_{0.5}Zr_{0.5}O₂ catalyst [3, 4].

M.A.A. Aziz et al. [3, 18] has reported about the plausible mechanism of CO₂ methanation on metal promoted mesostructured silica nanoparticles (M/MSN). The mechanism shows in Fig.2.2 revealed that the CO₂ and H₂ was adsorbed onto the metal sites and subsequently, dissociated to form CO, O and H atoms and migrated onto the MSN surface. Whilst there are the interaction between CO and oxide surface of the MSN to form (i) bridged carbonyl and (ii) linear carbonyl. In addition, (iii) bidentate formate was formed through the interaction with atomic hydrogen. Meanwhile, the O atom spilt over onto the MSN surface and was stabilized in the oxygen vacancy site near the metal site. Afterward, the hydroxyl was formed on the MSN surface due to the adsorbed oxygen was reacted with atomic hydrogen and the further reaction, the hydroxyl was reacted with another atomic hydrogen to form a water molecule. Finally, the adsorbed carbon species was further hydrogenated to methane and a water molecule as a byproduct. However, the work reported by M.A.A. Aziz et.al are in good agreement with the previous work [4, 19] that the main intermediate for CO₂ methanation reaction is the bidentate formate species.

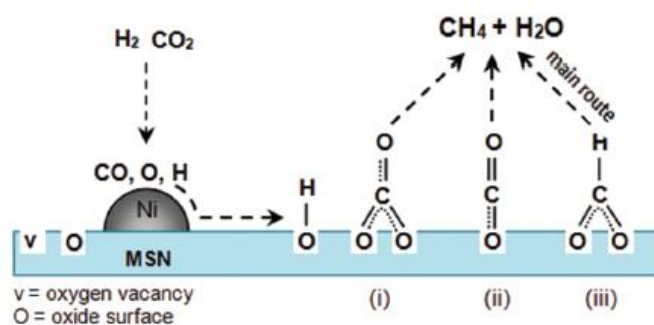



Figure 2.2 Plausible mechanism of CO₂ methanation on Ni/MSN; (i) bridged carbonyl, (ii) linear carbonyl and (iii) bidentate formate.

2.2 Characterisation of methanation catalysts

The development of thermally stable catalysts with high activities at low temperatures is a challenge. The suitable catalysts is determined by different qualities such as stability, selectivity, costs of catalyst, etc. The previous work are most discusses the following types of noble and non-noble metal-based catalysts – ruthenium (Ru), rhodium (Rh), palladium (Pd), platinum (Pt), nickel (Ni), iron (Fe), cobalt (Co) and molybdenum (Mo), respectively. In Table 2.2 basic characteristics of the most investigated CO₂ methanation catalysts are summarized.

Table 2.2 Characteristics of methanation catalysts

Methanation catalyst	Advantages	Disadvantage
Ruthenium (Ru) [3, 6-8, 14, 20-24]	<ul style="list-style-type: none"> - The most active metal for CO₂ methanation than Ni - Good result of CH₄ yield at low temperature without CO co-production - The most stable in CO₂ methanation process than Ni - Higher chemical activity than Ni - Easily reduced to the metallic state at low temperature - No obvious sintering of the active Ru particles happened (200-800°C) 	<ul style="list-style-type: none"> - About 3 times more expensive than Ni (costs dated by 2018 Ru 20 USD/lb Ni 6.21 USD/lb *) - High the Ru loading (>2.2wt%) affect to site-blocking mechanism
Rhodium (Rh) [3, 7, 8, 24-29]	<ul style="list-style-type: none"> - The activity shows lower than Ru and Ni - Can produce methane at low temperature (below 500°C) 	<ul style="list-style-type: none"> - Not occur the direct path way - The CO formation at high temperature (>500°C)

Methanation catalyst	Advantages	Disadvantage
Palladium (Pd) [3, 6-8, 24, 30-33]	<ul style="list-style-type: none"> - High methane selectivity - Beneficial impact on the stability of the nanoparticle against sintering 	<ul style="list-style-type: none"> - The CO₂ conversion exhibited lower than Ru,Ni - Easily deactivated from carbon deposition
Platinum (Pt) [6, 8, 24, 34]	<ul style="list-style-type: none"> - Highly selectivity than Ni - Effective reduction at low temperature 	<ul style="list-style-type: none"> - Lower activity than Ru and Ni
Iron (Fe) [24, 35-41]	<ul style="list-style-type: none"> - High activity - Environmentally friendly –long lifetime - Fe is lower price than Ni - Operating at high temperature (700-950°C) 	<ul style="list-style-type: none"> - Favor to produce long chain hydrocarbon - Very low CH₄ selectivity
Cobalt (Co) [24, 42-44]	<p style="text-align: center;">  จุฬาลงกรณ์มหาวิทยาลัย CHULALONGKORN UNIVERSITY Similar selectivity to Ni </p>	<ul style="list-style-type: none"> - Low CO₂ conversion - More expensive than Ni - Not widely used for commercial application as nickel catalysts

Methanation catalyst	Advantages	Disadvantage
Molybdenum (Mo) [24, 35, 45]	<ul style="list-style-type: none"> - Sulfur tolerant properties - High selectivity toward C₂₊ hydrocarbon than Ni 	<ul style="list-style-type: none"> - Lower activity compared to Ru,Fe,Co,Ni
Nickle (Ni) [2, 3, 6-9, 14, 16, 46-52]	<ul style="list-style-type: none"> - Low price - Commercial catalyst - Easily availability with reducible oxide material - High activity and selectivity of methane Operating temperature 300-600°C 	Easily deactivated at low temperature due to the sintering of Ni particle (short lifetime of catalyst)

2.3 The Ni based catalysts

Hydrogenation of CO₂ to methane has been widely investigated on Ni based catalysts because Ni metal material is commercially, low cost and easily availability. The Ni based catalyst is practical in this reaction and has high potential to convert CO₂ to methane in the range of reaction temperature 100 – 700°C. In addition, the catalytic activity of Ni based catalysts is dependent on various parameters such as the Ni loading, the support and the promoters.

2.3.1 The effect of Ni loading

Table 2.3 Summary of research on the effect of Ni content in CO₂ hydrogenation

Researchers	Objective of research	Methodology		Results
		Catalysts	Preparation method and reaction condition	
H.C.Wu et al 2015 [12]	The mechanism, reaction pathway and selectivity promoted by different Ni particle sizes	0.5Ni/SiO ₂ 10Ni/SiO ₂	-The catalysts were prepared by impregnation method and calcined at 500°C. -The reaction carried out at 400°C 1 atm.	- 0.5Ni/SiO ₂ shows the smaller crystallite size and proceed consecutive pathway. - 10Ni/SiO ₂ shows larger crystallite size and proceed both of consecutive and parallel pathway.
M. V. Gabrovska et al 2015 [18]	The effect on magnesium promoted on the properties and catalytic activity of Ni-Al LDHs with TKL structure	1.5NiAl 3.0NiAl 1.5NiMgAl 3.0NiMgAl	- The catalysts were prepared by co-precipitation method. - Reduction temperature	- 3.0NiMgAl show the highest conversion during 220-260°C. - The highly reduction temperature (530 and 600°C) resulted

Researchers	Objective of research	Methodology		Results
		Catalysts	Preparation method and reaction condition	
			various 400-600°C. - The reaction condition operated at 200-400°C 1 atm.	to sintering deactivation.
Soudabeh Rahmani et al 2014 [19]	The effect of Ni loading on catalytic activity and stability of catalysts supported on γ -Al ₂ O ₃	10Ni/Al ₂ O ₃ 15Ni/Al ₂ O ₃ 20Ni/Al ₂ O ₃ 25Ni/Al ₂ O ₃	- The catalysts were prepared by impregnation method and calcined at 450°C for 3 h. - Reduction temperature was 450°C for 2h. - The catalytic tests were carried out at	- The 20Ni on γ -Al ₂ O ₃ supported catalyst showed the highest activity (82.4%) and selectivity (100%) at 350°C.

Researchers	Objective of research	Methodology		Results
		Catalysts	Preparation method and reaction condition	
			different temperatures ranging from 200 to 500°C	
I. Grac,a et al 2014 [20]	The effect of Ni content (2, 5, 10, and 14) supported on HNaUSY zeolite	2.0Ni/HNaUSY 5.0Ni/HNaUSY 10Ni/HNaUSY 14Ni/HNaUSY	<ul style="list-style-type: none"> - The catalysts were prepared by incipient wetness impregnation method. - Pre-reduced in-situ at 470°C during 1 h. - The activity testing at 250-450°C and GHSV was 43000 h⁻¹. -The reaction carried out at 400°C 1 atm. 	- The 14Ni/HNaUSY zeolite catalyst showed the highest CO ₂ conversion (65.5%) and CH ₄ selectivity (94%) at 400°C.

Ni loading has affected of path way to achieve the reaction including the yield of methane and CO as by product.

H.C.Wu et al. 2015 [16] has investigated the effect of Ni content of 0.5wt% and 10wt% on SiO₂ supported catalysts and focused on the path way to produce CO and CH₄ in CO₂ methanation reaction. The 0.5wt% and 10wt% Ni loadings revealed the different effects in Ni particle size and the kinetic parameters of reaction. Figure 2.3 shows the formation path way of CO and CH₄. 0.5%wt Ni loading shows the smaller clusters and preference for consecutive pathway in the presence of CO as intermediate while both of consecutive and parallel reaction pathways were observed on the large Ni particles with 10%wt Ni loading. Lower Ni loading (0.5%wt) catalyst shows a higher catalytic activity for CO₂ hydrogenation with high CO selectivity. On the other hand, the selectivity is switched to favor CH₄ formation when Ni loading increased to 10wt% with 9 nm of particles. Small Ni particle size favored the consecutive pathway due to low H₂ coverage on Ni surface that led to dissociation of m-HCOO intermediates resulting to CO formation and high CO selectivity. In addition, the CO₂ hydrogenation on large Ni particles may be described to both of consecutive and parallel pathways. The part of parallel reaction may competitively hydrogenated the m-HCOO intermediate to CO or CH₄. The active site for H₂ adsorption in the 10wt% Ni/SiO₂ catalyst was more than the 0.5wt% Ni/SiO₂ catalyst resulting in higher H₂ coverage in the Ni surface proceeding to enable in the parallel pathway. The sites corresponding to corner or step position are attended as the primary active sites for CO₂ hydrogenation on both of Ni/SiO₂ catalysts.

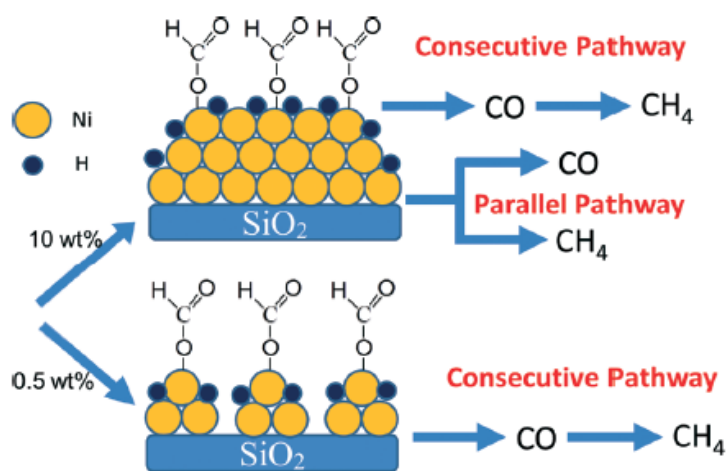


Figure 2.3 Proposed mechanism for CO₂ hydrogenation on Ni/SiO₂

M. V. Gabrovskaja et al. 2015 [46] studied about the effect of Ni content on Ni-Al layered double hydroxides (LDHs) for CO₂ methanation by the variation of Ni²⁺/Al³⁺ molar ratio (3, 1.5 and 0.5). After reduction at 400 and 450°C, the high nickel loading catalyst (3.0NiAl) revealed the highest conversion and a tendency to be more active than low Ni metal loaded (1.5NiAl and 0.5NiAl). The catalytic activity was ascribed to the larger specific surface areas and smaller particle sizes of Ni metal due to higher Ni dispersion. However, the pretreatment of catalyst at high temperature (530 and 600°C) induced to the sintering deactivation of nickel metal particles via the decreasing of methanation activity.

Soudabeh Rahmani et al. 2014 [52] studied the effect of Ni loading on catalytic activity and stability of catalysts supported on γ -Al₂O₃ in CO₂ methanation reaction. The nickel content affected to CO₂ conversion and CH₄ selectivity, the catalytic activity were increased with increasing in Ni loading from 10 to 20 wt%. But further increasing in Ni content resulted in the bigger crystallite size and lower surface area of catalyst and caused the decrease in conversion as seen in Fig.2.4. The 20wt%Ni on γ -Al₂O₃ supported catalyst showed the highest activity and selectivity among all the studied samples.

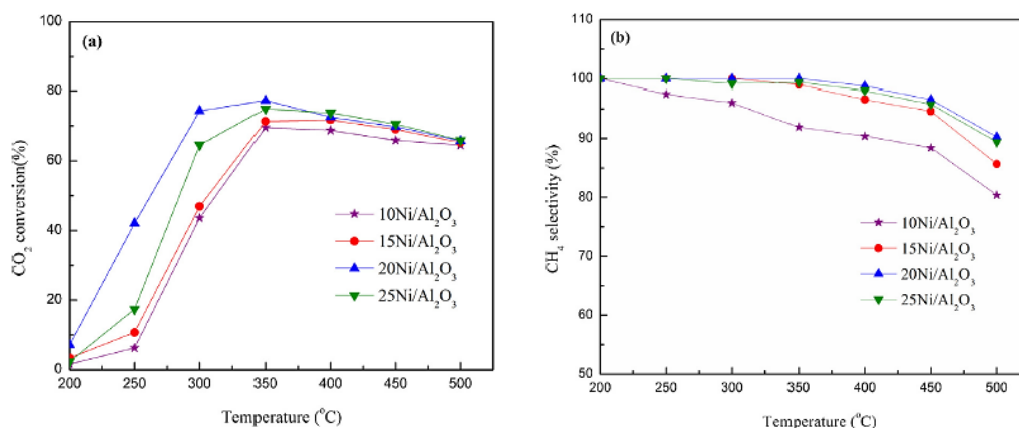


Figure 2.4 (a) Effect of Ni content on CO₂ conversion and (b) CH₄ selectivity, GHSV = 9000 ml/g_{cat} h, H₂/CO₂ molar ratio = 3.5

I. Grac_a et al. 2014 [51] investigated the effect of Ni contents (2, 5, 10, and 14) on HNaUSY zeolite for CO₂ methanation reaction. The enhancement of CO₂ conversion corresponded to an increase of the Ni content. The 14%Ni/HNaUSY zeolite catalyst showed the highest CO₂ conversion (65.5%) and CH₄ selectivity (94%) at 400°C and GHSV 43000 h⁻¹ due to the higher amount of Ni⁰ species after reduction. The resulting catalytic activity is shown in Figure 2.5.

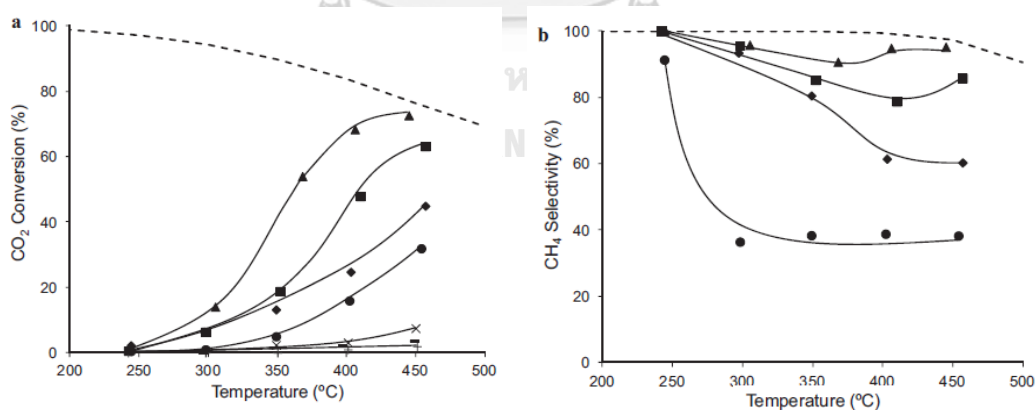


Figure 2.5 (a) CO₂ conversion and (b) CH₄ selectivity vs. temperature, at GHSV = 43,000 h⁻¹, for the USY (+), 10%NiO + USY (x), 2%NiUSY_{Ex} (-), 2%NiUSY_{Imp} (●), 5%NiUSY_{Imp} (◆), 10%NiUSY_{Imp} (■) and 14%NiUSY_{Imp} (▲) catalysts. Dashed line thermodynamic equilibrium conversion values.

2.3.2 The effect of supported catalysts

Table 2.4 Summary of research of supported on Ni catalysts

Researchers	Objective of research	Methodology		Results
		Catalysts	Preparation method and reaction condition	
Thien An Le et al. 2017 [2]	<ul style="list-style-type: none"> - The effect of metal oxide supported catalysts - The effect of difference CeO₂ surface area 	Ni/CeO ₂ (230) Ni/CeO ₂ (140) Ni/CeO ₂ (55) Ni/CeO ₂ (19) Ni/ γ -Al ₂ O ₃ Ni/SiO ₂ Ni/TiO ₂ Ni/ZrO ₂	<ul style="list-style-type: none"> - The catalysts were prepared by wet-impregnation method with 10wt% Ni loading. - Reduction temperature was 500°C. - The activity testing at 150-400°C 1 atm. 	<ul style="list-style-type: none"> - The Ni/CeO₂ (230) catalysts was revealed the best performance at low temperature (200-300°C). - The conversion of CO₂ were increased with the increasing of CeO₂ surface.
Hiroki Muroyama et al. 2016 [53]	The catalytic activity over Ni catalysts supported on various metal oxides	Ni/Y ₂ O ₃ Ni/Al ₂ O ₃ Ni/Sm ₂ O ₃ Ni/ZrO ₂ Ni/CeO ₂ Ni/La ₂ O ₃	<ul style="list-style-type: none"> - The catalysts were prepared by the impregnation method with 10wt%Ni loading and calcined at 600°C for 2h. 	<ul style="list-style-type: none"> - The Ni/Y₂O₃ (low s.v) shows the highest activity and CH₄ yield at 250°C.

Researchers	Objective of research	Methodology		Results
		Catalysts	Preparation method and reaction condition	
			<ul style="list-style-type: none"> - Reduction temperature was 600°C for 3 h. - The activity testing at 200-450°C with GHSV were 20,000 and 30,000 l kg⁻¹ h⁻¹. 	<ul style="list-style-type: none"> - The Ni/Al₂O₃ shows high stability within 75% CO₂ conversion for 48 h.

The CO₂ methanation reaction over supported Ni catalysts has been studied by Thien An Le and et al. 2017 [2] Their studies showed the comparative of some selected supports such as γ -Al₂O₃, SiO₂, TiO₂, CeO₂ and ZrO₂. Figure 2.6 showed the catalytic activity in the order; Ni/CeO₂ (230) > Ni/SiO₂ > Ni/ZrO₂ > Ni/ γ -Al₂O₃ > Ni/TiO₂ at 350-400 °C. Furthermore, the Ni/CeO₂ (230) catalysts revealed the best performance at low temperature (200-300°C). The smallest Ni particle size related to high Ni dispersion as long as the Ni species were completely reduced.

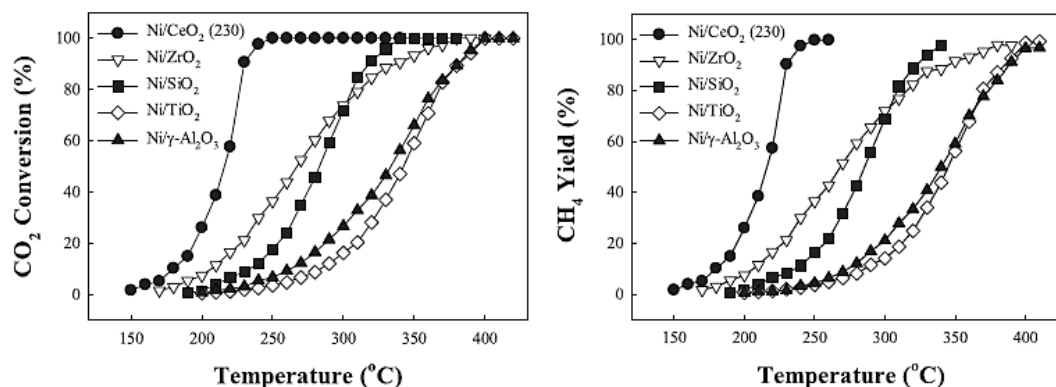


Figure 2.6 Catalytic performance of supported Ni catalysts for CO₂ methanation.

Reaction conditions: 1 mol% CO₂, 50 mol% H₂, 49 mol% He, F/W = 1000 mL/min/g_{cat}

In addition, they have found that the surface area of CeO₂ affected to the catalytic activity. The physicochemical properties of Ni/CeO₂ catalysts with different surface areas are shown in Table 2.4. The decreasing of Ni/CeO₂ surface area follows in the order Ni/CeO₂ (230) > Ni/CeO₂ (140) > Ni/CeO₂ (55) > Ni/CeO₂ (19).

Table 2.5 Physicochemical properties of Ni/CeO₂ catalysts with different surface areas [2].

Catalyst	S _{BET} (m ² /g)	Pore volume (cm ³ /g)	Average pore diameter (nm) ^a	Crystallite size (nm) ^b		H ₂ consumption (mmol H ₂ /g) ^c
				CeO ₂	Ni	
Ni/CeO ₂ (230)	117	0.13	4.4	9	n.d	2.4
Ni/CeO ₂ (140)	94	0.22	9.3	8	9	2.5
Ni/CeO ₂ (55)	44	0.22	20.1	18	21	2.3
Ni/CeO ₂ (19)	15	0.15	39.9	37	27	2.2

^a Average pore diameter was determined in BJH model.

^b Crystallite size of Ni was determined by Scherrer formula for supported Ni catalysts reduced at 500°C.

^c H₂ consumption was detected based in the H₂-TPR.

The catalytic activity of Ni/CeO₂ with different CeO₂ surface areas are shown in Figure 2.7. The conversion of CO₂ increased with increasing of CeO₂ surface, which may be due to the higher Ni dispersion and interaction between Ni and ceria which were responsible for the high catalytic activity.

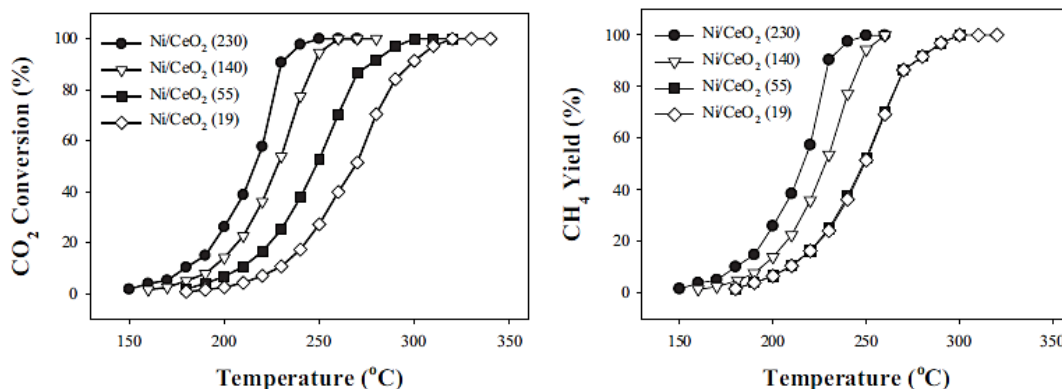
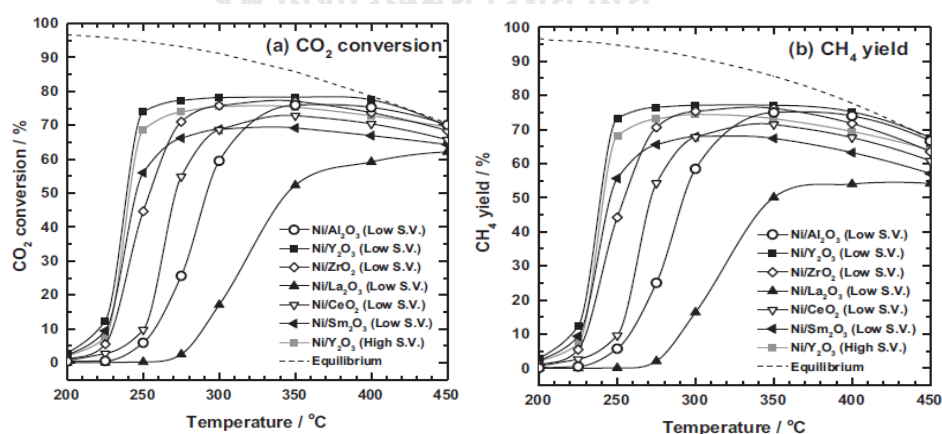


Figure 2.7 Catalytic performance of Ni/CeO₂ with different surface areas for CO₂ methanation. Reaction conditions: 1 mol% CO₂, 50 mol% H₂, 49 mol% He, F/W = 1000 mL/min/g_{cat}.

In the same way, Hiroki Muroyama et al. 2016 [53] investigated the CO₂ methanation over Ni catalysts supported on various metal oxides such as Y₂O₃, Al₂O₃, Sm₂O₃, ZrO₂, CeO₂ and La₂O₃. After reduction at 600°C, for most of the catalysts, the CO₂ conversion drastically increased at 225-250°C and reached a maximal value at 300-350°C. The order of CO₂ conversion and CH₄ yield at 250°C followed: Ni/Y₂O₃ > Ni/Sm₂O₃ > Ni/ZrO₂ > Ni/CeO₂ > Ni/Al₂O₃ > Ni/La₂O₃, be partly revealed to the basic properties of catalysts.



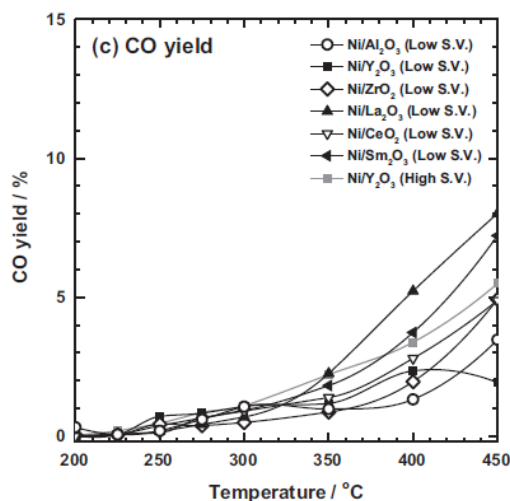


Figure 2.8 (a) CO₂ conversion, and (b) CH₄ and (c) CO yields in CO₂ methanation over 10 wt. % Ni/metal oxide catalysts (Al₂O₃, Y₂O₃, ZrO₂, La₂O₃, CeO₂, and Sm₂O₃). Reaction gas: 10% CO₂-40% H₂-50% N₂. Low S.V.: 20,000 l kg⁻¹ h⁻¹. High S.V.: 30,000 l kg⁻¹ h⁻¹.

In addition, the CO₂ desorption behavior of Ni catalysts has a positive effect on the catalytic activity for CO₂ methanation. The comparative species formed on the surface during CO₂ methanation for Ni/Y₂O₃, Ni/Al₂O₃ and Ni/La₂O₃ catalysts were detected. The CO species on Ni surface was confirmed on Ni/Al₂O₃ that proceeded via the formation of CO intermediate. Only carbonates were observed over Ni/La₂O₃ even under the methanation condition. On the other hand, On Ni/Y₂O₃ the carbonate-like species were observed, which converted to formate species by introducing H₂ to the CO₂ atmosphere while the formate species were decomposed in the H₂ atmosphere. Also, the decomposition of formate species affected to promote the high catalytic activity over Ni/Y₂O₃ catalyst.

Furthermore, the stability tests for the Ni/Y₂O₃, Ni/Sm₂O₃ and Ni/Al₂O₃ catalysts were carried out at 300°C and 20,000 kg⁻¹h⁻¹. Figure 2.9 shows the time on stream of CO₂ conversion, CH₄ and CO yields over the Ni/Y₂O₃, Ni/Sm₂O₃ and Ni/Al₂O₃ catalysts. The high stability was exhibited on Ni/Al₂O₃ catalyst within 75% CO₂ conversion for 48 h. For Ni/Y₂O₃ catalyst, the conversion of CO₂ slightly dropped from 77.0% to 74.2% with time and the CO yields were within 0.05% which were quite lower than Ni/Al₂O₃.

Conversely, Ni/Sm₂O₃ significantly decreases in CH₄ and CO yields. The degradation of catalysts may be derived from the carbon deposition and sintering of Ni particles.

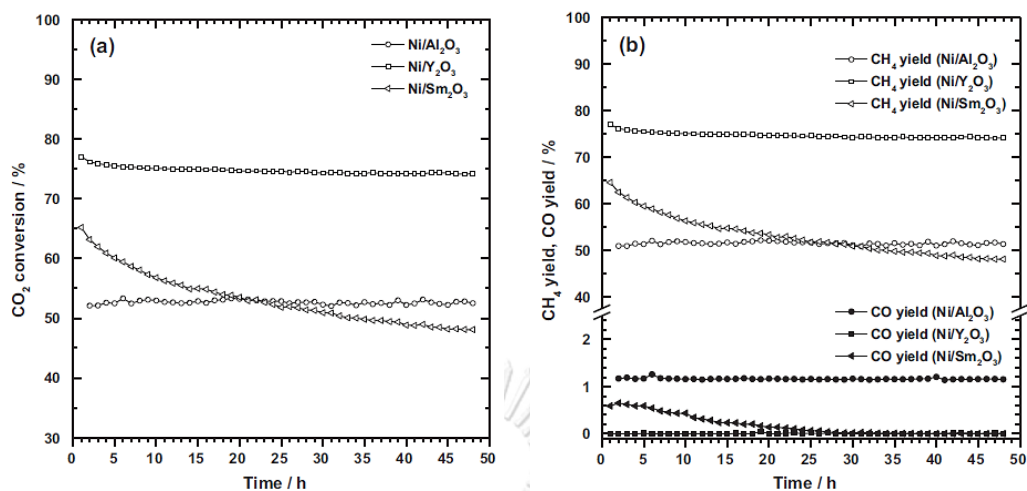


Figure 2.10 Time courses of (a) CO₂ conversion, and (b) CH₄ and CO yields in CO₂ methanation over 10 wt.% Ni/Al₂O₃, Ni/Y₂O₃, and Ni/Sm₂O₃. Reaction gas: 10% CO₂–40% H₂–50% N₂. S.V.: 20,000 l kg⁻¹ h⁻¹.

2.3.3. The effect of promoters on Ni based catalysts

The promoter of catalyst may be classified into two types. The first one, electron promoter to change the electron mobility of catalyst. Second one, structure promoter to inhibit the migration of active site under the high temperature of reaction including to improve the dispersion and thermal stability of catalyst by changing the chemical component, crystal texture, pore structure, dispersion state, and mechanical strength of catalyst [54].

2.3.3.1 Ruthenium (Ru), Rhodium (Rh), Palladium (Pd), Platinum (Pt)

Table 2.6 Summary of research of noble metal promoters

Researchers	Objective of research	Methodology		Results
		Catalysts	Preparation method and reaction condition	
Maria Mihet and Mihaela D. Lazar 2016 [15]	The effect of noble metals (Pt, Pd and Rh) promoted on Ni/ γ -Al ₂ O ₃ catalyst in the reduction of CO ₂ by H ₂ to methane	Ni-Pt/ γ -Al ₂ O ₃ Ni-Pd/ γ -Al ₂ O ₃ Ni-Rh/ γ -Al ₂ O ₃ Ni/ γ -Al ₂ O ₃	<ul style="list-style-type: none"> - The catalysts were prepared by impregnation method with 10wt% Ni, 0.5wt% promoter and calcined at 550°C for 3 h. - Reduction temperature was 550°C for 3 h. - The catalytic testing were carried out 30-300°C 1 atm. 	<ul style="list-style-type: none"> - The Ni-Pd/ γ-Al₂O₃ and Ni-Pt/ γ-Al₂O₃ shows the high CO₂ conversion and CH₄ selectivity in the range of temperature are 180-270°C. - The Ni-Pd / γ-Al₂O₃ shows the high stable CO₂ conversion of 74.6% and 96.6% CH₄ selectivity at 250°C

Researchers	Objective of research	Methodology		Results
		Catalysts	Preparation method and reaction condition	
Yi Liu et al. 2018 [24]	The effect of noble metal promoter (Ru,Pt,Pd) on 20wt%Ni/SiO ₂ catalyst during CO methanation reaction	Ni-Ru/SiO ₂ Ni-Pt/SiO ₂ Ni-Pd/SiO ₂	<ul style="list-style-type: none"> - The catalysts were prepared by aqueous incipient wetness impregnation method with 10wt% Ni, 0.5wt% promoter and calcined at 400°C for 2 h. - Reduction temperature was 400°C for 10 h. - The activity testing at 200-280°C with GHSV was 40,000 cm³ g⁻¹ h⁻¹. 	- The Ni-Ru/SiO ₂ shows the dramatically improvement of catalytic activity at 275°C.

Researchers	Objective of research	Methodology		Results
		Catalysts	Preparation method and reaction condition	
Wenlong Zhen et al. 2014 [25]	The long term stability testing on 10Ni-1.0Ru/ γ -Al ₂ O ₃	10Ni-1.0Ru/ γ -Al ₂ O ₃	<ul style="list-style-type: none"> - The catalysts were prepared by impregnation method with 10wt% Ni, 1.0wt% Ru and calcined at 450°C for 5 h. - Reduction temperature was 450°C for 2 h. - The activity testing at 400°C 1 atm with GHSV was 9000 h⁻¹ 	- The 10Ni-1.0Ru/ γ -Al ₂ O ₃ catalyst performed the high catalytic activities, selectivity and no deactivation up to 100h in long term stability testing at 400°C 1 atm

Maria Mihet and Mihaela D. Lazar (2016) [15] investigated the presence of Pt,Pd or Rh promotion on Ni/ γ -Al₂O₃ during CO₂ methanation. The addition of 0.5wt% noble metal promoter resulted in an increase of NiO reducibility (Ni-Rh > Ni-Pt > Ni-Pd > Ni), enhanced metal dispersion and increased H₂ chemisorption capacity (Ni-Pt > Ni-Rh > Ni-Pd > Ni) with no significant influence upon the support intrinsic activity given by the CO₂ adsorption capacity. The catalytic testing were carried out 30-300°C under atmospheric pressure. The Pt and Pd promoted on Ni/ γ -Al₂O₃ catalysts can enhance CO₂ conversion and CH₄ selectivity in the range of temperature are 180-270°C, while Ni-Rh/ γ -Al₂O₃ showed lower activity than Ni/ γ -Al₂O₃ as shown in Figure 2.11.

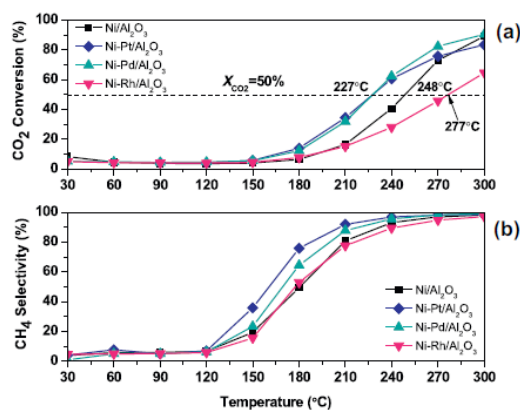


Figure 2.11 (a) CO_2 conversion, and (b) CH_4 selectivity profiles obtained on Ni/ $\gamma\text{-Al}_2\text{O}_3$, Ni-Pt/ $\gamma\text{-Al}_2\text{O}_3$, Ni-Pd/ $\gamma\text{-Al}_2\text{O}_3$, and Ni-Rh/ $\gamma\text{-Al}_2\text{O}_3$ ($\text{CO}_2:\text{H}_2 = 1:4$, GHSV = 5700 h^{-1}).

Considering the stability exhibited in Figure 2.12, all the catalysts showed stable catalytic performance over time range studied. The Ni-Pd / $\gamma\text{-Al}_2\text{O}_3$ revealed the most efficient catalyst with stable CO_2 conversion of 74.6% and 96.6% CH_4 selectivity at 250°C . Furthermore, during temperature programmed reaction tests the maximum values of 90.5% CO_2 conversion and 98.7% CH_4 selectivity were obtained at 300°C .

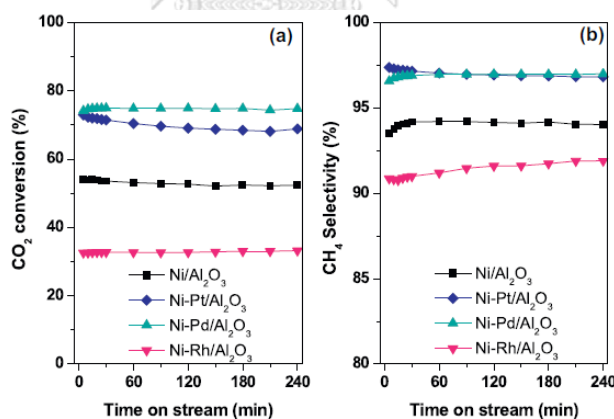


Figure 2.12 Effect of time on stream on the (a) conversion of CO_2 , and (b) CH_4 selectivity in the methanation reaction over Ni/ $\gamma\text{-Al}_2\text{O}_3$, Ni-Pt/ $\gamma\text{-Al}_2\text{O}_3$, Ni-Pd/ $\gamma\text{-Al}_2\text{O}_3$, and Ni-Rh/ $\gamma\text{-Al}_2\text{O}_3$ at 250°C ($\text{CO}_2:\text{H}_2 = 1:4$, GHSV = 5700 h^{-1}).

Yi Liu et al. (2018) [55] investigated the effect of noble metal promoter (Ru,Pt,Pd) on 20wt%Ni/ SiO_2 catalyst during CO methanation. They found that the addition of 0.5wt% of promoter showed the dramatically improvement of catalytic activity in the order Ru>Pt>Pd at the same temperature (275°C) comparable with

20Ni/SiO₂ catalyst, which may be due to the presence of Ru had decreased the crystallite size of Ni particle resulting to higher dispersion including the enhanced reducibility by hydrogen spillover.

In the same way, the positive effect by adding Ru promoter on 10wt%Ni/ γ -Al₂O₃ catalyst for CO₂ methanation were studied by Wenlong Zhen et al. 2014 [56] On 10Ni-1.0Ru/ γ -Al₂O₃ catalyst high catalytic activities, selectivity and no deactivation up to 100h in long term stability testing at 400°C 1 atm were established and were attributed to the easily reduced to the metallic state. For the possible reaction mechanism was revealed, the dissociation of CO₂ was activated in Ru surfaces to form carbon species (CO_{ads}) and further to react with activated H on Ni active site to form methane. In addition, Abe et al. 2009 [57] revealed 0.8wt%Ru/TiO₂ catalyst (Ru diameter 2.5nm) showed 100%yield CH₄ at 160°C and this catalyst showed no deactivation over at least 170 h testing.



2.3.3.2 Other metal promoter

Table 2.7 Summary of research of other metal promoters

Researchers	Objective of research	Methodology		Results
		Catalysts	Preparation method and reaction condition	
Zhenhua Li et al. 2014 [58]	The comparative of catalytic performance between Ni-Mg/Al ₂ O ₃ and Ni/Al ₂ O ₃	NiMg8 11Ni/Al ₂ O ₃	<ul style="list-style-type: none"> - 11Ni/Al₂O₃ was prepared by incipient wetness impregnation method and calcined at 600°C for 5 h - NiMg8 (Ni/Mg = 1/8) was prepared by co-precipitation method and calcined at 650°C for 8 h. - Reduction temperature was 800°C for 4 h. - The catalytic testing were operated at 600°C for 5 h. 	- The NiMg8 (Ni/Mg = 1/8) described the higher performance than Ni/Al ₂ O ₃ catalyst

Researchers	Objective of research	Methodology		Results
		Catalysts	Preparation method and reaction condition	
Lu et al. 2016 [59]	The effect of metal (La, Ce, Fe or Co) doped nickel catalysts supported on zirconia modified clays during CO methanation	Ni-La/ZrO ₂ Ni-Ce/ZrO ₂ Ni-Fe/ZrO ₂ Ni-Co/ZrO ₂	<ul style="list-style-type: none"> - The catalysts were prepared by the incipient wetness co-impregnation method with 15wt%Ni, 1wt% promoter and calcined temperature programmed from 25°C to 500 °C at a heating rate of 2 °C/min. - Reduction temperature was at 500 °C for 3 h. - The activity testing were operated at 300-500°C 	<ul style="list-style-type: none"> - The adding of metal promoter resulted to positive effect and improve better propertied of methanation catalyst. - The Fe and CO promoters preferred to beneficial for CO₂ methanation - The La and Ce promoters preferred to beneficial for CO methanation

Researchers	Objective of research	Methodology		Results
		Catalysts	Preparation method and reaction condition	
Javier Barrientos et al. 2017 [60]	<ul style="list-style-type: none"> - The effect of metal oxides promoted (Zr, Mg, Ba or Ca) nickel catalysts supported on alumina during CO methanation - To study the rate of polymeric carbon formation and the thermal sintering under accelerated ageing tests 	Ni-Zr/Al ₂ O ₃ Ni-Mg/Al ₂ O ₃ Ni-Ba/Al ₂ O ₃ Ni-Ca/Al ₂ O ₃	<ul style="list-style-type: none"> - The catalysts were prepared by Impregnation method with 30wt%Ni and 5wt%promoters and calcined at 500°C for 3 h. - Reduction temperature was 500°C for 4h. - The rate of carbon formation testing were operated at 300°C for 24 h. - The accelerated ageing testing were aged at 690°C in a H₂O/H₂ atmosphere for 7 days 	<ul style="list-style-type: none"> - None of all promoter has satisfactory effect on the thermal resistance in accelerated ageing condition. - The Zr promoter can inhibited the rate of polymeric carbon formation conversely with La promoted.

Zhenhua Li et al. 2014 [58] revealed the H₂-TPR results that the dispersed NiO interacting with MgO promoter and the support that inhibited the agglomeration of Ni metal active sites resulting in an improved activity and stability of catalyst at high temperature (up to 973K) in methanation reaction. Furthermore, MgO has positive effect to improve resistance of carbon deposition and minimize Ni particle sintering

[32]. In addition, The Ni/Al hydrotalcite- like with adding Mg as promoter and the catalyst designation NiMg8 (Ni/Mg = 1/8) described the higher performance than Ni/Al₂O₃ catalyst. Addition of Mg promoter can enhance activity and improve stability for the methanation of syngas corresponding to the minimize rate of carbonaceous deposits formation due to a higher extent of Ni dispersion in the NiMg8 catalyst [58].

Lu et al. 2016 [59] investigated the effect of metal (La, Ce, Fe or Co) doped nickel catalysts supported on zirconia modified clays. They found that doping metal promoter may promote NiO dispersion, increase the reducibility of Ni species and enhance the thermal stability for CO₂ methanation. In addition, doping of Fe and Co shows the positive effect on CO₂ methanation while La and Ce preferred proceed the beneficial in CO methanation.

Javier Barrientos et al. 2017 [60] studied about the effect of metal oxides promoted (Zr, Mg, Ba or Ca) nickel catalysts supported on alumina. The CO methanation was carried out under low temperature (300°C) in order to study the rate of polymeric carbon formation and the thermal sintering under accelerated aging test conditions. Apparently, none of the promoter has satisfactory effect on the thermal resistance due to the Ni metal surface area was loss corresponding to sintering and pore collapse. However, the Zr promoter can inhibited the rate of polymeric carbon formation while Ca promoter has adverse effect on carbon formation.

2.4 The NiAl₂O₄ spinel catalyst on steam reforming reaction

N. Sahli et al. [61] studied the NiAl₂O₄ catalyst that prepared by using sol-gel method (propionic acid) during CO₂ reforming of methane. They found the spinel structure was unaltered of nickel to aluminum ratio higher than 0.5 and the excess of nickel may give the large particle size of NiO on spinel phase. For the ratio of nickel to aluminum higher than 0.5, free NiO was observed on spinel and the reduction of nickel preferred to proceed at low temperature while the Ni/Al ratio lower than 0.5 revealed the formation of Al₂O₃ and NiAl₂O₄ and high surface area was obtained. To get high performance, coke formation on small metallic particles and the growing of Ni particle needed to be limited. In addition, the substoichiometric spinel structure showed properties that proceeded as the active catalyst following the high stability of structure at low temperature, high dispersion of NiO into the spinel. The growing Ni particles

were limited probably due to the interaction between nickel metal out of structure and Ni oxide of structure.

Cristina Jiménez-González et al. 2013 [13] investigated two series of nickel aluminates supported (15wt% and 70wt% of $\text{NiAl}_2\text{O}_4/\text{Al}_2\text{O}_3$) and unsupported (NiAl_2O_4) catalysts. The Ni^{2+} was detected on surface nickel of $\text{NiAl}_2\text{O}_4/\text{Al}_2\text{O}_3$ calcined at 850°C . Furthermore, the Ni surface composition of all the catalysts was the mixture of NiO and NiAl_2O_4 structures. The distribution of nickel between NiO and NiAl_2O_4 species depended on Ni loading and the preparation method. The nano-structural and chemical properties of supported catalysts were modified by the interaction among the phases lying on the carrier after reduction at high temperature. Considering the relationship between the Ni particle size and NiO/ NiAl_2O_4 ratios, low NiO/ NiAl_2O_4 ratio resulted in the smallest Ni particle size (6nm) leading to the highest dispersion that observed on 70% $\text{NiAl}_2\text{O}_4/\text{Al}_2\text{O}_3$ catalyst. These interesting results allowed us to conclude. Conversely, the previous literature data reported the small metallic Ni particle size was controlled by the NiO/ NiAl_2O_4 ratio initially present in the calcined samples. Moreover, in this work, several Ni contents from 15% to 70% were modulated the surface acidity of NiAl_2O_4 supported catalysts and no dramatic loss of active sites. For the catalytic activity results on steam reforming of methane, the 70% $\text{NiAl}_2\text{O}_4/\text{Al}_2\text{O}_3$ catalyst showed a higher activity and hydrogen yield than the other investigated nickel based catalysts. The stability improvement and the resistance towards sintering and carbon formation corresponded to the higher dispersion and smaller Ni crystallite size. Also, the dispersion of nickel aluminate phase on high surface area transition alumina provided better textural and nano-structural stability than pure NiAl_2O_4 .

CHAPTER III

MATERIALS AND METHODOLOGY

This chapter explains about the details of co-precipitation method and conditions of catalyst preparation including precipitation and calcination temperatures. It is divided into three parts consisting of catalyst preparation, catalyst characterization and catalytic reaction test. The first part describes the preparation method of catalysts by co-precipitation method. Second part shows the details of characterization techniques such as N_2 physisorption (BET), X-ray diffraction (XRD), temperature program reduction (TPR), temperature program desorption (TPD), thermogravimetric analysis (TGA) and transmission electron microscopy (TEM). And finally, the reaction test for CO_2 methanation is exhibited in the third part.

Part I: Catalysts preparation

3.1 Materials

The chemicals used in the catalyst preparation were analytical grades as shown in Table 3.1.

Table 3.1 List of chemicals prepared catalysts by co-precipitation method.

Chemicals	Formula	Assay (%)	Manufacture
Nickel(II)nitrate hexahydrate	$Ni(NO_3)_2 \cdot 6H_2O$	99.99	Sigma-Aldrich
Aluminium nitrate	$Al(NO_3)_3 \cdot 9H_2O$	98	Ajax Finechem
Ruthenium (III) nitrosyl nitrate solution	$Ru(NO)(NO_3)_3$	75	Sigma-Aldrich
Tetramminepalladium (II) chloride monohydrate	$Pd(NH_3)_4Cl_2 \cdot H_2O$	39	Alfa Aesar
Rhodium (III) Chloride hydrate	$RhCl_3 \cdot xH_2O$	38.5-45.5	Alfa Aesar
Aluminum oxide	Al_2O_3	-	Fluka

3.2 Catalysts preparation by co-precipitation method

3.2.1 NiAl₂O₄ spinel catalysts preparation

NiAl₂O₄ catalysts were prepared by co-precipitation method with molar ratio of Ni/Al was 1:2. Nickel nitrate (Ni (NO₃)₂ • 6H₂O) and aluminium nitrate (Al (NO₃)₃ • 9H₂O) were used as the metal precursors. Firstly, nickel nitrate and aluminium nitrate were diluted in DI water with concentration of solution 0.5 molar and then adjust pH of solution by adding NH₄OH from pH 4 to 8.5 and stirring until precipitated. The temperature of co-precipitation were varied at 30 and 80°C After that the precipitate powder were filtrated and dried at 110°C for 12 h in air and calcined at temperature 500, 700, 900 or 1200°C for 5 h. The preparation conditions and the nomenclature of the prepared catalysts are shown in Table 3.2

Table 3.2 Co-precipitation and calcination conditions of the prepared catalysts

No	Co-precipitation temperature (°C)	Calcination temperature (°C)	Catalysts nomenclature
1	30	500	NiAl ₃₀ - 500
2	30	700	NiAl ₃₀ - 700
3	30	900	NiAl ₃₀ - 900
4	80	500	Ni-Al ₈₀ - 500
5	80	700	Ni-Al ₈₀ - 700
6	80	900	Ni-Al ₈₀ - 900
7	80	1200	Ni-Al ₈₀ - 1200

3.2.2 Ni/Al₂O₃ catalyst preparation

36.5Ni/Al₂O₃ was also prepared by impregnation method with a similar molar ratio of Ni/Al 1:2 using nickel nitrate (Ni (NO₃)₂ • 6H₂O) and Al₂O₃ commercial (Fluka s.f. 155 sq.m/g) as precursor of metal and support, respectively. The catalyst was dried at 110°C overnight and calcined at 550°C for 5 h.

20Ni/Al₂O₃ was also prepared by impregnation method with 20wt% of Ni loading onto the Al₂O₃ commercial support catalyst (Fluka s.f. 155 sq.m/g). The catalyst was dried at 110°C overnight and calcined at 550°C for 5 h.

3.2.3 Promoted catalysts preparation

The various metal catalysts were promoted on NiO/NiAl₂O₄ catalyst that precipitated at 80°C and calcined at 900°C. The Ru (NO) (NO₃)₃, Pd (NH₃)₄Cl₂ • H₂O and RhCl₃ • xH₂O were used as metal precursor with metal loading 1%wt. The catalyst was dried at 110°C overnight and calcined at 350°C for 2 h.

Part II: Catalysts characterization

3.3 Catalysts characterization

3.3.1 N₂ physisorption (BET)

BET surface area, total pore volume and average pore size diameter were calculated from the nitrogen adsorption isotherms at 77 K using a BEL-SORP automated system. The surface area was calculated according to Brunauer – Emmett – Teller (BET). Pore volume and average pore size diameter were calculated by Barrett – Joyner – Halenda (BJH) analysis.

3.3.2 X-ray diffraction (XRD)

Powder X-ray diffraction (XRD) patterns were the technique for examine the crystallite phase and elemental distribution of the catalyst particle. The XRD pattern were performed by using SIEMENS XRD D5000 X-ray diffractometer with CuK α radiation. The scanning were recorded over a range of 2 θ angles from 10° to 80°. The average crystallite size of catalysts were calculated from line broadening according to the Scherrer's equation.

3.3.3 Temperature program reduction (TPR)

TPR measurements were carried in quartz u- tube reactor to determine the behavior of reduction temperature of the catalysts. Prior the measurement, the samples were pretreated by N₂ with flow rate 30 cm³/min at 200°C for 1 h then cooled down to the room temperature. After that, flowing the carrier gas (10%H₂/Ar) through the catalysts samples at 30 cm³/min and temperature ramping from 300°C to 800°C with the temperature rating 10°C/min.

3.3.4 Scanning Electron Microscopy (SEM)

The morphologies of all catalysts sample were performed by using JEOL mode JSM-5800L V. scanning electron microscopy.

3.3.5 Transmission Electron Microscopy (TEM)

The transmission electron microscope of TECNAI F20 G with field emission gun operating at voltage rang of 50-200 kV and optical point resolution of 0.23 nm was performed for TEM analysis. This TEM technique provide morphology images (TEM images) and crystallite size.

Part III: Catalytic activity

3.4 Catalytic activity

3.4.1 Materials

The catalytic activity of the prepared catalysts were evaluated in CO₂ methanation reaction at 350°C for 3 h under atmospheric and the molar gas mix ratio of CO₂:H₂:N₂ 1:10:4 with the total flow rate is 40 cm³/min. Approximately 0.1 g catalyst was packed in 9 mm diameter of the tubular quartz reactor. Prior to the reaction test, the samples were pretreated in pure H₂ at 450°C for 2.30 h with flow rate is 30 cm³/min. The composition of outlet gas was analyzed by pulse inlet to GC-TCD with molecular sieve and Porapack Q columns.

3.4.2 Apparatus

A flow diagram of the system for testing the catalytic activity is shown in Figure 3.1. An apparatus consisted of a quartz tubular reactor, an automation temperature controller, an electrical furnace, a gas controlling system and gas chromatography that was thermal conductivity detector (TCD). The instruments used in this system were listed and explained as follows:

Table 3.3 The operating conditions of TCD gas chromatographs for the catalytic activity test.

Gas chromatograph	Shimadzu GC-14B
Detector	TCD
Column	Porapak Q (2m) , Molecular sieve
Carrier gas	Helium
Carrier gas flow	30 ml/min
Injector temperature	100°C
Detector temperature	70°C
Column temperature	70°C
Analysis gas	CO ₂ , CH ₄ , CO

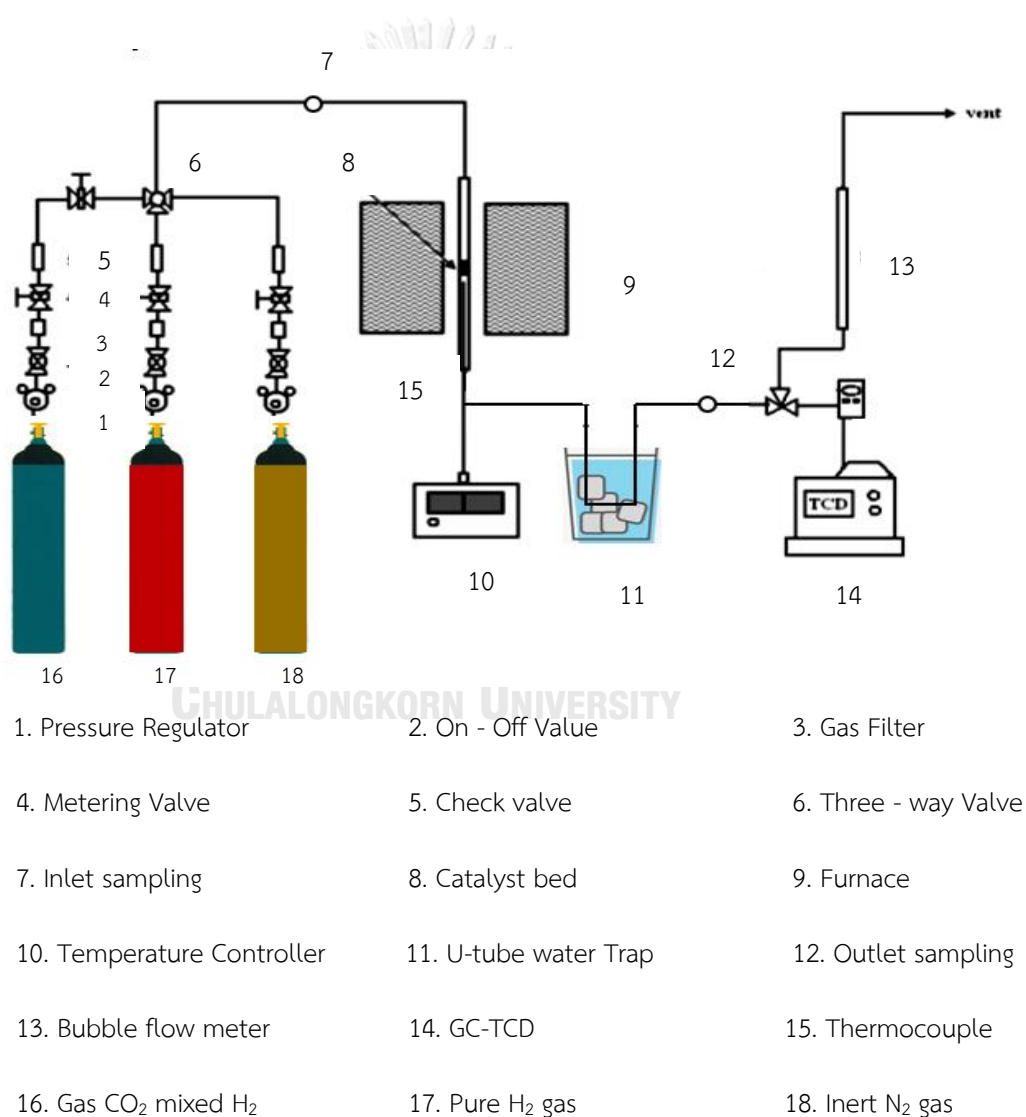


Figure 3.1 Schematic diagram of the reaction line for testing the CO₂ methanation analyzed by GC – TCD equipped with molecular sieve and Porapak Q columns.

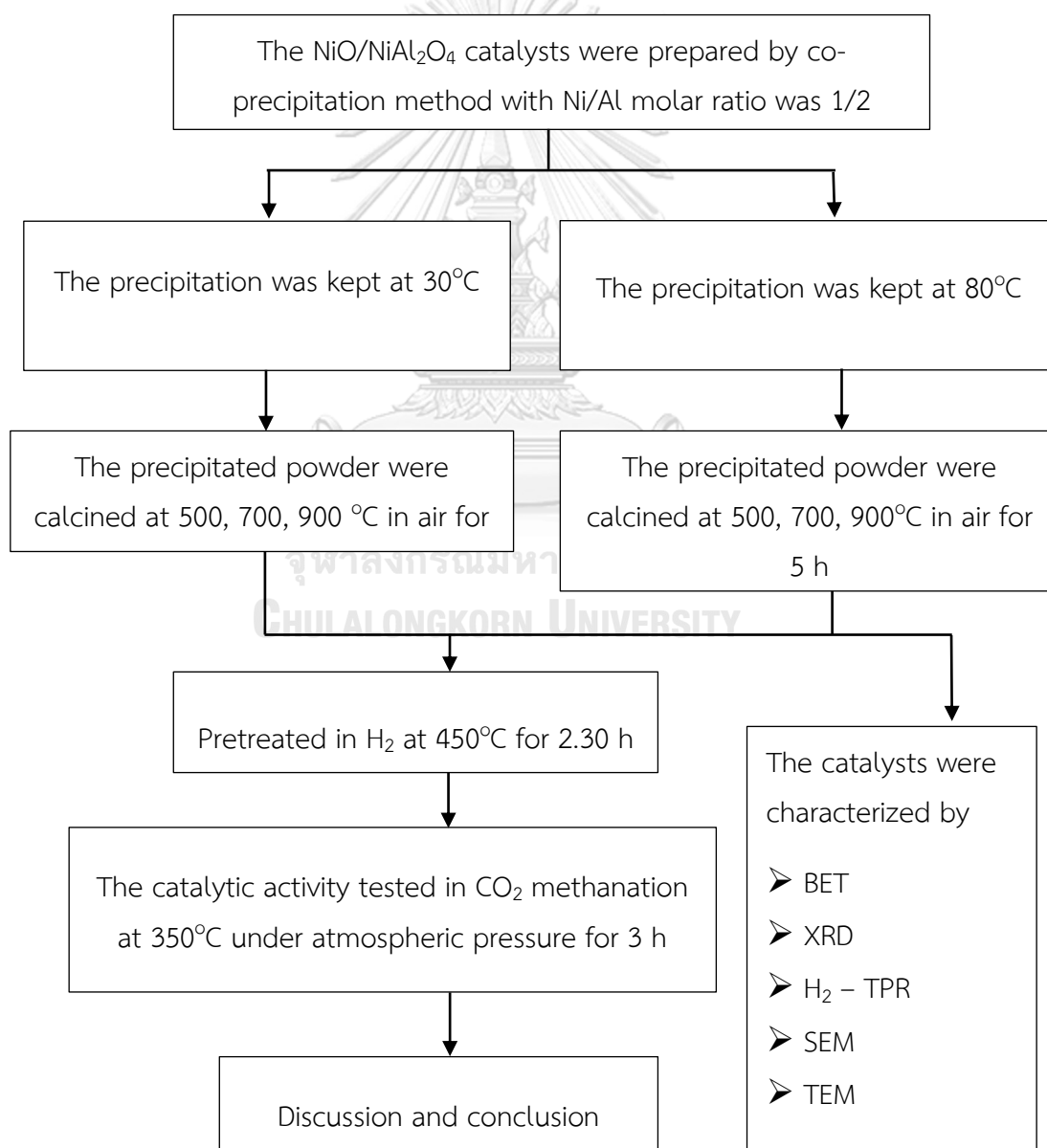
CHAPTER IV

RESEARCH METHODOLOGY AND RESEARCH PLAN

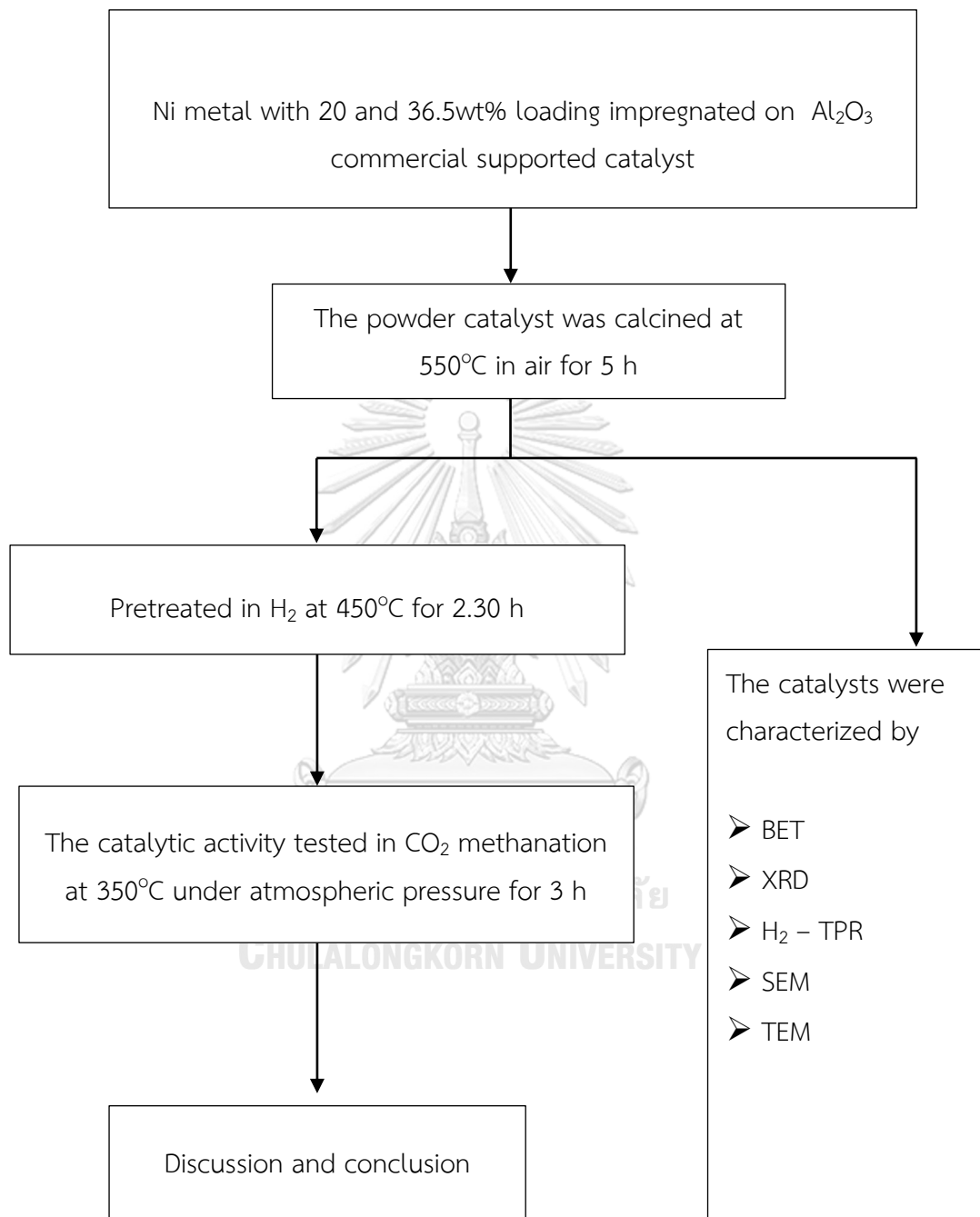
4.1 Research methodology

In this work, the research were divided into three parts according to

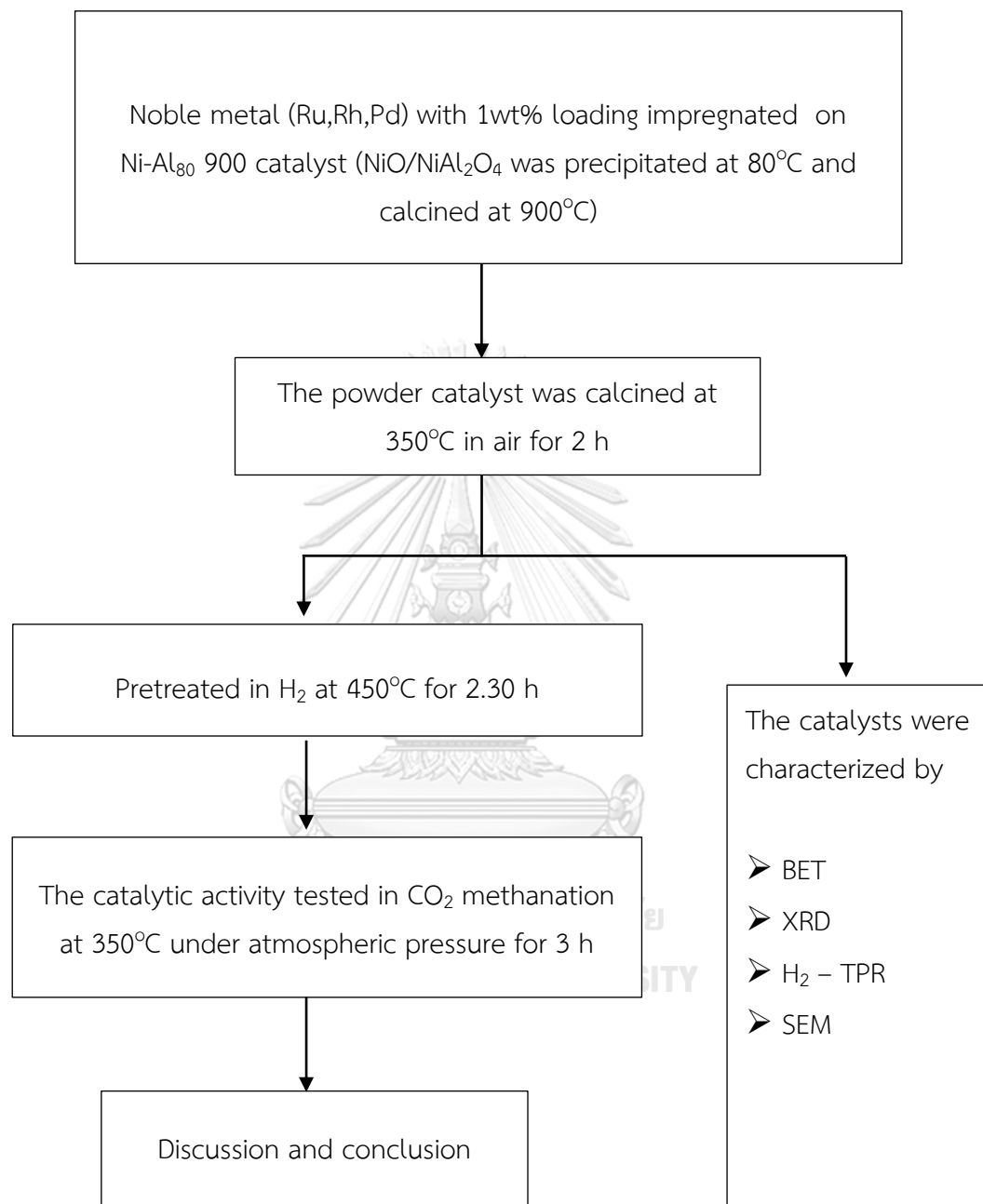
4.1.1 The effect of preparation and calcination temperatures of NiO/NiAl₂O₄ spinel catalyst during CO₂ methanation reaction



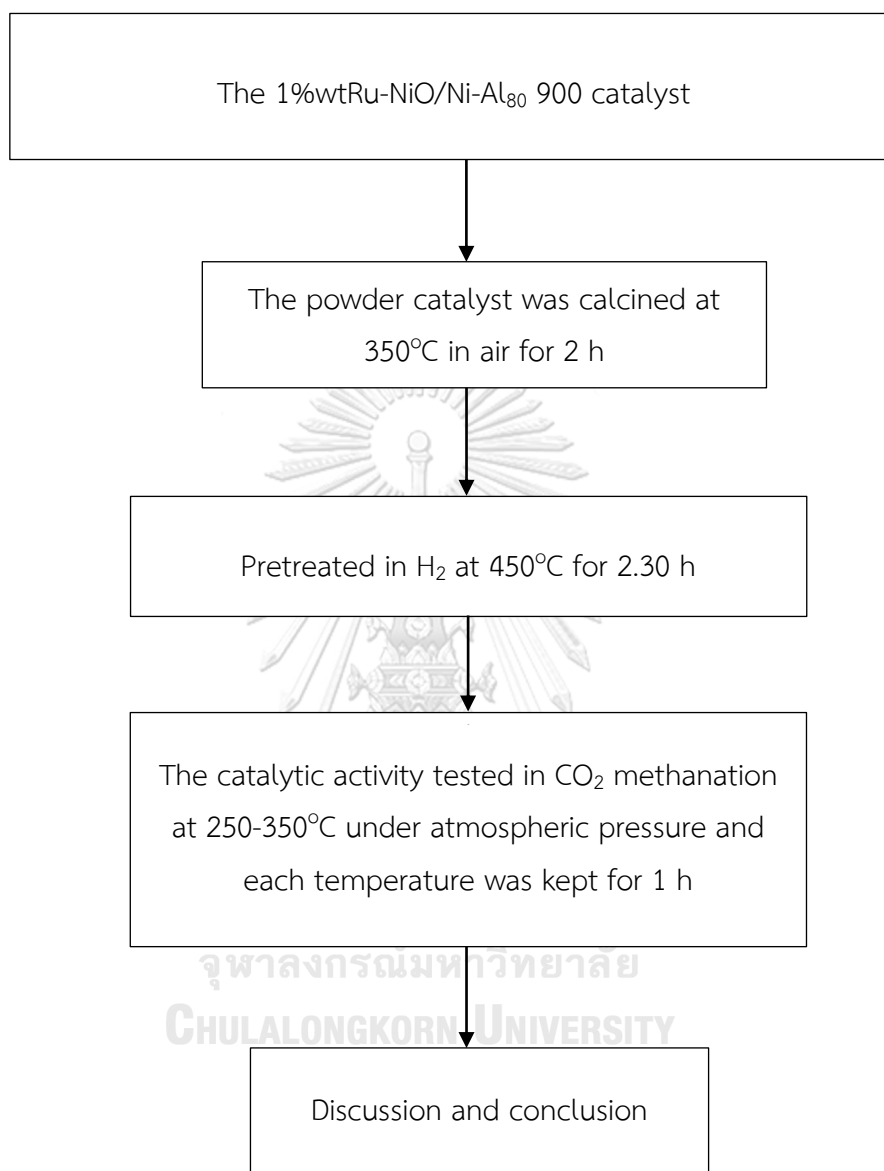
4.1.1.1 The effect of spinel phase formation compared Ni support on commercial Al_2O_3



4.1.2 The effect of noble metal loading support on NiO/NiAl₂O₄ spinel catalyst during CO₂



4.1.2.1 The effect of reaction temperature over Ru-NiO/NiAl₂O₄ catalyst during CO₂ methanation



CHARTER V

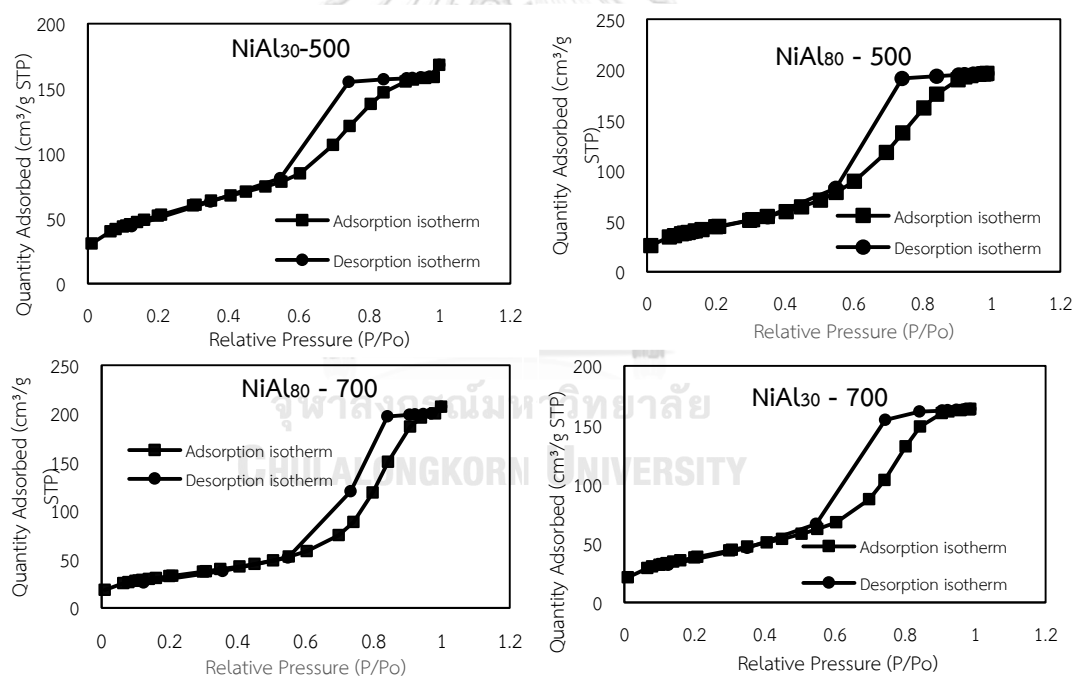
RESULTS AND DISSCUSSION

Part I: The effect of preparation and calcination temperatures of NiO/NiAl₂O₄ spinel catalysts during CO₂ methanation reaction

5.1 Characterization of NiO/NiAl₂O₄ spinel catalysts

5.1.1 N₂- physisorption (BET)

The adsorption-desorption isotherm of the NiO/NiAl₂O₄ spinel catalysts are shown in Figure 5.1. All the catalysts exhibited type IV isotherm that indicated mesoporous structure with pore size 2-50 nm with significantly reduced hysteresis loops.



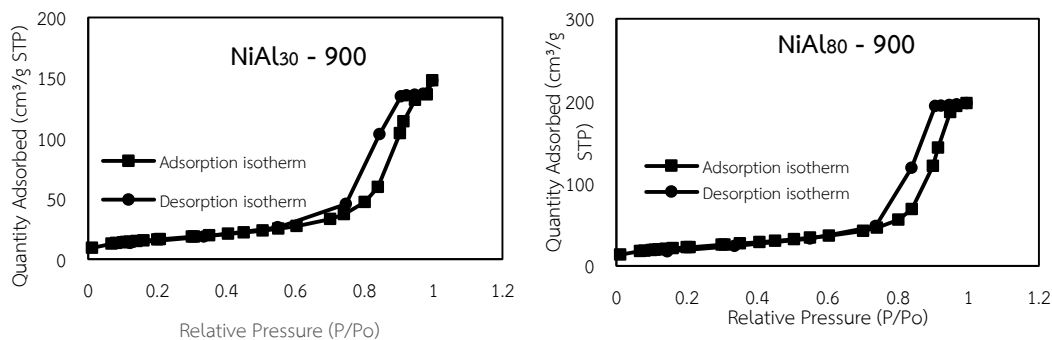


Figure 5.1 Adsorption-Desorption Isotherm of all NiO/NiAl₂O₄ – spinel based catalysts

The results of surface area, pore volume and average pore size diameter are summarized in Table 5.1. For the catalysts prepared by precipitation at temperature 30°C, the NiAl₃₀ – 500 had the higher BET surface area (190.2 m²/g) than NiAl₃₀-700 (138.8 m²/g). The lowest surface area 58.7 m²/g was found for NiAl₃₀ – 900. In the same way, the total pore volume had slightly decreased from 0.27 to 0.23 cm³/g with increasing calcination temperature from 500 to 900°C. In contrast, the average pore diameter decreased with increasing calcination temperature in the order to NiAl₃₀ – 900 (9.7 nm) > NiAl₃₀ – 700 (4.8 nm) > NiAl₃₀ – 500 (4.4 nm). In addition, the catalysts prepared at precipitation temperature 80°C revealed the similar trend of surface area and total pore volume to the catalysts that precipitated at 30°C. From Table 5.1, the NiAl₈₀ – 500 had the highest surface area 161.4 m²/g subordinated to NiAl₈₀ – 700 with the surface area 118.4 m²/g and the lowest surface area 80.6 was NiAl₈₀ – 900. The total pore volume of NiAl₈₀ – 500, NiAl₈₀ – 700 and NiAl₈₀ – 900 were around 0.31-0.32 cm³/g that described the similarity when the calcination temperature increased. On the other hand, the average pore diameter increased with increasing calcination temperature in the order of NiAl₈₀ – 500 (4.8 nm) < NiAl₈₀ – 700 (6.5 nm) < NiAl₈₀ – 900 (10.8 nm)

For the NiAl₈₀ – 1200 catalyst the BET surface area dramatically decreased to 2.33 m²/g due to the migration of nanoparticles with very low total pore volume. The catalyst exhibited a similar pore diameter to NiAl₃₀ – 500 catalyst.

The surface area of 36.5Ni/Al₂O₃ catalyst was similar to NiO/NiAl₂O₄ calcined around 700°C but the total pore volume decreased to 0.14 because of pore blocking from impregnated Ni particles on the commercial Al₂O₃.

However, both precipitation and calcination temperatures affected BET surface area as seen in Table 5.1. The surface area decreased as a result of higher crystallinity of spinel and/or the particle size increased from sintering and nucleation after calcined at high temperature. The total pore volume slightly decreased when the calcination temperature increased probably due to pore blocking of spinels after calcination. In addition, the average pore diameter increased with increasing preparation and calcination temperatures [62, 63]. However, the larger total pore volume and the bigger average pore diameter were revealed towards higher calcination temperature that phenomena related to benefit gas molecules diffusing into the holes [56].

Table 5.1. The BET surface area, total pore volume and average pore size diameter of all NiO/NiAl₂O₄ – spinel based catalysts

Catalyst	BET surface area (m ² /g)	Total pore volume (cm ³ /g)	Avg pore diameter (nm)
NiAl ₃₀ – 500	190.2	0.27	4.4
NiAl ₃₀ – 700	138.8	0.26	4.8
NiAl ₃₀ – 900	58.7	0.23	9.7
NiAl ₈₀ – 500	161.4	0.31	4.8
NiAl ₈₀ – 700	118.4	0.32	6.5
NiAl ₈₀ – 900	80.6	0.31	10.8
NiAl ₈₀ – 1200	2.3	0.0024	4.2
20Ni/Al ₂ O ₃	91.9	0.0937	4.1
36.5Ni/Al ₂ O ₃	124.9	0.14	4.4

5.1.2 X-ray diffraction (XRD)

The XRD patterns of NiO/NiAl₂O₄ catalysts are shown in Figure 5.2. The crystalline phases were identified using JCPDS files. The patterns of NiO/NiAl₂O₄ precipitated at 30 and 80°C with calcination temperature 500°C and 700°C (NiAl₃₀ – 500, NiAl₈₀ – 500, NiAl₃₀ – 700 and NiAl₈₀ – 700) were similar. The nickel oxide phase were observed (NiO, JCPDS 89-7131) at 2 θ degrees 37.5°, 43.5° and 63.1°. There a partial transformation of nickel aluminate phase but this results were not clearly seen because there were the overlapping of NiO and NiAl₂O₄ at 2 θ degrees 37.5° and very small shoulder at 45.3°, 65.8° and 71.3° [13, 61, 64, 65]. It is well known that under high calcination temperature, there are sufficient energy of nickel ion to overcome the surface of alumina and integrate into the alumina lattice to form spinel structure [64]. Interestingly, the corresponding patterns of NiO/NiAl₂O₄ calcined at highly temperature at 900°C (NiAl₃₀ – 900 and NiAl₈₀ – 900) were clearly observed which the high intensity of nickel aluminate phase (NiAl₂O₄, JCPDS 78-1601) at 2 θ degrees 31.7°, 45.3°, 65.8° and 71.3°. For NiO/NiAl₂O₄ calcined at very high temperature 1200°C, the width of nickel aluminate peaks decreased indicating the increase in both crystallinity and crystallite size but the presence of NiO phase was still observed [66].

The crystallite size of NiO/NiAl₂O₄ – spinels catalysts are shown in Table 5.2. For the NiO/NiAl₂O₄ prepared by precipitated at 30°C, the crystallite size of NiO increased from 7.4 to 8.4 nm and the crystallite size of NiAl₂O₄ also increased from 4.8 to 7.4 nm. The revelation of increased calcination temperature from 500 to 900 °C slightly increased crystallite size. In the same way, the higher precipitation temperature at 80°C had some effect to increase the crystallite size for both of NiO and NiAl₂O₄ as there was a slightly increasing of NiO crystallite size from 6.6 to 8.8 nm towards high calcination temperature from 500 to 900°C and dramatically increased to 36.6 nm when calcined at 1200°C. There were similar trend of the increasing crystallite size of NiAl₂O₄ from 9.4 to 14.4 nm with higher calcination temperature and dramatically increased to 37.3 nm when calcined at 1200°C probably to migration of nanoparticles corresponding to low surface area as shown in the results of N₂ – physisorption and decreasing of peaks width resulting in more crystallinity. Also, the crystallinity of NiO/NiAl₂O₄ – spinels catalysts prepared at higher calcination temperature was higher than lower calcination temperature [62, 66].

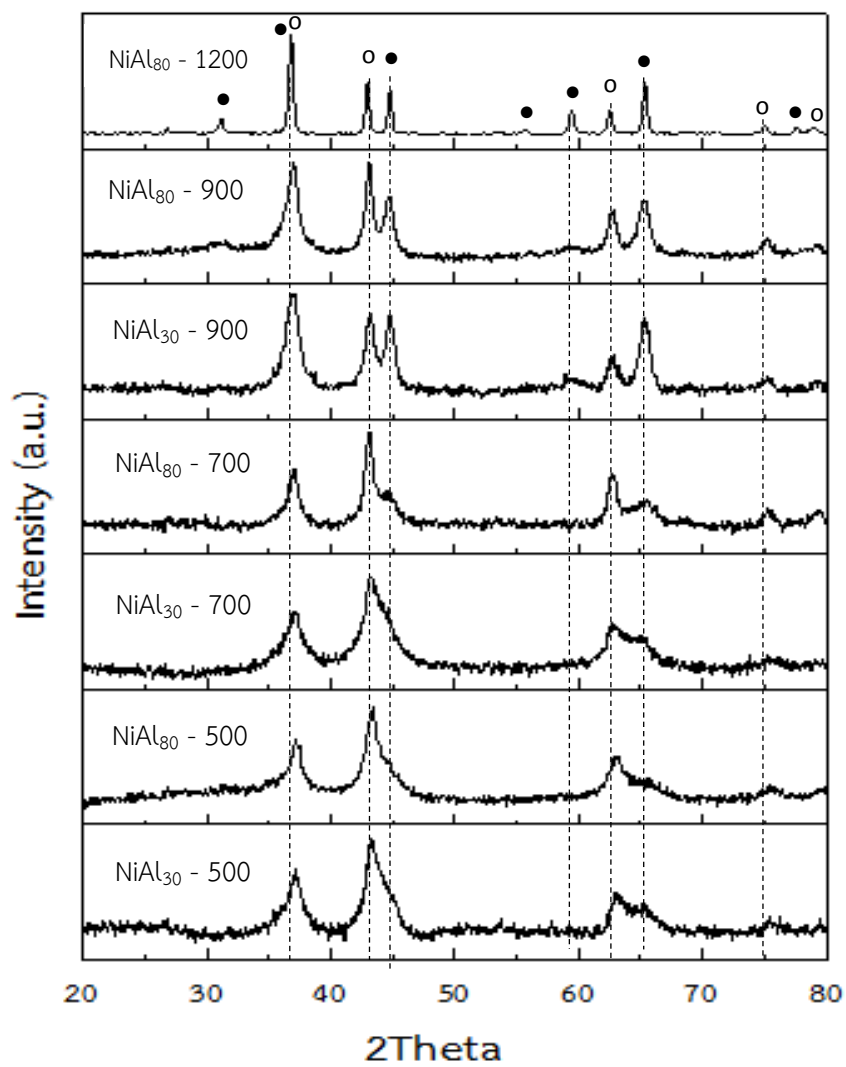


Figure 5.2 The XRD patterns of fresh NiO/NiAl₂O₄ spinel – based catalysts;

• NiAl₂O₄; ○ NiO

Table 5.2 The average crystallite size and phase amount of NiO/NiAl₂O₄- spinel based catalysts

Catalyst	Average crystallite size of fresh catalyst (nm) ^a		Phase amount (Wt %) ^b		NiO:NiAl ₂ O ₄ Weight ratio
	NiO	NiAl ₂ O ₄	NiO	NiAl ₂ O ₄	
NiAl ₃₀ – 500	7.4	4.8	81.4	18.6	4.4
NiAl ₃₀ – 700	8.2	5.5	70.1	29.9	2.4
NiAl ₃₀ – 900	8.9	7.4	26.5	73.5	0.4
NiAl ₈₀ – 500	6.6	9.4	78.8	21.3	3.7
NiAl ₈₀ – 700	7.3	11.3	55.9	44.1	1.3
NiAl ₈₀ – 900	8.8	14.2	24.7	75.3	0.3
NiAl ₈₀ – 1200	36.6	37.3	18.3	81.7	0.2

^a Calculated by using Shcerrer equation

^b Determine by Rietveld quantitative phase analysis in Material Analysis Using Diffraction (Maud) programmed.

From Table 5.2. The quantitative phase analysis by Rietveld method into Material Analysis Using Diffraction program were ascribed [66-69]. The calcination temperature affected to amount of NiO and NiAl₂O₄ phases in both of precipitation temperatures (30 and 80°C). NiO/NiAl₂O₄ catalysts calcined at 500°C and precipitated at 30°C had the highest quantitative of 81.4wt% NiO and lowest 18.6wt% NiAl₂O₄ compared with all the catalysts calcined at higher temperature (700, 900 and 1200°C), that resulting to highest NiO:NiAl₂O₄ weight ratio 4.4. In contrast, the increasing of calcination temperature at 1200°C of NiO/NiAl₂O₄ decreased the quantitative of

18.3wt% NiO while NiAl_2O_4 phase became highest at 81.7 wt%. However, the increasing of both precipitation and calcination temperatures affected to decrease the quantitative of NiO and improved the quantitative of NiAl_2O_4 phase formation that corresponding to NiO: NiAl_2O_4 weight ratio.

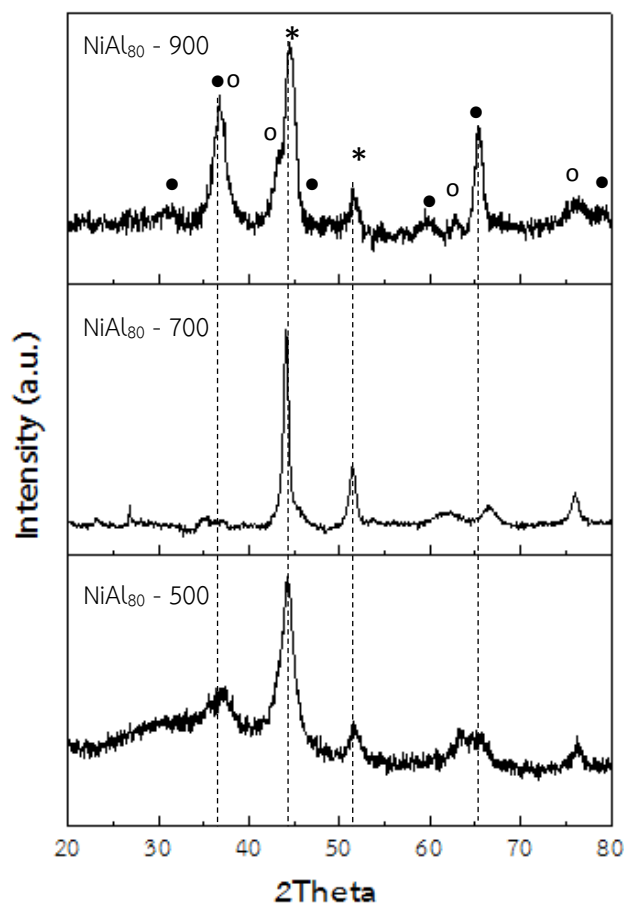



Figure 5.3 The XRD patterns spent NiO/ NiAl_2O_4 spinel – based catalysts;

• NiAl_2O_4 ; ○ NiO ; * Ni metallic

Figure 5.3 showed the XRD patterns of spent of NiO/ NiAl_2O_4 spinel- based catalysts. The merging of NiO and NiAl_2O_4 peaks at 2θ degrees 37° , $43\text{-}45^\circ$ and $62\text{-}67^\circ$ were observed in the pattern of $\text{NiAl}_{80} - 500$ catalyst while the Ni metallic at 2θ degrees 52° was clearly observed. In the same way, the $\text{NiAl}_{80} - 700$ catalyst exhibited the major peaks of Ni metallic (JCPDS 89-7128) at 2θ degrees 44.6° , 52° and 76.5° [13] while the combination of NiO and NiAl_2O_4 peaks were still observed at 2θ degrees around 37° , $61\text{-}65^\circ$ with a small shoulder peak around 45° with low intensity. In

contrast, the NiAl_2O_4 peaks were still clearly observed on $\text{NiAl}_{80} - 900$ at 2θ degrees 31.7° , 37.5° , 60.2° and 65.8° except the peak at 2θ degrees 45.3° shows the small shoulder peak due to the combination peak with Ni metallic at 2θ degrees 44.6° and clearly Ni metallic at 2θ degrees 52° with low intensity. Moreover, the shoulder peak of NiO still was presented at 2θ degrees 37.5° (overlapping to NiAl_2O_4) and 43.5° (combined with Ni metallic peak).

Table 5.3 The average crystallite size of spent $\text{NiO}/\text{NiAl}_2\text{O}_4$ - spinel based catalysts



Catalyst	Average crystallite size of spent catalyst (nm) ^a		
	NiO	Ni methallic	NiAl_2O_4
$\text{NiAl}_{80} - 500$	7.3	6.1	17.8
$\text{NiAl}_{80} - 700$	15.3	14.9	7.3
$\text{NiAl}_{80} - 900$	6.1	6.7	10.4

^a calculated by using Shcerrer equation.

However, there were difficultly defining species due to the combination and overlapping of peaks species so the calculation of crystallite size were investigated by using the Gaussian deconvolution [13, 50]. Table 5.3 shows the average crystallite size of spent $\text{NiO}/\text{NiAl}_2\text{O}_4$ - spinel based catalysts. The increasing of crystallite size of NiO were observed on $\text{NiAl}_{80} - 500$ and $\text{NiAl}_{80} - 700$ spent catalyst which may be due to migration of NiO particles while the $\text{NiAl}_{80} - 500$ catalyst ascribed the largest crystallite size of NiAl_2O_4 compared with spinel catalysts calcined at 700 and 900°C . On the other hand, the $\text{NiAl}_{80} - 900$ spent catalyst revealed the decreasing of crystallite size of NiO and NiAl_2O_4 to 6.1 and 10.4 nm, respectively. The $\text{NiAl}_{80} - 500$ and $\text{NiAl}_{80} - 900$ catalysts revealed the similar crystallite size of Ni metallic around 6.1 and 6.7 nm, respectively probably the formation of NiAl_2O_4 corresponded to limitation of mobility

on the surface of support and resistance sintering [70], which was in good agreement with Paternina Berrocal et al. [65]. They suggested that the formation of large Ni crystallite was inhibited during reduction of the nickel aluminate phase. Also, crystallite size of Ni metallic for NiAl₈₀ – 700 catalyst was increased to 14.9 nm maybe due to the agglomeration or sintering after reaction test, corresponding to the broad peak of the combination of NiO and NiAl₂O₄ peaks as seen in the XRD results.

In addition, the XRD patterns of fresh and spent Ni/Al₂O₃ catalysts are shown in Figure 5.4a and 5.4b. For both of 36.5Ni/Al₂O₃ and 20Ni/Al₂O₃ NiO and γ – Al₂O₃ phases was evidently observed with high intensity and sharp of peaks. The NiO phase of 36.5Ni/Al₂O₃ catalyst were observed at 2θ degrees 37.5°, 43.5°, 63.1° and 71.3° (JCPDS 89-7131) while γ – Al₂O₃ phase were observed at 2θ degrees 31.6°, 37.8° and 67.1° (JCPDS 79-1558) and the remaining peak were not clearly observed at 2θ degrees 45.7° and 62°. In contrast, the small shoulder peak of γ – Al₂O₃ were observed on the 20Ni/Al₂O₃ catalyst at 2θ degrees 45.7° and 62°. After reaction test, Ni metallic phase were exhibited on both 36.5Ni/Al₂O₃ and 20Ni/Al₂O₃ catalysts at at 2θ degrees 44.6°, 52° and 76.5° (JCPDs 89-7128). The NiO peak were evidently disappeared on 36.5Ni/Al₂O₃ catalyst while it was still observed small shoulder peak on 20Ni/Al₂O₃ catalyst.

The crystallite size of fresh and spent Ni/Al₂O₃ catalysts are shown in Table 5.3. The 20Ni/Al₂O₃ catalyst had larger crystallite size of both NiO and γ – Al₂O₃ (23.41 and 16.24, respectively) than 36.5Ni/Al₂O₃. The 36.5Ni/Al₂O₃ had the crystallite size of NiO and γ – Al₂O₃ around 16.2 and 13.8 nm, respectively that corresponded to the sharper peak as seen in the XRD pattern. For spent catalysts, crystallite size of NiO decreased because of the reduction of NiO to Ni metallic. The 20Ni/Al₂O₃ catalyst revealed the larger the crystallite size of γ – Al₂O₃ than fresh catalyst to 20.5 nm. Nevertheless, the crystallite of γ – Al₂O₃ for 36.5Ni/Al₂O₃ catalyst cannot be calculated due to the very sharp peak.

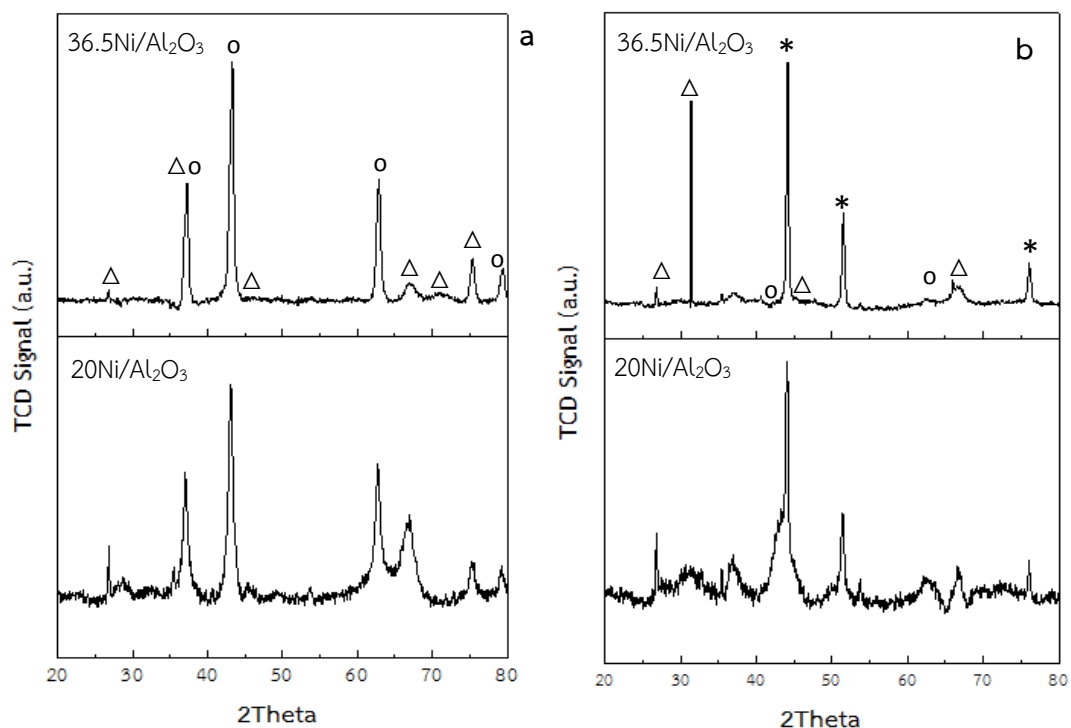


Figure 5.4 The XRD patterns of (a) fresh Ni/Al₂O₃ catalysts (b) spent Ni/Al₂O₃ catalysts;

Δ γ -Al₂O₃; o NiO ; * Ni metallic

Table 5.4 The average crystallite size of fresh and spent Ni/Al₂O₃ catalysts

Catalyst	Average crystallite size of fresh catalyst (nm) ^a		Average crystallite size of spent catalyst (nm) ^a		
	NiO	γ -Al ₂ O ₃	NiO	Ni metallic	γ -Al ₂ O ₃
20Ni/Al ₂ O ₃	23.41	16.24	8.76	5.88	20.45
36.5Ni/Al ₂ O ₃	16.22	13.84	N/D	8.67	N/D

^a calculated by using Shcerrer equation.

5.1.3 Temperature programmed reduction (H_2 - TPR)

The reducibility of nickel species and the metal-support interaction were investigated proceeding H_2 - TPR experiment as shown in Figure 5.6a and 5.6b. In principle, the reducible NiO species are usually divided into three types: α , β and γ . The peak located low temperature (300-550°C) was assigned to α - type NiO species, which were free nickel oxides having a weak interaction with support. The medium temperature (550-700°C) expected to β - type NiO species with stronger interaction with alumina than α - type and finally, the high temperature (>700°C) related to γ - type NiO species which the stable nickel aluminate phase with spinel structure were ascribed [13, 50, 65].

Figure 5.5 shows the reduction profiles of the NiO/ Al_2O_3 catalysts series and bulk NiO commercial. For bulk NiO commercial, clearly two distinct reduction peak were noted at 206 and 373°C. The types of reducible nickel species of all catalysts were applied by Gaussian-type.

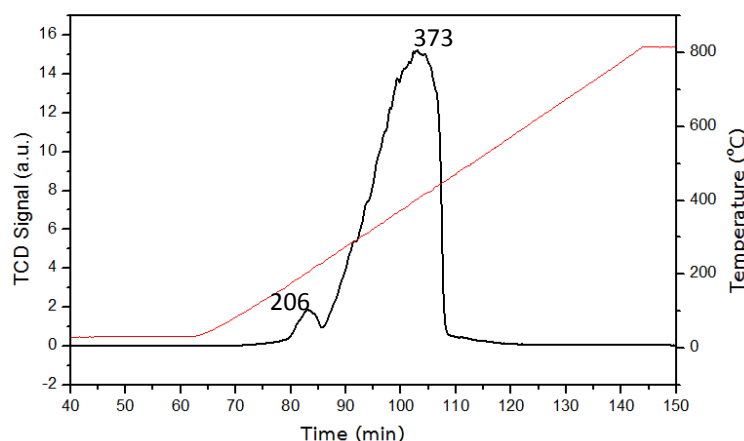


Figure 5.5 The H_2 - TPR profile of NiO commercial catalysts plot against time

For the NiO/ $NiAl_2O_4$ catalysts precipitated at 30°C and calcined under various calcination temperature (500, 700 and 900), there were three reduction peaks that related to presence of three types of NiO species. In the case of NiO/ $NiAl_2O_4$ calcined at 500°C ($NiAl_{30}$ - 500), it exhibited initial reduction temperature at 511, 581 and 699°C which were lower than NiO/ $NiAl_2O_4$ calcined at higher temperatures. Consequently, NiO/ $NiAl_2O_4$ with calcination temperature at 700°C ($NiAl_{30}$ - 700), the initial reduction peaks were shifted toward higher temperature in order to 528, 586 and 740°C. In the

same way, the initial reduction peaks of NiO/NiAl₂O₄ calcined at 900 (NiAl₃₀ – 900) were shifted toward higher temperature in order of 580, 707 and 814°C, respectively.

Contrastingly, the increasing of precipitation to 80°C of NiO/NiAl₂O₄ with various calcination temperatures (500, 700, 900 and 1200°C), the similar trends of three reduction peaks were observed except for the NiO/NiAl₂O₄ calcined 1200°C that had two reduction peaks. The NiO/NiAl₂O₄ calcined at 500°C (NiAl₈₀ – 500) had initial reduction temperature peak at 496°C and the second and third peaks were exhibited at 563 and 680°C, respectively. The increasing of calcination temperature to 700°C, the reduction peaks were shifted toward higher temperature position in order to 572, 617 and 765°C. Interestingly, NiO/NiAl₂O₄ calcined at 900°C (NiAl₈₀ – 900) had initial reduction temperature at 426°C that lower than NiAl₈₀ – 500 (496°C) and NiAl₈₀ – 700 (572°C) probably due to lower NiO/support interaction so the NiO can be reduced more easily [62]. Finally, NiO/NiAl₂O₄ calcined at 1200°C (NiAl₈₀ – 1200), broad peak around 573 to 729°C were observed with very low intensity. The increasing of reduction temperature peak was due to very strongly interaction of NiO into nickel aluminate spinel structure and their dramatically larger crystallite sizes probably makes the reduction process more difficult [10].

By comparing of precipitation temperature, the spinel catalysts precipitated at higher temperature (80°C) (except calcined 700), the reducing of NiO species started earlier probably due to different rates of NiO formation compared to the catalysts prepared at low temperature (30°C) during calcination. Also, the presence of NiO particles interacted considerable with spinel phase and only small amount of NiO maybe more easily for reduction process [10, 71] as suggested by Yolanda C. et al. [10]. They reported the comparing of NiAl₂O₄ spinel with differential precipitation temperatures (25°C and 75°C) and observed that spinel precipitated at 25°C shows initial reducing earlier at low temperature probably because the NiO favor proceed with the different precipitation rate of the nickel aluminum hydroxide at 25°C.

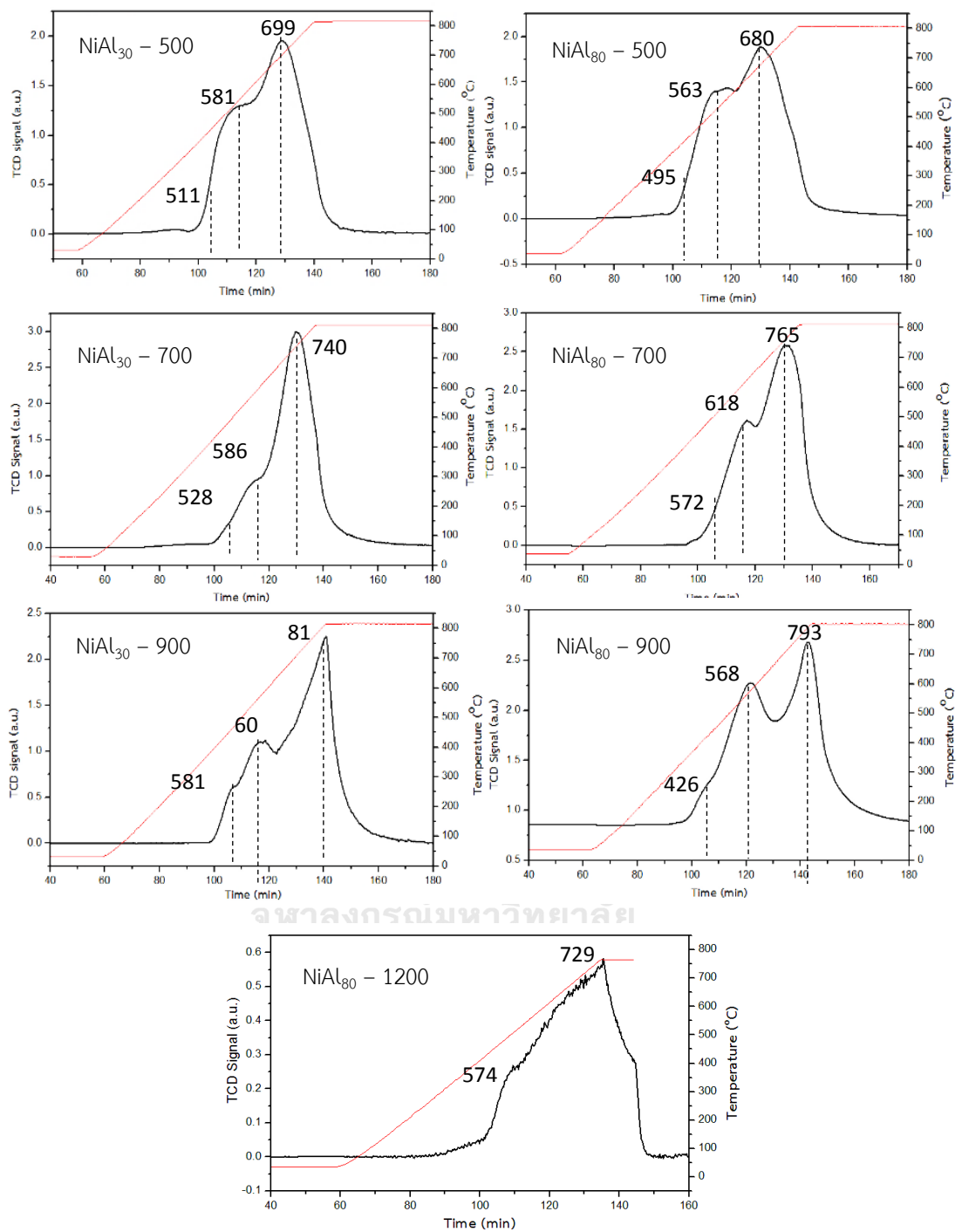


Figure 5.6 The H₂ – TPR profile of NiO/NiAl₂O₄ – spinel catalysts plot against time

Moreover, the calcination temperature had a significant effect to the residual amount of NiO from nickel interacted with alumina proceeding to nickel aluminate phase formation including to different crystallite size of particles. The increasing of calcination temperature related to more crystallite size and showed higher value of initial reduction temperature so the larger crystallite size can be more difficult to reduce [10, 72] except NiO/NiAl₂O₄ calcined at 900 and 1200°C, their peaks shifts to lower temperature probably lower content of NiO (as shown by XRD and quantitative phase analysis) and lower NiO/support interaction since they were more crystalline and can be reduced more easily [62, 65]. In addition, the serious aggregation resulting to the larger particle size that can be attributed to the weak interaction between the impregnated Ni species and the support [70].

In case of lower calcination temperature, the catalysts exhibited higher surface area and smaller particle size. Free NiO usually result in stronger interaction bonded to the support and is normally reduced at higher temperatures than large particles with poor metal-support interaction [70, 73, 74]

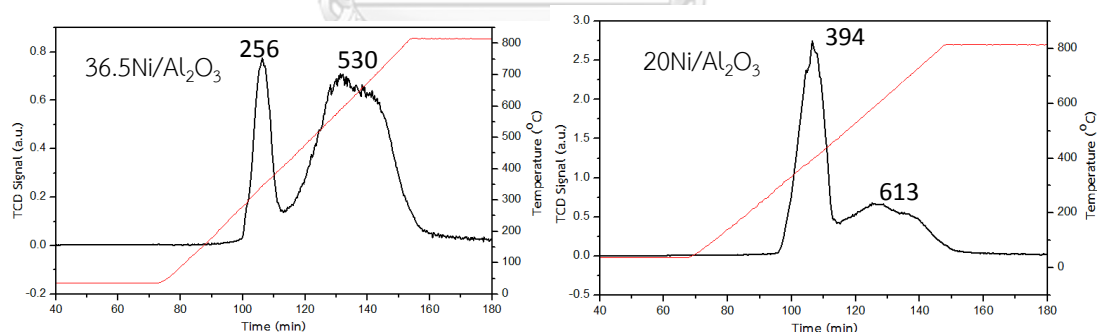


Figure 5.7 The H₂ – TPR profile of 36.5Ni/Al₂O₃ and 20Ni/Al₂O₃ catalysts plot against time

Figure 5.7 shows the reduction profile of 36.5 wt% and 20 wt% of Ni loading on Al₂O₃ commercial support. The 20NiO/Al₂O₃ catalyst exhibited clearly two distinct reduction peaks at 394 and 613°C without the strong interaction of NiO into NiAl₂O₄ spinel phase. Lower reduction temperature were observed on 36.5NiO/Al₂O₃ catalyst which revealed two distinct peaks at 256 and 530°C. There were no observed γ -type

NiO at high temperature or the peak of spinel phase interaction. The reduction peak were shifted to lower temperature with higher Ni loading. Highly dispersed NiO exhibited a stronger interaction with the support, while the lower reduction temperature can be related to larger NiO particles having interactions of lower strength with the support. In addition, the increasing of Ni content ascribed to the decreasing metal – support interaction so the interaction of Ni species with alumina support became weaker at higher Ni content [52, 75].

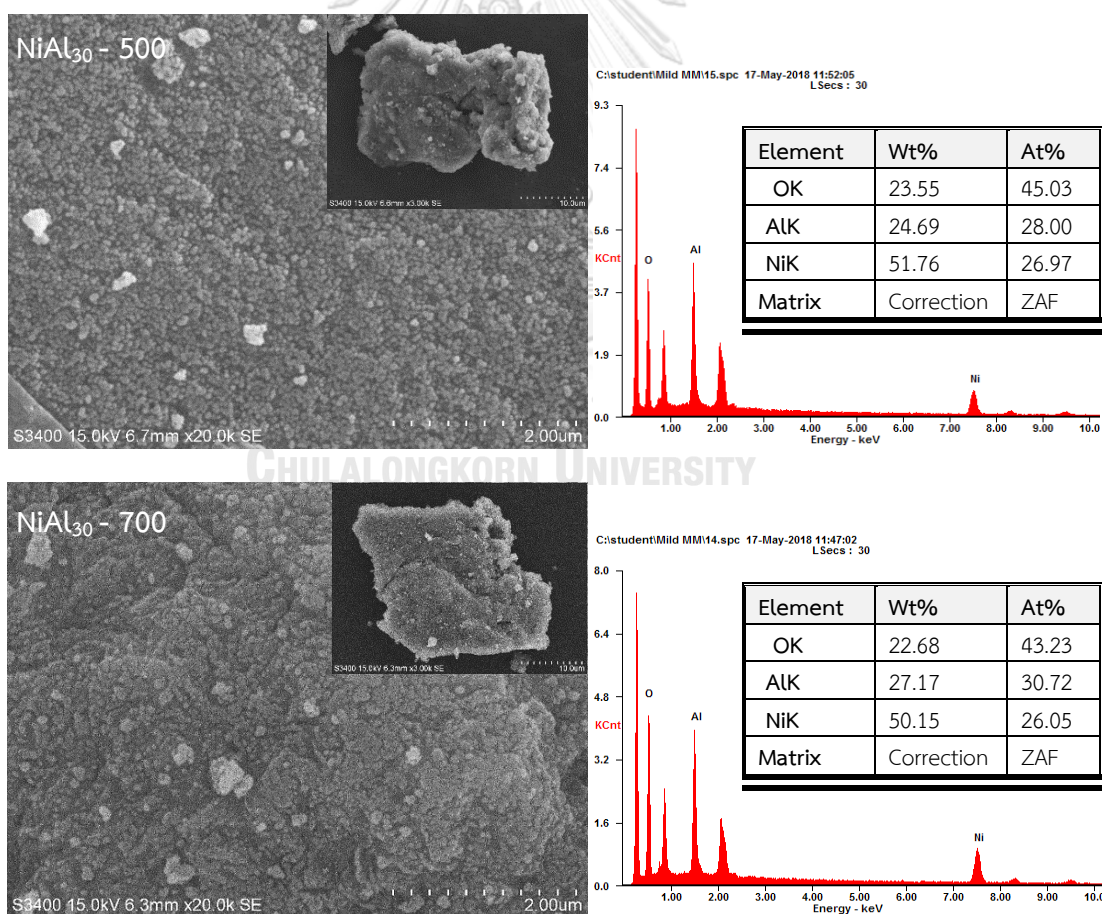
Table 5.5 The summary of H₂ – TPR results

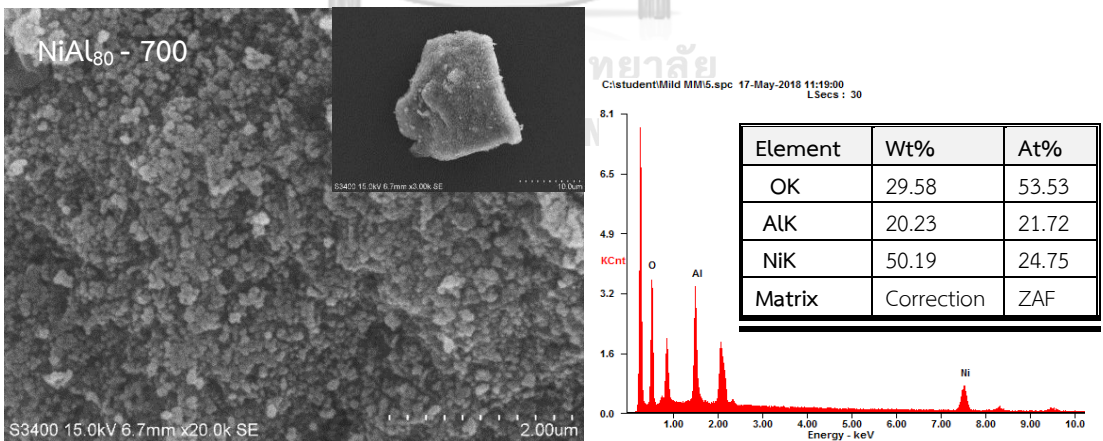
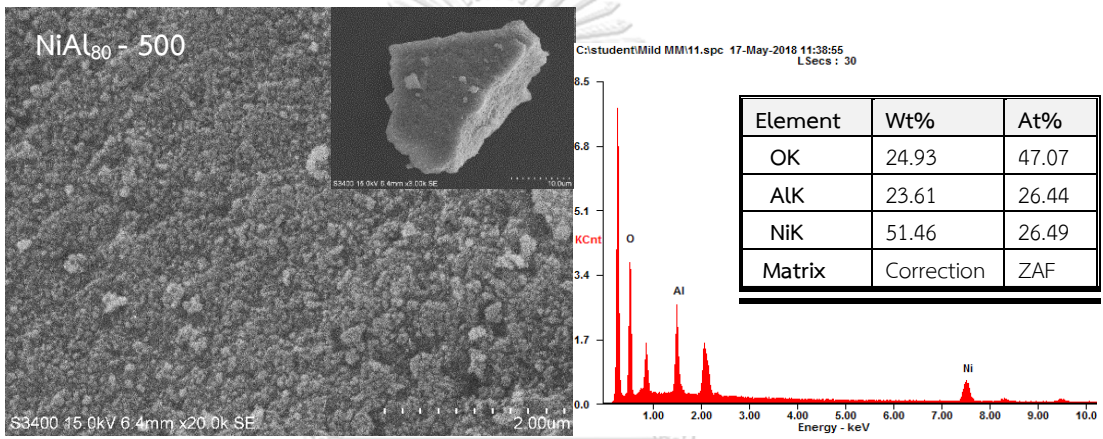
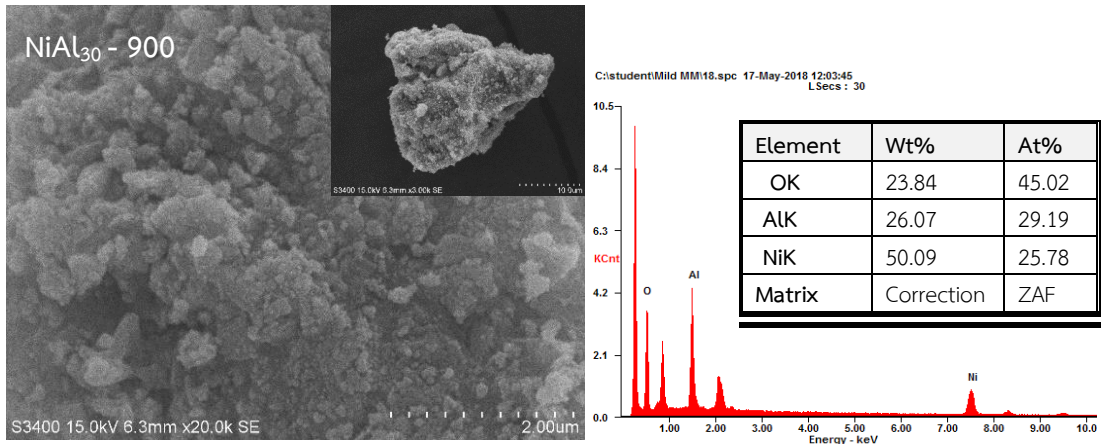
Catalyst	Peak position temperature (°C)		
	α – type NiO species	β – type NiO species	γ – type NiO species
NiAl ₃₀ – 500	511	581	699
NiAl ₃₀ – 700	528	586	740
NiAl ₃₀ – 900	581	600	814
NiAl ₈₀ – 500	496	563	680
NiAl ₈₀ – 700	572	618	765
NiAl ₈₀ – 900	426	568	793
NiAl ₈₀ – 1200	-	574	729
20Ni/Al ₂ O ₃	394	613	-
36.5Ni/Al ₂ O ₃	256	530	-

5.1.5 Scanning Electron Microscopy (SEM)

The surface morphology of NiO/NiAl₂O₄ – spinel based catalysts were investigated by scanning electron microscopy and are shown in Figure 5.8. For NiO/NiAl₂O₄ calcined at 500°C the higher dispersion was observed with smaller particle size and lower crystallite size corresponded to the XRD results. In addition, the lower surface area were observed on the catalysts which calcined at higher temperature due to nucleation of metallic particles and/or clustering of the nanoparticles including to more crystallite size.

The presence of Ni, Al and O was confirmed by means of energy dispersive X-ray analysis (EDX). The EDX spectrum revealed Ni, Al and O peaks.





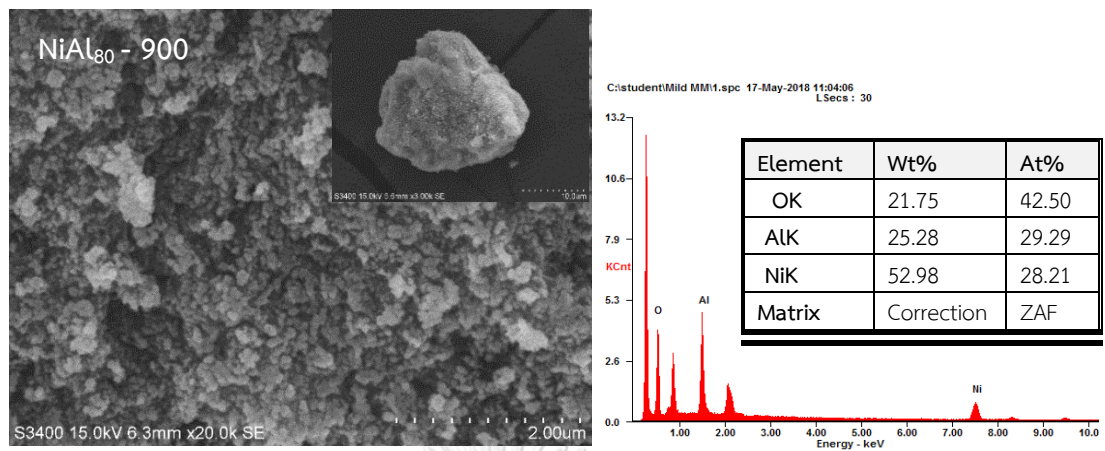
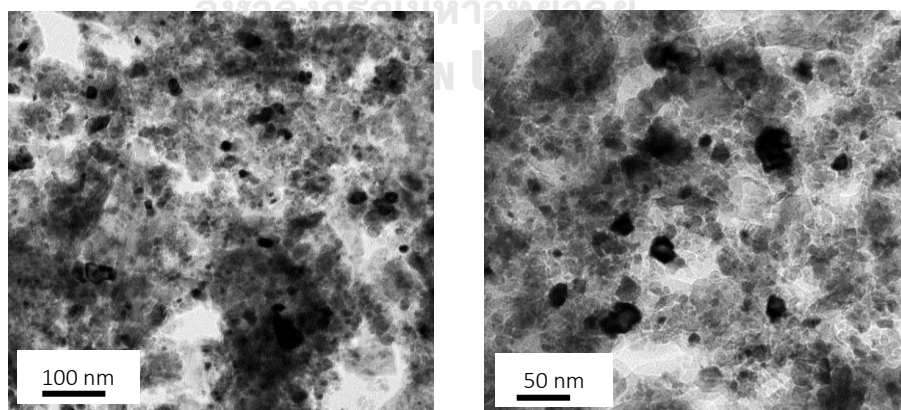


Figure 5.8 The SEM images of NiO/NiAl₂O₄ spinel – based catalysts

5.1.6 Transmission Electron Microscopy (TEM)

The morphology of catalyst were investigated by using transmission electron microscopy (TEM). The TEM images of fresh NiAl₈₀ – 900 catalyst were displayed in Figure 5.9a. The irregular shape were observed and the average particle size was 7.5 nm. The spent NiAl₈₀ – 900 catalyst had the average particle size are smaller than fresh catalyst (3.2 nm) as seen in Figure 5.9b.



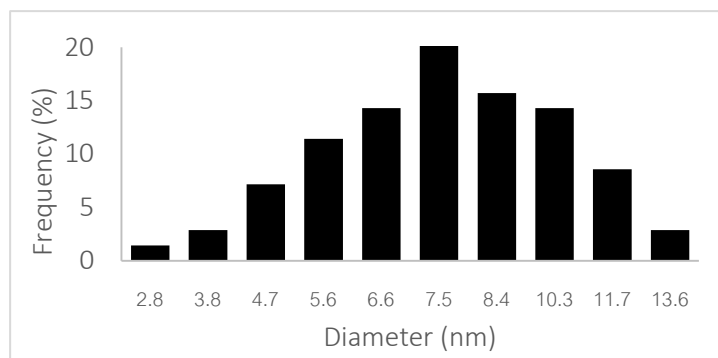


Figure 5.9a. The TEM images of fresh NiAl₈₀ – 900 catalyst

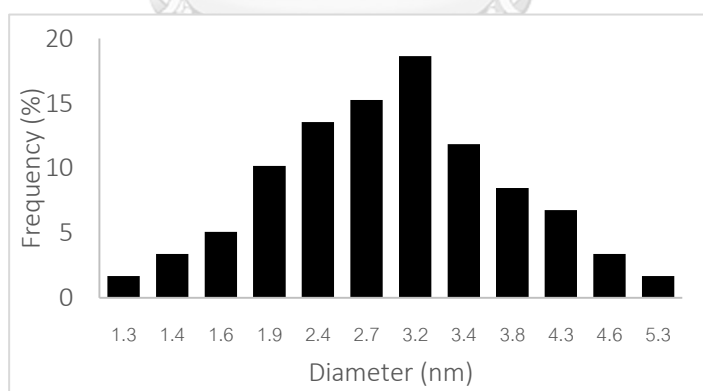
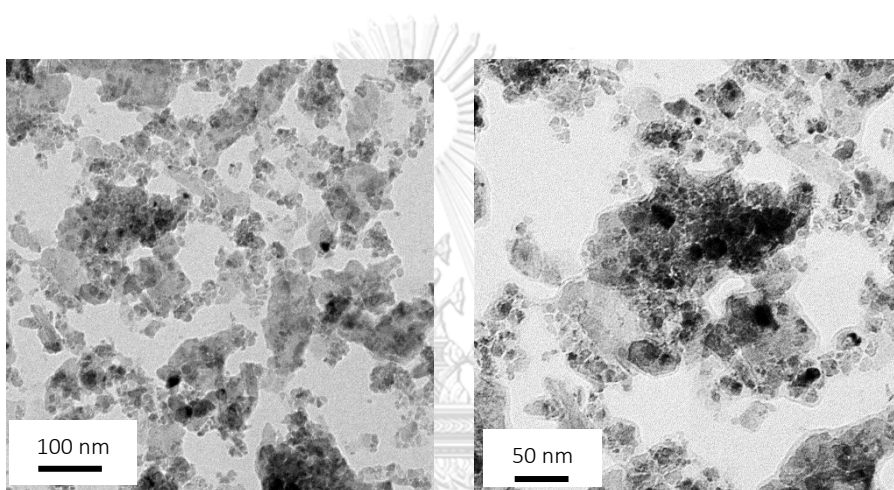


Figure 5.9b. The TEM images of spent NiAl₈₀ – 900 catalyst

The TEM images of the Ni/Al₂O₃ commercial catalysts with 20 and 36.5 %wt Ni loading are shown in Figure 5.10a, 5.10b, 5.11a and 5.11b, showing the metal distribution on the commercial Al₂O₃ supports. For the spent catalyst, sintering or agglomeration of metal particles with relatively larger size were observed.

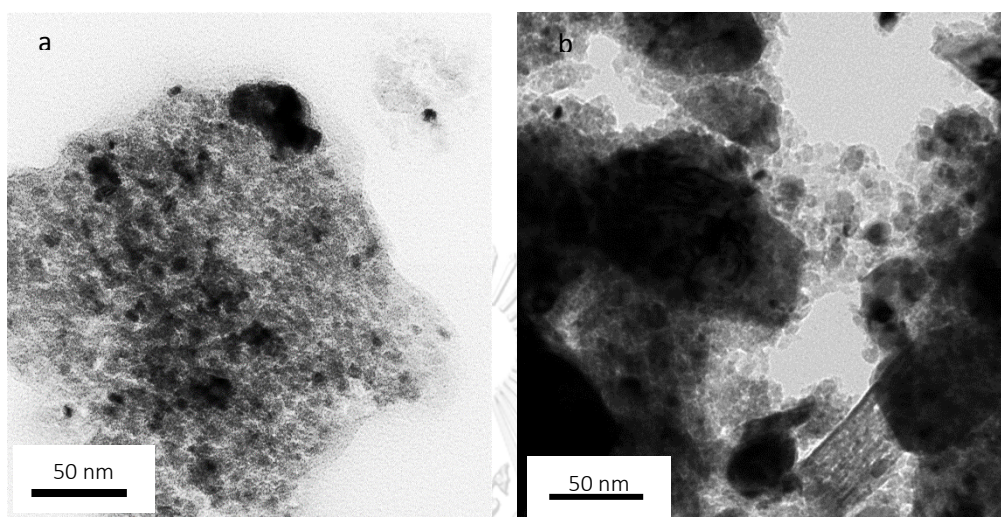


Figure 5.10 (a) The TEM image of fresh 20Ni/Al₂O₃ catalyst (b) The TEM image of spent 20Ni/Al₂O₃ catalyst.

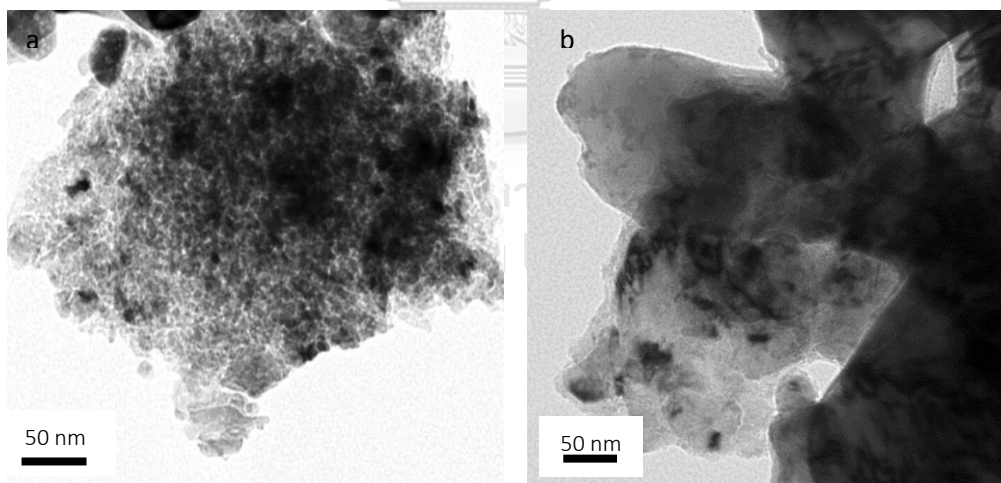


Figure 5.11 (a) The TEM image of fresh 36.5Ni/Al₂O₃ catalyst (b) The TEM image of spent 36.5Ni/Al₂O₃ catalyst.

5.2. Catalytic activity of NiO/NiAl₂O₄ catalysts

The catalytic activity tests for CO₂ methanation were carried out at 350°C for 180 min (3 h). The catalyst performances in terms of CO₂ conversion, CH₄ yield and CO yield are shown in Fig. 5.12. All the catalysts showed high stability during the 3 h time on stream and the outlet product showed no CO formation except NiAl₃₀ – 500, NiAl₈₀ – 1200 and 20Ni/Al₂O₃ catalysts. The NiAl₈₀ – 900 catalyst exhibited the highest CO₂ conversion among of the catalysts studied at 92% and 100% methane selectivity without CO formation. For the NiAl₈₀ – 900 catalyst also showed slightly lower conversion of CO₂ than the NiAl₃₀ – 900 catalyst at 88% conversion. Interestingly, The CO₂ conversion of NiAl₃₀ – 500 (82%), NiAl₈₀ – 500 (82.5%), NiAl₃₀ – 700 (81.9%), and NiAl₈₀ – 700 (81%) were essentially similar at around 82% conversion but only NiAl₃₀ – 500 catalysts exhibited a slight of CO formation in 20 min after that the CO formation was disappeared. The NiAl₈₀ – 1200 catalyst showed the highest stability but the lowest conversion among all the catalysts studied at 23 % conversion with CO yield that slightly decreased during reaction operated.

By comparing the series of NiO/NiAl₂O₄ catalysts with the Ni/Al₂O₃ catalysts prepared by impregnation method with similar amount of Ni loading (36.5wt %) and another one with 20% Ni loading. The conversion of impregnated catalysts were lower than all the precipitated NiO/NiAl₂O₄ catalysts and only 20Ni/Al₂O₃ catalyst revealed the CO formation during 180 min operated. The 36.5Ni/Al₂O₃ catalyst exhibited 75% CO₂ conversion with 100% methane selectivity. For lower Ni content, 20Ni/Al₂O₃ catalyst showed conversion of CO₂ at 68 % conversion with less CO yield around 1.3 % after reaction test for 180 min. The observation of CO formation on Ni/Al₂O₃ were intermediate during CO₂ methanation proceeded. The CO species were dissociated into carbon and oxygen species that proceed hydrogenated to form CH₄ and water. The dissociation of CO was reported to be the rate determining step on CO₂ methanation via the formation of CO intermediate [76] [77].

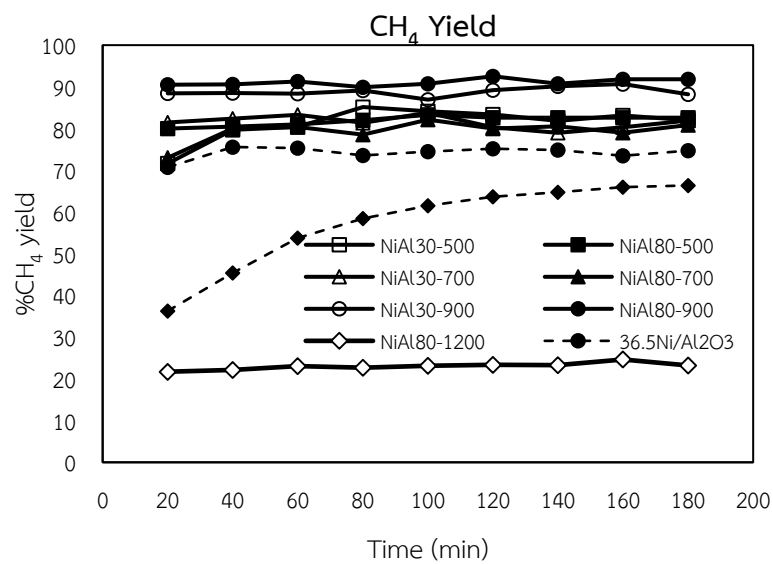
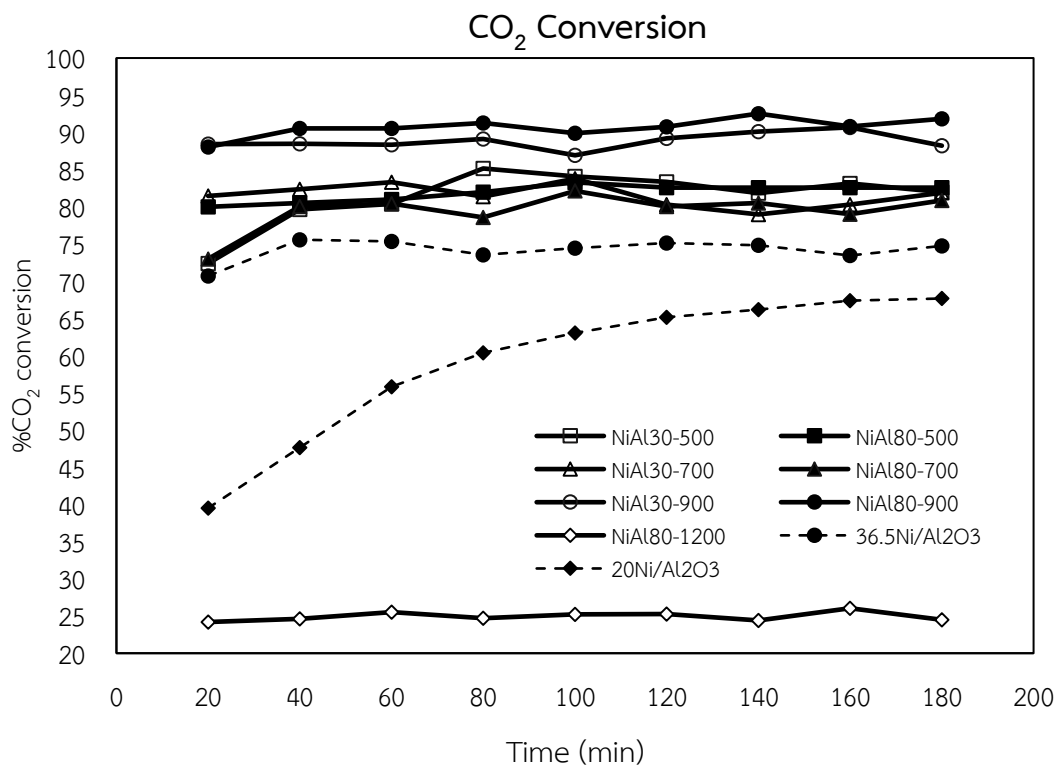
In general, CO₂ was dissociated over the catalyst support into carbon species (CO_{ads}) and oxygen species (O_{ads}), the H₂ was activated on the Ni surface to form the H_{ads} species and finally reacted with CO_{ads} to generate CH₄ over the Ni surface [78]. The ability of H₂ activation would decrease as a result of thermal agglomeration of metallic Ni active so the selectivity of CH₄ would decreased due to lack of the H_{ads}

source. The previous work reported that 20wt% of Ni showed the highest activity and selectivity including stable performance during 10h of reaction but the conversion of CO_2 had decreased with increasing of Ni loading resulting in bigger crystallite size and lower surface area [52]. In this work, 36.5Ni/ Al_2O_3 catalysts showed higher conversion and selectivity without CO as byproduct probably due to the 36.5Ni/ Al_2O_3 can be reduced more easily at lower temperature as shown in the H_2 – TPR results.

The best catalytic performance were obtained on the NiAl₈₀ – 900 catalyst probably due to the lowest reduction temperature from H_2 – TPR results compared to all of spinel catalysts that can make the reduction more easily so that NiO was completely reduced to metallic Ni under reduction temperature conditions (450°C for 2.3h) before operated. The higher reduction rate of catalyst can improve the higher selectivity toward methane and higher activity [79]. Furthermore, the larger crystallite size of the bulk NiAl₂O₄ also showed high activity in the steam reforming of methane reaction that reported by Sahli. L et al.[61]

Although, the low surface area but the large total pore volume could provide sufficient exposed metallic active sites for reactants which accounted for its much higher catalytic [80].

In addition, the formation of NiAl₂O₄ in optimal ratio with NiO form (24.67wt% NiO and 75.33%wt based on 36.5%wtNi loading) on the NiAl₈₀ – 900 catalyst showed the positive effect to conversion, selectivity, and stability. The presence of NiAl₂O₄ could probably exert a positive effect on Ni sintering. The particle size of Ni metal can changed to smaller size after reduced in pure H_2 at high temperature and resulted in high disposition on the NiAl₂O₄ support[6, 61]. In the CO_2 reforming of methane, an enhancement of CO_2 conversion and CH_4 yield over NiAl₂O₄ was attributed to the presence of spinel structure that was active and highly stable, high dispersion of NiO on the spinel, and the interaction of nickel metal and the support [71]. Moreover, in the hydrogenation of acetylene over Ni/NiAl₂O₄ catalyst, the formation of NiAl₂O₄ can provide a stabilizing effect resulting in the inhibition of metal aggregation and lowering coking rate formation[13]. Furthermore, the formation of NiAl₂O₄ can improve of coke resistance, and enhance stability of catalyst for dry reforming of methane reaction [64]. In the present work, the presence of both NiO and NiAl₂O₄ led to high activity in CO_2 methanation due probably to the formation of active substoichiometric spinel structure and high dispersion of Ni on NiAl₂O₄ upon reduction.



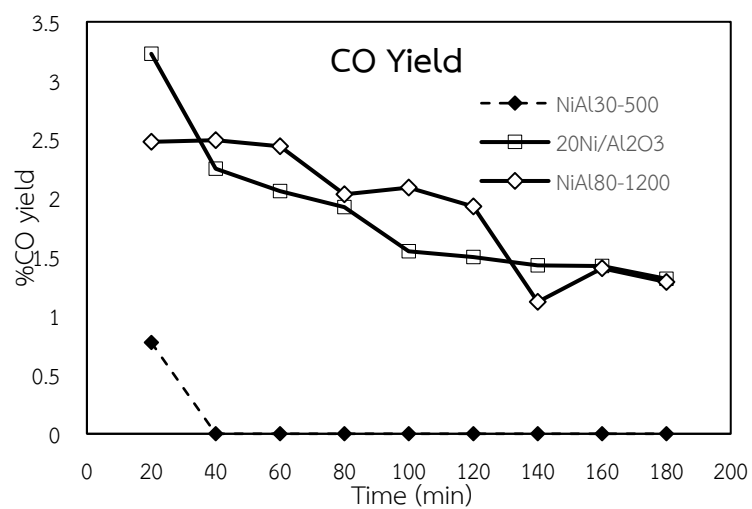


Figure 5.12 The activity of NiO/NiAl₂O₄-spinel based catalysts during CO₂ methanation reaction under atmospheric (1 atm) at 350°C for 180 min



Part II : The effect of noble metal loading on the NiO/NiAl₂O₄ spinel catalyst during CO₂ methanation

5.3 Characterization of metal-NiO/NiAl₂O₄ spinel catalysts

5.3.1 N₂ - physisorption (BET)

The adsorption-desorption isotherm of the metal doped onto NiO/NiAl₂O₄ spinel catalysts are shown in Figure 5.13. The type IV isotherms were exhibited indicated mesoporous (2-50 nm) with significantly reduced hysteresis loops for all catalysts. Also the doping of metal had no effect on the catalyst pore structure.

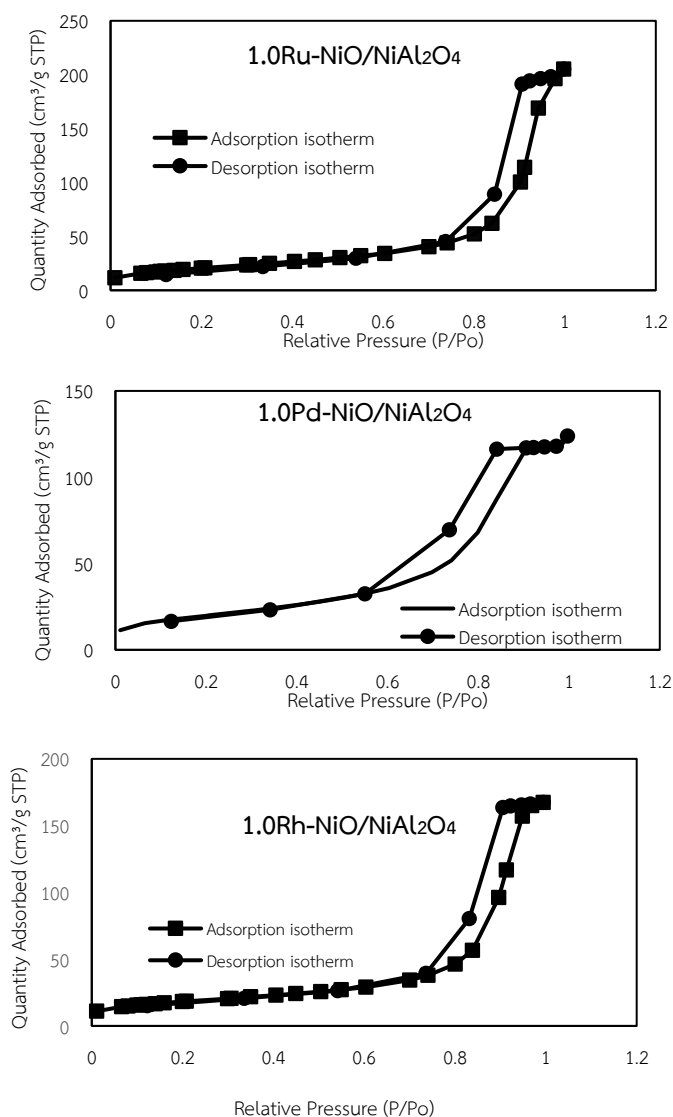


Figure 5.13 Adsorption-Desorption Isotherm of metal doped (Ru,Pd and Rh) into NiO/NiAl₂O₄ – spinel based catalysts

The results of surface area, pore volume and average pore size diameter summarized in Table 5.6. The BET surface area of unpromoted NiAl₈₀ – 900 catalyst decreased by adding noble metal in the order 1.0Ru-NiO/NiAl₂O₄ (75 m²/g) > 1.0Pd-NiO/NiAl₂O₄ (71.5 m²/g) > 1.0Rh-NiO/NiAl₂O₄ (65.4 m²/g) because of pore blocking and/or agglutinated of metal into NiO/NiAl₂O₄. In addition, doping of Pd and/or Rh into NiO/NiAl₂O₄ catalysts had significant decreased to 0.19 and 0.26 cm³/g, respectively. Interestingly, the total pore volume slightly increased to 0.32 cm³/g by doping Ru metal. Moreover, the average pore diameter increased with Ru and Pd dopants to 12.3 and 11.4 nm, respectively. Opposite result was found for 1.0Rh-NiO/NiAl₂O₄ in which average pore diameter decreased to 6.7 nm.

Table 5.6 The BET surface area, total pore volume and average pore size diameter of metal doped onto NiO/NiAl₂O₄ – spinel based catalysts

Catalyst	BET surface area (m ² /g)	Total pore volume (cm ³ /g)	Avg pore diameter (nm)
NiAl ₈₀ – 900	80.5	0.31	10.8
1.0Ru-NiO/NiAl ₂ O ₄	75.0	0.32	12.3
1.0Pd-NiO/NiAl ₂ O ₄	71.5	0.19	11.4
1.0Rh-NiO/NiAl ₂ O ₄	65.4	0.26	6.7

5.2.2 X-ray diffraction (XRD)

The XRD patterns of metal doping (Ru, Rh and Pd) on NiAl₈₀ – 900 catalysts are shown in Figure 5.11a. The 1.0Ru-NiO/NiAl₈₀ – 900 catalyst exhibited three phases corresponding to NiO, NiAl₂O₄. The Ru metal dopant had no significant to gradate the XRD pattern of NiO and NiAl₂O₄ peaks. Also, the major XRD peaks of RuO₂ were not observed at 2θ degree 28.1°, 35.1°, 40.8° and 54.5° (PDF 70-2662) [81-83]. On the same way, the peak for rhodium oxide in RhO₂ and/or Rh₂O₃ phases from the XRD pattern of 1.0Rh-NiO/NiAl₈₀ – 900 were not detected probably to very small crystallite size less than 5 nm that the XRD cannot detect.

The XRD pattern of reduced catalysts at high temperature (450°C) are shown in Figure 5.14b. For 1.0Ru-NiO/NiAl₈₀ - 900 and 1.0Rh-NiO/NiAl₈₀ - 900 catalysts, there was the disappearance of NiO phased while presence of metallic Ni peaks at 2θ degree 44.6° , 52° and 76.5° (JCODS 89-7128) that evidenced completely reduced NiO into metallic Ni [13] and no observed the peak of Ru metallic may be the crystallite size decreased to less than 5 nm that XRD cannot detected. On the other hand, there was no clearly metallic Ni peak observed on 1.0Pd-NiO/NiAl₈₀ - 900 and NiO phase still presence. Similar, results of the XRD patterns of NiAl₈₀ - 900 catalyst were obtained. There were no clearly observation metallic Ni phase but the intensity of major NiO peak at 2θ degree 37° had decreased.

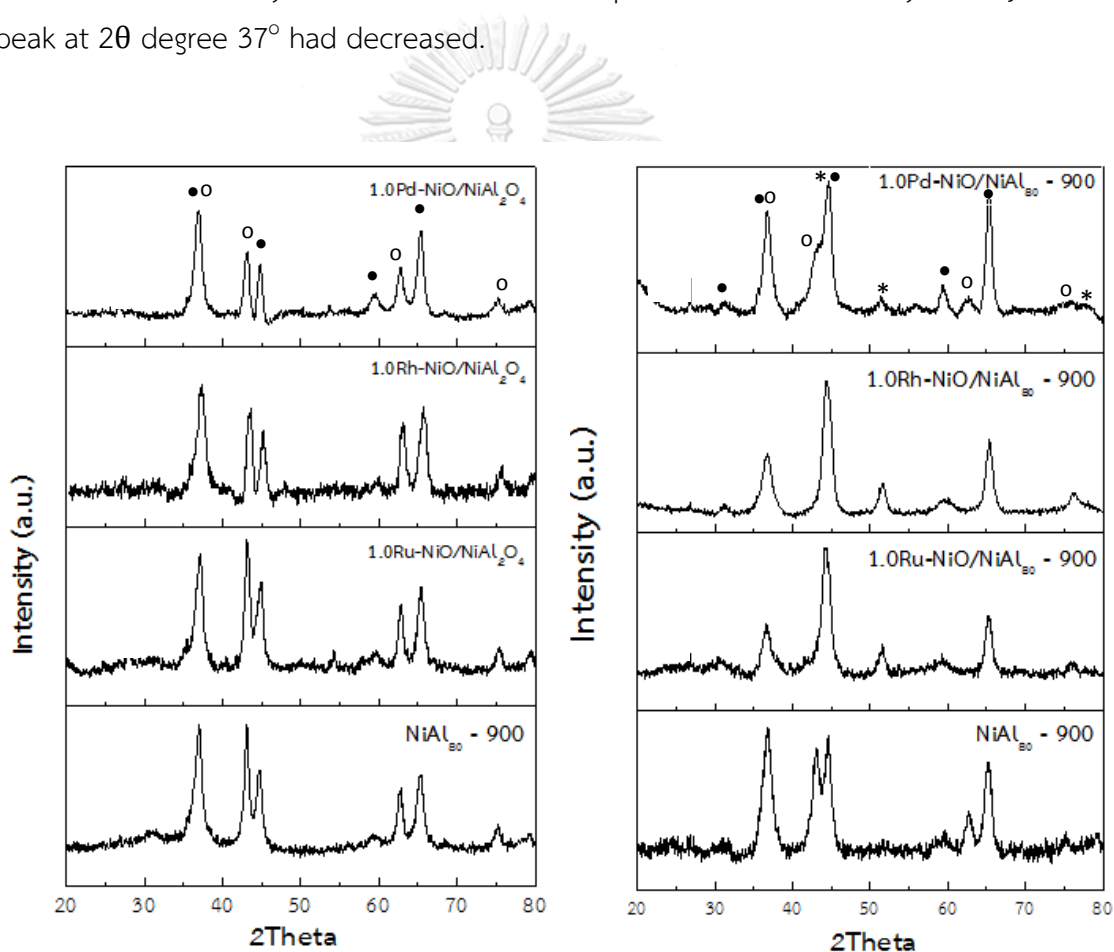


Figure 5.14. The XRD patterns of (a) fresh metal doping (Ru,Rh,Pd) on NiAl₈₀ - 900 catalysts and (b) reduced metal doping (Ru,Rh,Pd) on NiAl₈₀ - 900 catalysts ;

• NiAl₂O₄; ○ NiO; * Ni⁰

The calculated crystallite size of Ni species are shown in Table 5.7. After doping Ru onto NiAl₈₀ – 900 the crystallite size of both NiO and NiAl₂O₄ were slightly decreased to 8.2 and 11.5 nm, respectively. In the same way, Rh metal dopant related to decrease the crystallite size of NiO and NiAl₂O₄ to 7.6 and 9.6 nm, respectively. Moreover, Pd metal dopant showed similar trend to decrease the crystallite size of NiO and NiAl₂O₄ to 8.3 and 9.1 nm, respectively.

Table 5.7 The average crystallite size and phase amount of metal doping (Ru,Rh,Pd) on NiAl₈₀ – 900 catalysts

Catalyst	Average crystallite size (nm) ^a		
	Nobel metal oxide form	NiO	NiAl ₂ O ₄
NiAl ₈₀ – 900	-	8.8	14.2
1.0Ru-NiO/NiAl ₂ O ₄	N/D	8.2	11.5
1.0Rh-NiO/NiAl ₂ O ₄	N/D	7.6	9.6
1.0Pd-NiO/NiAl ₂ O ₄	N/D	8.3	9.1

^a calculated by using Shcerrer equation.

5.2.3 Temperature programed reduction (H₂-TPR)

The reduction profiles of metal doping onto NiAl₈₀ – 900 catalysts are shown in Figure 5.15. The reduction temperature in unpromoted NiO/NiAl₂O₄ calcined 900°C was significantly decreased by Ru and Rh addition except Pd addition. The 1.0Ru-NiO/NiAl₈₀ – 900 catalyst had initial reduction temperature at 179°C corresponding the Ru species reduce to Ru oxide (RuO₂) in agreement with Masae K. et al [84], that reported the completely Ru oxide reduced below 200°C and the reduction of Ni species at 454°C. The higher reduction temperature at 775°C was attributed to the

reduction of nickel aluminate spinel [85]. For the 1.0Pd-NiO/NiAl₈₀ – 900 catalyst revealed two peaks of reduction at 421 that attributed to NiO reduction peak and NiAl₂O₄ spinel reduction peak at high temperature 745°C without palladium oxide reduction peak being observed. The 1.0Rh-NiO/NiAl₂O₄ catalyst exhibited the reduction peak at 246°C related to rhodium interact with nickel that higher than reduction peak of rhodium alone (exhibited around 112°C) [86]. The second peak of NiO reduction was exhibited at 436°C and the reduction peak of nickel aluminate spinel was evidenced at 781°C.

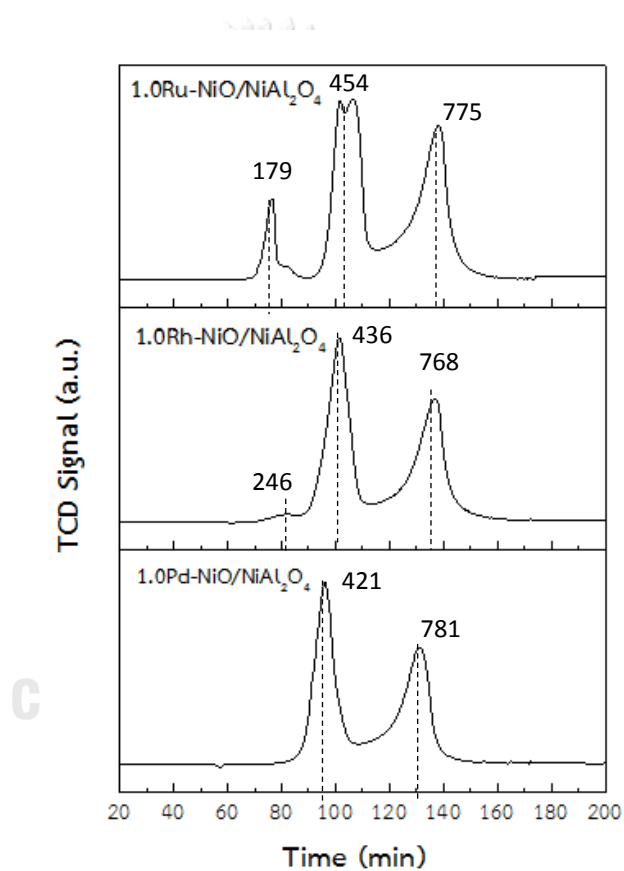
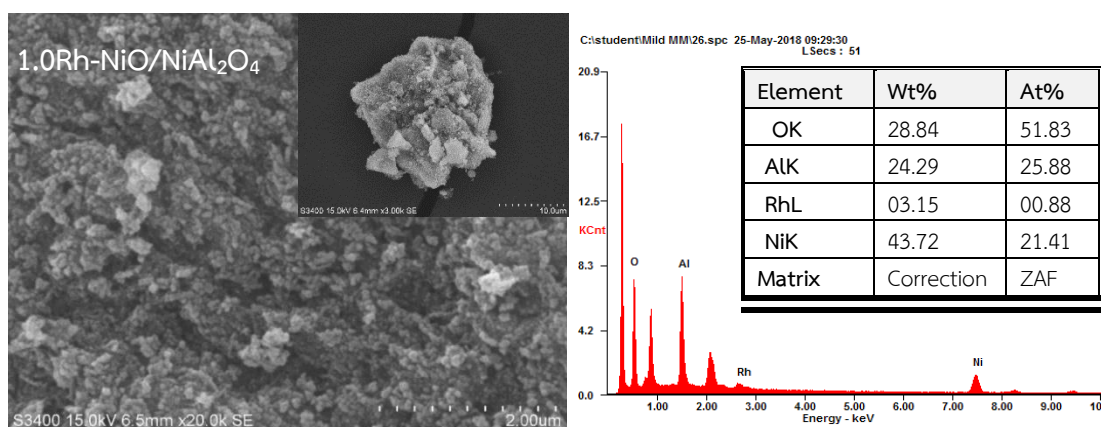
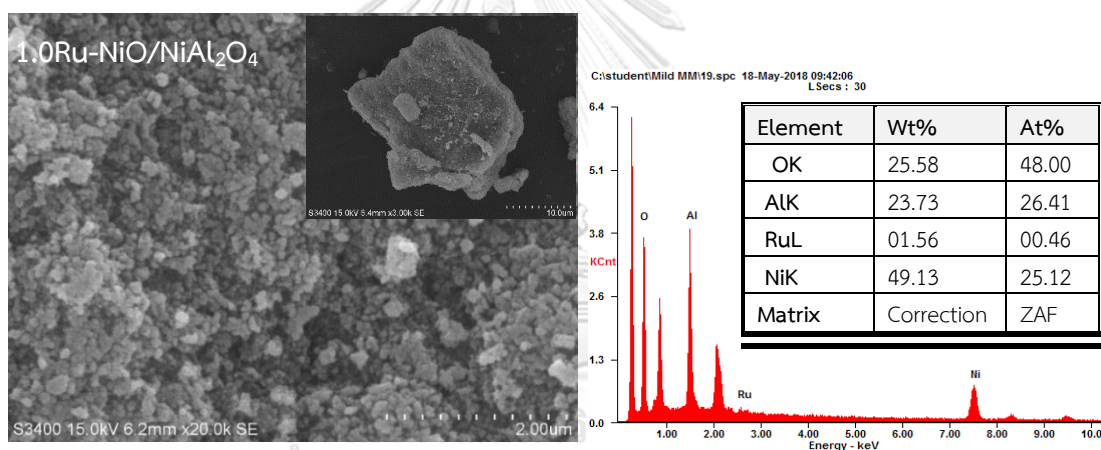


Figure 5.15 The H₂ – TPR profile of metal doping onto NiAl₈₀ – 900 catalysts plot against time

5.2.5 Scanning Electron Microscopy (SEM)

The surface morphology of metal doping on NiAl_{80} – 900 catalysts were investigated by scanning electron microscopy and are shown in Figure 5.16. For all the catalysts, the SEM – EDX results were similarly with the agglutination of nanoparticle cluster corresponding to decreasing of surface area which reported from N_2 – physisorption.

However, from XRD result the noble metal phase were not detected but the X-ray analysis (EDX) confirmed the presence of noble metal. Moreover, The EDX spectrum revealed Ru, Rh, Pd, Ni, Al and O peak, indicating the presence of Ru ,Rh and/or Pd supported on NiAl_2O_4 phase.



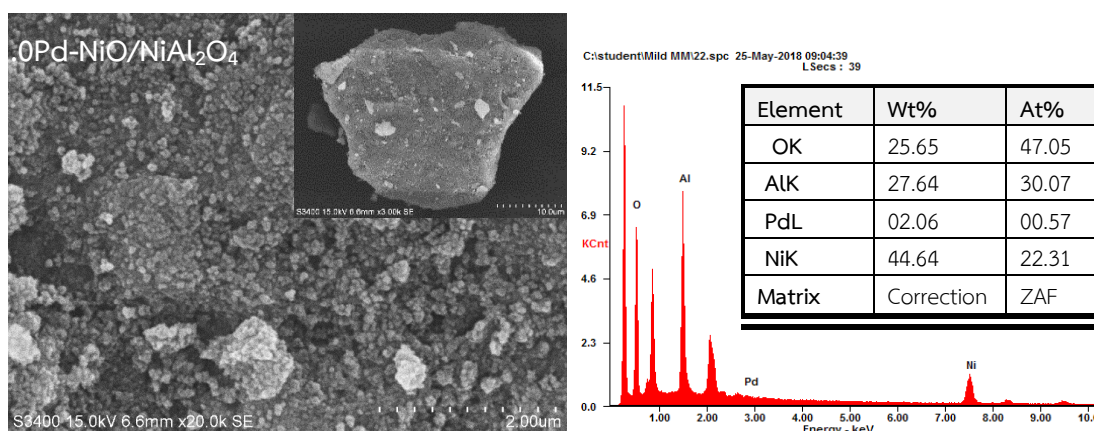


Figure 5.16 The SEM images of metal doping onto NiAl₈₀ – 900 catalysts

5.4. Catalytic activity of noble metal doping on NiO/NiAl₂O₄ catalysts

The catalytic activity tests for CO₂ methanation were carried out at 350°C for 180 min (3 h). The catalyst performances in terms of CO₂ conversion, CH₄ yield and CO yield are shown in Fig. 5.17. All metal doping catalysts exhibited 100% of methane selectivity corresponding to invisible CO formation during reaction test. The 1.0Ru-NiO/NiAl₈₀ – 900 catalyst showed the best stability and the highest conversion of CO₂ at 92% with 100% methane. The CO₂ conversion was closed to NiAl₈₀ – 900 catalyst activity. Meanwhile, the 1.0Rh-NiO/NiAl₂O₄ catalyst showed lower conversion of CO₂ at 49% conversion and finally the 1.0Pd-NiO/NiAl₂O₄ catalyst exhibited the lowest conversion at 11% among all the NiO/NiAl₂O₄ and Ni/Al₂O₃ series.

In addition, the activity had slightly decreased corresponding to presence of Rh and/or Pd promoter. For pure Pd/ γ -Al₂O₃, the CO_(ads) species are too strongly adsorbed, and the reaction is slow [33]. And the presence of NiO phase after reduction suggest an incomplete reduction of NiO to metallic active site, hence the lowest conversion of CO₂ was obtained.

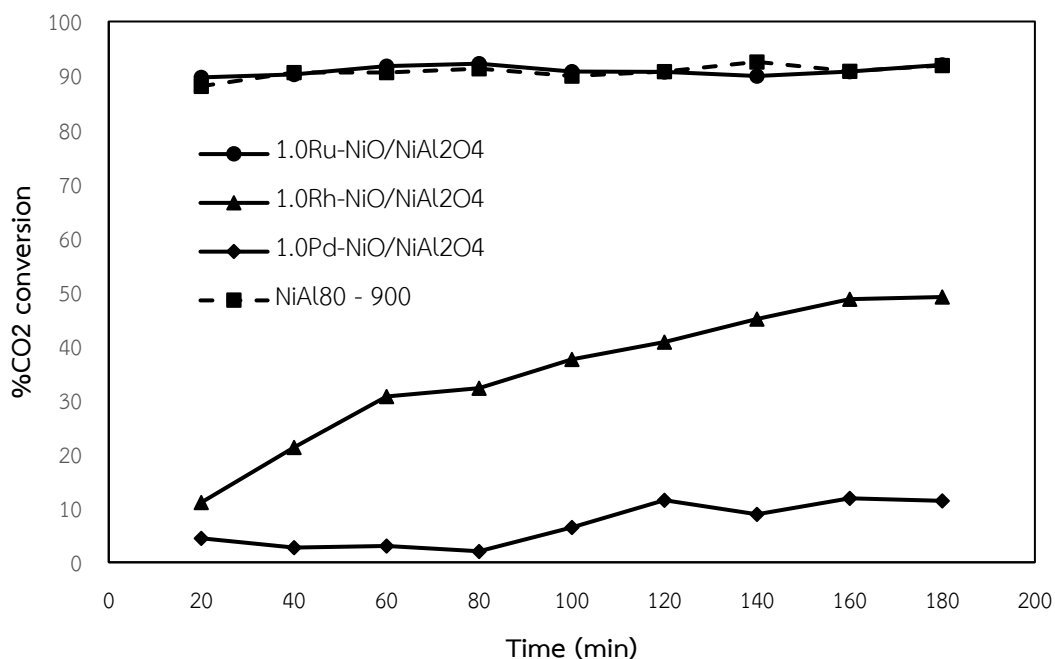


Figure 5.17 The activity of 1 wt% metal (Ru,Rh,Pd) doping into NiO/NiAl₂O₄-spinel based catalysts during CO₂ methanation reaction under atmospheric (1 atm) at 350°C for 180 min

However, the activities of 1.0Ru-NiO/NiAl₈₀-900 and NiAl₈₀-900 catalysts were similar during the reaction operated at 350°C. Nevertheless, the difference in activities testing for both of 1.0Ru-NiO/NiAl₈₀-900 and NiAl₈₀-900 catalysts were observed during the temperature profile reaction test from 250 to 350°C for each temperature kept for 1 h.

The 1.0Ru-NiO/NiAl₈₀-900 catalyst showed increased conversion of CO₂ from 19% at initial temperature 250°C to 43% and 74% at 275 and 300°C, respectively which exhibited higher performance than the NiAl₈₀-900 catalyst with 18% CO₂ conversion at 250°C and slightly increased to 19% at 275°C and dramatically increased to 63% at 300°C.

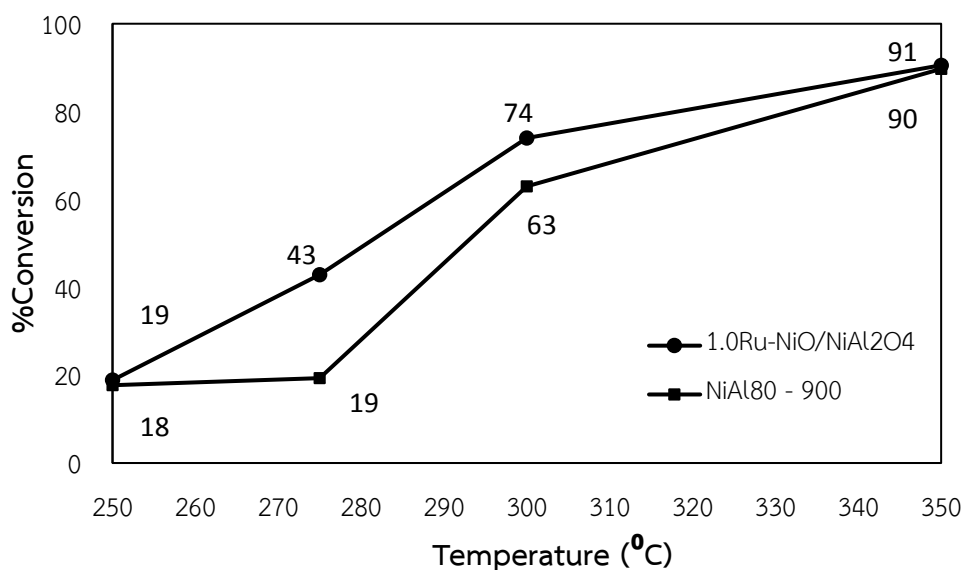


Figure 5.18 The activity of comparison of 1.0Ru-NiO/NiAl₂O₄ and NiAl₈₀ - 900 catalysts during CO₂ methanation reaction under atmospheric and temperature profile (250, 275 and 300°C) condition

In many previous works [6, 14, 20, 22], Ru metal was reported to be the most efficient catalyst for CO₂ methanation in terms of both conversion and selectivity. They showed the potentially a synergistic effect of the Ru containing with Ni as bimetallic catalyst that contributed to the high activity at lower temperatures. Thus, the results demonstrated that small amount of Ru can significantly improve the reaction rate at relatively low temperatures for Ni based catalysts as well as improved the selectivity of CH₄. The increase of the activity could be explained by the improved reducibility of Ni and the synergistic effect between Ni and Ru [87]. Furthermore, the adding of Ru decreased the crystallite size of Ni particles, resulting in higher dispersion including the enhanced reducibility by hydrogen spillover [55].

CHARTER VI

CONCLUSION

6.1 Conclusion

Among the various NiO/NiAl₂O₄ catalysts prepared by co-precipitation at different precipitation and calcination temperatures, the NiO/NiAl₂O₄ precipitated at 80°C and calcined at 900°C showed the best activity in CO₂ methanation at 350°C with CO₂ conversion 92% and 100% methane without CO formation. The optimal of NiO and NiAl₂O₄ phase composition at 24.7%wt and 75.3%wt, could provide a stabilizing effect resulting in the inhibition of metal aggregation and the lower reduction temperature of NiO to metallic Ni. In addition, the calcination at higher temperature led to larger total pore volume, which was good to provide sufficient exposed metallic active sites for reactants.

Doping metal (Ru, Rh and Pd) onto NiAl₈₀ – 900 catalysts resulted in lower surface area and less of pore volume except for 1.0Ru-NiO/NiAl₈₀ – 900 catalyst that retained similar physical properties as the unpromoted one.

Comparison to the unpromoted catalyst, the Ru promoted NiO/NiAl₈₀-900 exhibited higher activity at low temperature (250 - 300°C) due to a decrease of the crystallite size of Ni particles resulting in higher dispersion and the enhanced reducibility due to hydrogen spillover and the synergistic effect between Ni and Ru. For the Rh- and Pd- promoted ones, poorer catalytic performances were obtained.

6.2 Recommendations

6.2.1 The NiO/NiAl₂O₄ spinel – based catalyst should be modified for higher activity at lower temperature (below 300°C).

6.2.2 The effect of various ratios of Ni/Al for CO₂ methanation catalysts should be investigated.

REFERENCES

- [1] H. J. K. Sang Joon Choe, Su-Jin Kim, Sung-Bae Park, Dong Ho Park, and Do Sung Huh, "Adsorbed Carbon Formation and Carbon Hydrogenation for CO₂ Methanation on the Ni(111) Surface: ASED-MO Study," *Bull. Korean Chem. Soc.* 2005, vol. 26, 2005.
- [2] T. A. Le, M. S. Kim, S. H. Lee, T. W. Kim, and E. D. Park, "CO and CO₂ methanation over supported Ni catalysts," *Catalysis Today*, vol. 293-294, pp. 89-96, 2017.
- [3] M. A. A. Aziz, A. A. Jalil, S. Triwahyono, and A. Ahmad, "CO₂ methanation over heterogeneous catalysts: recent progress and future prospects," *Green Chemistry*, vol. 17, no. 5, pp. 2647-2663, 2015.
- [4] Q. Pan, J. Peng, S. Wang, and S. Wang, "In situ FTIR spectroscopic study of the CO₂ methanation mechanism on Ni/Ce_{0.5}Zr_{0.5}O₂," *Catal. Sci. Technol.*, vol. 4, no. 2, pp. 502-509, 2014.
- [5] R. Kadam and N. L. Panwar, "Recent advancement in biogas enrichment and its applications," *Renewable and Sustainable Energy Reviews*, vol. 73, pp. 892-903, 2017.
- [6] X. Su, J. Xu, B. Liang, H. Duan, B. Hou, and Y. Huang, "Catalytic carbon dioxide hydrogenation to methane: A review of recent studies," *Journal of Energy Chemistry*, vol. 25, no. 4, pp. 553-565, 2016.
- [7] P. Frontera, A. Macario, M. Ferraro, and P. Antonucci, "Supported Catalysts for CO₂ Methanation: A Review," *Catalysts*, vol. 7, no. 12, 2017.
- [8] W. Wei and G. Jinlong, "Methanation of carbon dioxide: an overview," *Frontiers of Chemical Science and Engineering*, vol. 5, no. 1, pp. 2-10, 2010.
- [9] Y. Zeng, H. Ma, H. Zhang, W. Ying, and D. Fang, "Highly efficient NiAl₂O₄-free Ni/γ-Al₂O₃ catalysts prepared by solution combustion method for CO methanation," *Fuel*, vol. 137, pp. 155-163, 2014.

- [10] P. S. Yolanda Cesteros, Francisco Medina, and J. s. E. Sueiras, "Preparation and Characterization of Several High-Area NiAl₂O₄ Spinel. Study of Their Reducibility," *Chem. Mater*, vol. 331-335, p. 12, 2000.
- [11] K. Zhao, Z. Li, and L. Bian, "CO₂ methanation and co-methanation of CO and CO₂ over Mn-promoted Ni/Al₂O₃ catalysts," *Frontiers of Chemical Science and Engineering*, vol. 10, no. 2, pp. 273-280, 2016.
- [12] M. Muraleedharan Nair and S. Kaliaguine, "Structured catalysts for dry reforming of methane," *New Journal of Chemistry*, vol. 40, no. 5, pp. 4049-4060, 2016.
- [13] C. Jiménez-González *et al.*, "Structural characterisation of Ni/alumina reforming catalysts activated at high temperatures," *Applied Catalysis A: General*, vol. 466, pp. 9-20, 2013.
- [14] G. Garbarino, D. Bellotti, P. Riani, L. Magistri, and G. Busca, "Methanation of carbon dioxide on Ru/Al₂O₃ and Ni/Al₂O₃ catalysts at atmospheric pressure: Catalysts activation, behaviour and stability," *International Journal of Hydrogen Energy*, vol. 40, no. 30, pp. 9171-9182, 2015.
- [15] M. Mihet and M. D. Lazar, "Methanation of CO₂ on Ni/γ-Al₂O₃: Influence of Pt, Pd or Rh promotion," *Catalysis Today*, 2016.
- [16] H. C. Wu, Y. C. Chang, J. H. Wu, J. H. Lin, I. K. Lin, and C. S. Chen, "Methanation of CO₂ and reverse water gas shift reactions on Ni/SiO₂ catalysts: the influence of particle size on selectivity and reaction pathway," *Catalysis Science & Technology*, vol. 5, no. 8, pp. 4154-4163, 2015.
- [17] R. D. a. A. R. Michel Marwood, "In-situ surface and gas phase analysis for kinetic studies under transient conditions The catalytic hydrogenation of CO₂," *Applied Catalysis A: General*, vol. 151 (1997) 223-246, 1997.
- [18] M. A. A. Aziz, A. A. Jalil, S. Triwahyono, and S. M. Sidik, "Methanation of carbon dioxide on metal-promoted mesostructured silica nanoparticles," *Applied Catalysis A: General*, vol. 486, pp. 115-122, 2014.

- [19] M. N. Shin-ichiro Fujita, Tosiaki Doi and Nobutsune and Takezawa, "Mechanisms of methanation of carbon dioxide and carbon monoxide over nickel/alumina catalysts," *Applied Catalysis A: General*, vol. 104, pp. 87-100, 1993.
- [20] J. Xu *et al.*, "Influence of pretreatment temperature on catalytic performance of rutile TiO₂ -supported ruthenium catalyst in CO₂ methanation," *Journal of Catalysis*, vol. 333, pp. 227-237, 2016.
- [21] G.-y. Wang, Y.-x. Gao, W.-d. Wang, and W.-x. Huang, "Selective CO Methanation over Ru Catalysts Supported on Nanostructured TiO₂ with Different Crystalline Phases and Morphology," *Chinese Journal of Chemical Physics*, vol. 25, no. 4, pp. 475-480, 2012.
- [22] D. C. Upham, A. R. Derk, S. Sharma, H. Metiu, and E. W. McFarland, "CO₂ methanation by Ru-doped ceria: the role of the oxidation state of the surface," *Catalysis Science & Technology*, vol. 5, no. 3, pp. 1783-1791, 2015.
- [23] M. Kuśmierz, "Kinetic study on carbon dioxide hydrogenation over Ru/ γ -Al₂O₃ catalysts," *Catalysis Today*, vol. 137, no. 2-4, pp. 429-432, 2008.
- [24] S. Rönsch *et al.*, "Review on methanation – From fundamentals to current projects," *Fuel*, vol. 166, pp. 276-296, 2016.
- [25] B. A. S. A. G. X. QOMOHJAI, "The Hydrogenation of CO and CO₂ over Polycrystalline Rhodium: Correlation of Surface Composition, Kinetics and Product Distributions," *JOURNAL OF CATALYSIS*, vol. 46, pp. 167-189, 1997.
- [26] C. Swalus, M. Jacquemin, C. Poleunis, P. Bertrand, and P. Ruiz, "CO₂ methanation on Rh/ γ -Al₂O₃ catalyst at low temperature: "In situ" supply of hydrogen by Ni/activated carbon catalyst," *Applied Catalysis B: Environmental*, vol. 125, pp. 41-50, 2012.
- [27] T. Szailer, É. Novák, A. Oszkó, and A. Erdőhelyi, "Effect of H₂S on the hydrogenation of carbon dioxide over supported Rh catalysts," *Topics in Catalysis*, vol. 46, no. 1-2, pp. 79-86, 2007.

- [28] S. Ma *et al.*, "Elucidation of the high CO₂ reduction selectivity of isolated Rh supported on TiO₂: a DFT study," *Catalysis Science & Technology*, vol. 6, no. 15, pp. 6128-6136, 2016.
- [29] R. Büchel, A. Baiker, and S. E. Pratsinis, "Effect of Ba and K addition and controlled spatial deposition of Rh in Rh/Al₂O₃ catalysts for CO₂ hydrogenation," *Applied Catalysis A: General*, vol. 477, pp. 93-101, 2014.
- [30] J. P. Peter Albers, Stewart F. Parker "Poisoning and deactivation of palladium catalysts," *Journal of Molecular Catalysis A: Chemical*, vol. 173, pp. 275-286, 2001.
- [31] X. Wang, H. Shi, J. H. Kwak, and J. Szanyi, "Mechanism of CO₂ Hydrogenation on Pd/Al₂O₃ Catalysts: Kinetics and Transient DRIFTS-MS Studies," *ACS Catalysis*, vol. 5, no. 11, pp. 6337-6349, 2015.
- [32] H. M. L. Hyun You Kim, and Jung-Nam Park, "Bifunctional Mechanism of CO₂ Methanation on Pd-MgO/SiO₂ Catalyst: Independent Roles of MgO and Pd on CO₂ Methanation," *J. Phys. Chem.*, vol. 114, pp. 7128-7131, 2010.
- [33] A. Karelovic and P. Ruiz, "Improving the Hydrogenation Function of Pd/ γ -Al₂O₃ Catalyst by Rh/ γ -Al₂O₃ Addition in CO₂ Methanation at Low Temperature," *ACS Catalysis*, vol. 3, no. 12, pp. 2799-2812, 2013.
- [34] M. Schubert *et al.*, "Highly active Co-Al₂O₃-based catalysts for CO₂ methanation with very low platinum promotion prepared by double flame spray pyrolysis," *Catalysis Science & Technology*, vol. 6, no. 20, pp. 7449-7460, 2016.
- [35] J. G. Inga Kuznecova, "Property based ranking of CO and CO₂ methanation catalysts," *Energy Procedia*, vol. 128 pp. 255-260, 2017.
- [36] H. M. Mar'ia Luisa Cubeiro, Mireya R. Goldwasser, M. Josefina Pérez-Zurita, and C. U. d. N. Fernando González-Jiménez "Hydrogenation of carbon oxides over Fe/Al₂O₃ catalysts," *Applied Catalysis A: General* vol. 189, pp. 87-97, 1999.

- [37] H. Wang *et al.*, "Carbon dioxide hydrogenation to aromatic hydrocarbons by using an iron/iron oxide nanocatalyst," *Beilstein J Nanotechnol*, vol. 5, pp. 760-9, 2014.
- [38] M.-W. L. Gurram Kishan, Sang-Sung Nam, Myoung-Jae Choi and Kyu-Wan Lee, "The catalytic conversion of CO₂ to hydrocarbons over Fe–K supported on Al₂O₃–MgO mixed oxides," *Catalysis Letters*, vol. 56, pp. 215-219, 1998.
- [39] Z. You, W. Deng, Q. Zhang, and Y. Wang, "Hydrogenation of carbon dioxide to light olefins over non-supported iron catalyst," *Chinese Journal of Catalysis*, vol. 34, no. 5, pp. 956-963, 2013.
- [40] G. P. Van Der Laan and A. A. C. M. Beenackers, "Kinetics and Selectivity of the Fischer–Tropsch Synthesis: A Literature Review," *Catalysis Reviews*, vol. 41, no. 3-4, pp. 255-318, 1999.
- [41] M. Iglesias G, C. de Vries, M. Claeys, and G. Schaub, "Chemical energy storage in gaseous hydrocarbons via iron Fischer–Tropsch synthesis from H₂/CO₂— Kinetics, selectivity and process considerations," *Catalysis Today*, vol. 242, pp. 184-192, 2015.
- [42] E. Kok, J. Scott, N. Cant, and D. Trimm, "The impact of ruthenium, lanthanum and activation conditions on the methanation activity of alumina-supported cobalt catalysts," *Catalysis Today*, vol. 164, no. 1, pp. 297-301, 2011.
- [43] T. A. Le, M. S. Kim, S. H. Lee, and E. D. Park, "CO and CO₂ Methanation Over Supported Cobalt Catalysts," *Topics in Catalysis*, vol. 60, no. 9-11, pp. 714-720, 2017.
- [44] R. Silva *et al.*, "Effect of support on methane decomposition for hydrogen production over cobalt catalysts," (in English), *International Journal of Hydrogen Energy*, vol. 41, no. 16, pp. 6763-6772, 2016.
- [45] B. Wang *et al.*, "Effects of MoO₃ loading and calcination temperature on the activity of the sulphur-resistant methanation catalyst MoO₃/V–Al₂O₃," *Applied Catalysis A: General*, vol. 431-432, pp. 144-150, 2012.

- [46] R. M. E.-K. M. V. Gabrovska, M. G. Shopska, D. A. Nikolova, L. P. Bilyarska, D. Crişan, M. Crişan, "Purification of hydrogen-rich streams from CO₂ by methanation," *Bulgarian Chemical Communications*, vol. 47, no. Special issue C, pp. 66-72, 2015.
- [47] R. A. Hubble, J. Y. Lim, and J. S. Dennis, "Kinetic studies of CO₂ methanation over a Ni/gamma-Al₂O₃ catalyst," *Faraday Discuss*, vol. 192, pp. 529-544, Oct 20 2016.
- [48] S. Hwang *et al.*, "Methanation of carbon dioxide over mesoporous Ni-Fe-Al₂O₃ catalysts prepared by a coprecipitation method: Effect of precipitation agent," (in English), *Journal of Industrial and Engineering Chemistry*, vol. 19, no. 6, pp. 2016-2021, 2013.
- [49] K. Stangeland, D. Kalai, H. Li, and Z. Yu, "CO₂ Methanation: The Effect of Catalysts and Reaction Conditions," *Energy Procedia*, vol. 105, pp. 2022-2027, 2017.
- [50] Z. Boukha, C. Jiménez-González, B. de Rivas, J. R. González-Velasco, J. I. Gutiérrez-Ortiz, and R. López-Fonseca, "Synthesis, characterisation and performance evaluation of spinel-derived Ni/Al₂O₃ catalysts for various methane reforming reactions," *Applied Catalysis B: Environmental*, vol. 158-159, pp. 190-201, 2014.
- [51] I. Graça *et al.*, "CO₂ hydrogenation into CH₄ on NiHNaUSY zeolites," *Applied Catalysis B: Environmental*, vol. 147, pp. 101-110, 2014.
- [52] S. Rahmani, M. Rezaei, and F. Meshkani, "Preparation of highly active nickel catalysts supported on mesoporous nanocrystalline γ -Al₂O₃ for CO₂ methanation," *Journal of Industrial and Engineering Chemistry*, vol. 20, no. 4, pp. 1346-1352, 2014.
- [53] H. Muroyama *et al.*, "Carbon dioxide methanation over Ni catalysts supported on various metal oxides," *Journal of Catalysis*, vol. 343, pp. 178-184, 2016.

- [54] J. Gao, Q. Liu, F. Gu, B. Liu, Z. Zhong, and F. Su, "Recent advances in methanation catalysts for the production of synthetic natural gas," *RSC Advances*, vol. 5, no. 29, pp. 22759-22776, 2015.
- [55] Y. Liu, W. Sheng, Z. Hou, and Y. Zhang, "Homogeneous and highly dispersed Ni-Ru on a silica support as an effective CO methanation catalyst," *RSC Advances*, vol. 8, no. 4, pp. 2123-2131, 2018.
- [56] W. Zhen, B. Li, G. Lu, and J. Ma, "Enhancing catalytic activity and stability for CO₂ methanation on Ni-Ru/ γ -Al₂O₃ via modulating impregnation sequence and controlling surface active species," *RSC Adv.*, vol. 4, no. 32, pp. 16472-16479, 2014.
- [57] T. Abe, M. Tanizawa, K. Watanabe, and A. Taguchi, "CO₂ methanation property of Ru nanoparticle-loaded TiO₂ prepared by a polygonal barrel-sputtering method," *Energy & Environmental Science*, vol. 2, no. 3, 2009.
- [58] Z. Li, L. Bian, Q. Zhu, and W. Wang, "Ni-based catalyst derived from Ni/Mg/Al hydrotalcite-like compounds and its activity in the methanation of carbon monoxide," *Kinetics and Catalysis*, vol. 55, no. 2, pp. 217-223, 2014.
- [59] X. Y. Huailiang Lu, Guanjun Gao, Jie Wang, Chenhui Han, Xiaoyuan Liang, Changfu Li, Yuanyuan Li, Weida Zhang, Xuetao Chen, "Metal (Fe, Co, Ce or La) doped nickel catalyst supported on ZrO₂ modified mesoporous clays for CO and CO₂ methanation," *Fuel* vol. 183, pp. 335-344, 2016.
- [60] J. Barrientos, N. Gonzalez, M. Boutonnet, and S. Järås, "Deactivation of Ni/ γ -Al₂O₃ Catalysts in CO Methanation: Effect of Zr, Mg, Ba and Ca Oxide Promoters," *Topics in Catalysis*, vol. 60, no. 17-18, pp. 1276-1284, 2017.
- [61] N. Sahli, C. Petit, A. C. Roger, A. Kiennemann, S. Libs, and M. M. Bettahar, "Ni catalysts from NiAl₂O₄ spinel for CO₂ reforming of methane," *Catalysis Today*, vol. 113, no. 3-4, pp. 187-193, 2006.

- [62] P. S. a. Y. Cesteros a, F. Medina b, J.E. Sueiras, "Synthesis and characterization of several Ni/NiAl₂O₄ catalysts active for the 1,2,4-trichlorobenzene hydrodechlorination," *Applied Catalysis B: Environmental*, vol. 25, pp. 213-227, 2000.
- [63] C. Ragupathi, J. J. Vijaya, P. Surendhar, and L. J. Kennedy, "Comparative investigation of nickel aluminate (NiAl₂O₄) nano and microstructures for the structural, optical and catalytic properties," *Polyhedron*, vol. 72, pp. 1-7, 2014.
- [64] L. Zhou, L. Li, N. Wei, J. Li, and J.-M. Basset, "Effect of NiAl₂O₄ Formation on Ni/Al₂O₃ Stability during Dry Reforming of Methane," *ChemCatChem*, vol. 7, no. 16, pp. 2508-2516, 2015.
- [65] R. López-Fonseca, C. Jiménez-González, B. de Rivas, and J. I. Gutiérrez-Ortiz, "Partial oxidation of methane to syngas on bulk NiAl₂O₄ catalyst. Comparison with alumina supported nickel, platinum and rhodium catalysts," *Applied Catalysis A: General*, vol. 437-438, pp. 53-62, 2012.
- [66] I. A. D. A.-H. a. S. J. I. A.-M. Mohammed M. Hussein Al-Marzooqee, "Synthesis of Stoichiometric Phase Pure NiAl₂O₄ Using Molten Salt Method," *Applied Engineering Research*, vol. 12, pp. 14818-14827, 2017.
- [67] F. Deng, X. Lin, Y. He, S. Li, R. Zi, and S. Lai, "Quantitative Phase Analysis by the Rietveld Method for Forensic Science," *J Forensic Sci*, vol. 60, no. 4, pp. 1040-5, Jul 2015.
- [68] R. F. K. a. D. S. BURNETT, "Quantitative Phase Analysis by X-Ray Diffraction," *ANALYTICAL CHEMISTRY*, vol. 38, no. 1741-1745, 1966
- [69] D. L. Bish and S. A. Howard, "Quantitative phase analysis using the Rietveld method," *Journal of Applied Crystallography*, vol. 21, no. 2, pp. 86-91, 1988.
- [70] Q. Zhang *et al.*, "Facile synthesis of hollow hierarchical Ni/Al₂O₃ nanocomposites for methane dry reforming catalysis," *RSC Adv.*, vol. 4, no. 93, pp. 51184-51193, 2014.

- [71] J. H. J.A. Pena, C.Guimon, A. Monzon and J. Santanaria, "Hydrogenation of Acetylene over Ni/NiAl₂O₄ Catalyst: Characterization, Coking, and Reaction Studies," *JOURNAL OF CATALYSIS*, vol. 159, 313–322, p. 159, 1995.
- [72] P. S. Y. Cesteros , F. Medina , J.E. Sueiras "Synthesis and characterization of several Ni/NiAl₂O₄ catalysts active for the 1,2,4-trichlorobenzene hydrodechlorination," *Applied Catalysis B: Environmental*, vol. 25, pp. 213-227, 2000.
- [73] L. Xu, H. Song, and L. Chou, "Carbon dioxide reforming of methane over ordered mesoporous NiO–MgO–Al₂O₃ composite oxides," *Applied Catalysis B: Environmental*, vol. 108-109, pp. 177-190, 2011.
- [74] Z. Liu *et al.*, "Dry Reforming of Methane on a Highly-Active Ni-CeO₂ Catalyst: Effects of Metal-Support Interactions on C-H Bond Breaking," *Angew Chem Int Ed Engl*, vol. 55, no. 26, pp. 7455-9, Jun 20 2016.
- [75] S. Sepehri and M. Rezaei, "Preparation of Highly Active Nickel Catalysts Supported on Mesoporous Nanocrystalline γ -Al₂O₃ for Methane Autothermal Reforming," *Chemical Engineering & Technology*, vol. 38, no. 9, pp. 1637-1645, 2015.
- [76] M. N. Shin-ichiro Fujita, Tosiaki Doi and Nobutsune and Takezawa, "Mechanisms of methanation of carbon dioxide and carbon monoxide over nickel/alumina catalysts," *Applied Catalysis A: General*, vol. 104, pp. 87-100, 1993.
- [77] J. Ren, H. Guo, J. Yang, Z. Qin, J. Lin, and Z. Li, "Insights into the mechanisms of CO₂ methanation on Ni(111) surfaces by density functional theory," *Applied Surface Science*, vol. 351, pp. 504-516, 2015.
- [78] H. J. K. Sang Joon Choe, Su-Jin Kim, Sung-Bae Park, Dong Ho Park, and Do Sung Huh, "Adsorbed Carbon Formation and Carbon Hydrogenation for CO₂ Methanation on the Ni(111) Surface: ASED-MO Study," *Bull. Korean Chem. Soc.* 2005, vol. 26, no. 11, 2005.

- [79] O. R. By E. B. M. DOESBURGS., J. R. H. Ross,*t and L. L. VAN REIJEN, "Effect of Temperature of Reduction on the Activity and Selectivity of a Coprecipitated Ni-Al₂O₃, Catalyst for the Fischer-Tropsch and Methanation Reactions," *J.C.S. CHEM.. COMM.*, , 1977.
- [80] L. Xu *et al.*, "CO₂ methanation over a Ni based ordered mesoporous catalyst for the production of synthetic natural gas," *RSC Advances*, vol. 6, no. 34, pp. 28489-28499, 2016.
- [81] E. C. P. Ailton J. Terezo, "Preparation and characterisation of Ti/RuO₂ anodes obtained by sol-gel and conventional routes," *Materials Letters*, vol. 53, pp. 339-345, 2002.
- [82] A. W. a. T. M. J. Málek¹, "SOL-GEL PREPARATION OF RUTILE TYPE SOLID SOLUTION IN TiO₂-RuO₂ SYSTEM," *Journal of Thermal Analysis and Calorimetry*, vol. 60, pp. 699-705, 2000.
- [83] Z. Gao, L. Cui, and H. Ma, "Selective methanation of CO over Ni/Al₂O₃ catalyst: Effects of preparation method and Ru addition," *International Journal of Hydrogen Energy*, vol. 41, no. 12, pp. 5484-5493, 2016.
- [84] M. Kimura *et al.*, "Selective methanation of CO in hydrogen-rich gases involving large amounts of CO₂ over Ru-modified Ni-Al mixed oxide catalysts," *Applied Catalysis A: General*, vol. 379, no. 1-2, pp. 182-187, 2010.
- [85] Y. Guo, H. Li, L. Jia, and H. Kameyama, "Trace Ru-doped anodic alumina-supported Ni catalysts for steam reforming of kerosene: Activity performance and electrical-heating possibility," *Fuel Processing Technology*, vol. 92, no. 12, pp. 2341-2347, 2011.
- [86] A. Le Valant, N. Bion, F. Can, D. Duprez, and F. Epron, "Preparation and characterization of bimetallic Rh-Ni/Y₂O₃-Al₂O₃ for hydrogen production by raw bioethanol steam reforming: influence of the addition of nickel on the catalyst performances and stability," *Applied Catalysis B: Environmental*, vol. 97, no. 1-2, pp. 72-81, 2010.

- [87] K. Stangeland, D. Kalai, H. Li, and Z. Yu, "The Effect of Temperature and Initial Methane Concentration on Carbon Dioxide Methanation on Ni Based Catalysts," *Energy Procedia*, vol. 105, pp. 2016-2021, 2017.



APPENDIX

APPENDIX A

CALCULATION FOR CATALYST PREPARATION

Preparation of NiO/NiAl₂O₄ catalysts by using Co-precipitation method

Preparation of NiO/NiAl₂O₄ catalysts by using Co-precipitation method with Ni/Al molar ratio 1/2 is presented as follows:

Precursor

- Nickel nitrate (Ni (NO₃)₂ • 6H₂O), MW = 290.79
- Aluminium nitrate (Al (NO₃)₃ • 9H₂O), MW = 212.996

Calculation

For concentration of (Ni (NO₃)₂ • 6H₂O) at 0.17 mol/lit

$$\begin{aligned} \text{Using (Ni (NO}_3)_2 \cdot 6\text{H}_2\text{O)} &= 0.17 \text{ mol/lit} \times 290.79 \text{ g/mol} \\ &= 49.43 \text{ g/lit} \end{aligned}$$

For concentration of (Al (NO₃)₃ • 9H₂O) at 0.34 mol/lit

$$\begin{aligned} \text{Using (Al (NO}_3)_3 \cdot 9\text{H}_2\text{O)} &= 0.34 \text{ mol/lit} \times 212.996 \text{ g/mol} \\ &= 72.418 \text{ g/lit} \end{aligned}$$

Based on total volume 1 lit (1000 ml)

For 1 liter using (Ni (NO₃)₂ • 6H₂O) 49.43 g

$$\therefore 0.5 \text{ liter required (Ni (NO}_3)_2 \cdot 6\text{H}_2\text{O)} = \frac{49.43 \times 0.5}{1} = 24.71 \text{ g}$$

For 1 liter using (Al (NO₃)₃ • 9H₂O) 72.418 g

$$\therefore 0.5 \text{ liter required (Al (NO}_3)_3 \cdot 9\text{H}_2\text{O)} = \frac{72.418 \times 0.5}{1} = 36.209 \text{ g}$$

Preparation of Ni/Al₂O₃ catalysts by using impregnation method

Preparation of Ni/Al₂O₃ catalyst by using Co-precipitation method with Ni/Al molar ratio 1/2 is presented as follows:

Precursor

- Nickel nitrate (Ni (NO₃)₂ • 6H₂O), MW = 290.79
- Aluminum oxide (Al₂O₃), MW = 101.961

Based on 5 g of Al₂O₃ commercial supported catalyst

Find mole of Al₂O₃

$$\begin{aligned} \text{Mol of Al}_2\text{O}_3 &= \frac{5 \text{ g}}{101.961 \text{ g/mol}} \\ &= 0.049 \text{ mol Al}_2\text{O}_3 \end{aligned}$$

For Al₂O₃ 101.961 g presence of Al = 26.98 X 2

$$\begin{aligned} \therefore \text{Al}_2\text{O}_3 \text{ 5 g presence of Al} &= \frac{26.98 \times 2 \times 5}{101.961} \\ &= 2.646 \text{ g} \end{aligned}$$

Find mole of Al and mole of Ni

$$\begin{aligned} \text{Mol of Al} &= \frac{2.646 \text{ g}}{26.98 \text{ g/mol}} \\ &= 0.098 \text{ mol Al} \end{aligned}$$

So, mol of Ni = 0.098 X 0.5

$$= 0.049 \text{ mol Ni}$$

Find gram of Ni

$$\begin{aligned} \text{Ni } 0.049 \text{ mol} &: 0.049 \text{ mol} \times 58.69 \text{ g/mol} \\ &= 2.875 \text{ g Ni} \end{aligned}$$

Find $(\text{Ni}(\text{NO}_3)_2 \cdot 6\text{H}_2\text{O})$ precursor requirement

$$\text{Ni } 58.69 \text{ g require } (\text{Ni}(\text{NO}_3)_2 \cdot 6\text{H}_2\text{O}) 290.79 \text{ g}$$

$$\text{So, Ni } 2.875 \text{ g require } (\text{Ni}(\text{NO}_3)_2 \cdot 6\text{H}_2\text{O}) = \frac{290.79 \times 2.875}{58.69} = 14.24 \text{ g}$$

Find %wt loading of Ni based on Al_2O_3 5 g

$$\text{For } \text{Al}_2\text{O}_3 \text{ 5 g contained Ni } 2.875 \text{ g}$$

$$\therefore \text{ Total amount of catalyst} = 7.875 \text{ g}$$

$$\begin{aligned} \text{So, catalyst } 100 \text{ g contained Ni} &= \frac{100 \times 2.875}{7.875} \\ &= 36.5 \text{ g} \end{aligned}$$

∴ The molar ratio of Ni/Al = 1/2 equal 36.5%wt of Ni loading

Preparation of metal dope onto NiAl_2O_4 catalysts by using impregnation method

Preparation of 1%wt metal dope onto NiAl_2O_4 catalysts by using impregnation method are presented follow:

Precursor

- Ruthenium (III) nitrosyl nitrate solution ($\text{Ru}(\text{NO})(\text{NO}_3)_3$) , concentration = 0.75 g in 50 ml solution
- Tetramminepalladium (II) chloride monohydrate ($\text{Pd}(\text{NH}_3)_4\text{Cl}_2 \cdot \text{H}_2\text{O}$) , assay Pd 39%
- Rhodium (III) Chloride hydrate ($\text{RhCl}_3 \cdot x\text{H}_2\text{O}$) , assay Rh 42 %

Support

- NiAl_2O_4 prepared by co-precipitation method with Ni/Al molar ratio 1/2 precipitated at 80°C and calcined at 900°C ($\text{NiAl}_{80} - 900$)

Calculation

For 1%wt Ru loading on $\text{NiAl}_{80} - 900$ catalyst

Based on 1 g NiAl_2O_4 supported catalyst

NiAl_2O_4 99 g required Ru 1 g

So, NiAl_2O_4 1 g required Ru 0.01 g

Find the amount of precursor requirement

From Ru 0.75 g contained in solution 50 ml

So, Ru 0.01 g required solution 0.67 ml

For 1%wt Rh loading on $\text{NiAl}_{80} - 900$ catalyst

Based on 1 g NiAl_2O_4 supported catalyst

NiAl_2O_4 99 g required Rh 1 g

So, NiAl_2O_4 1 g required Rh 0.01 g

Find the amount of precursor requirement

From RhCl_3 100 g contained in Rh 42 g

So, Rh 0.01 g required $\text{RhCl}_3 = 0.0042$ g

For 1%wt Pd loading on NiAl_{80} – 900 catalyst

Based on 1 g NiAl_2O_4 supported catalyst

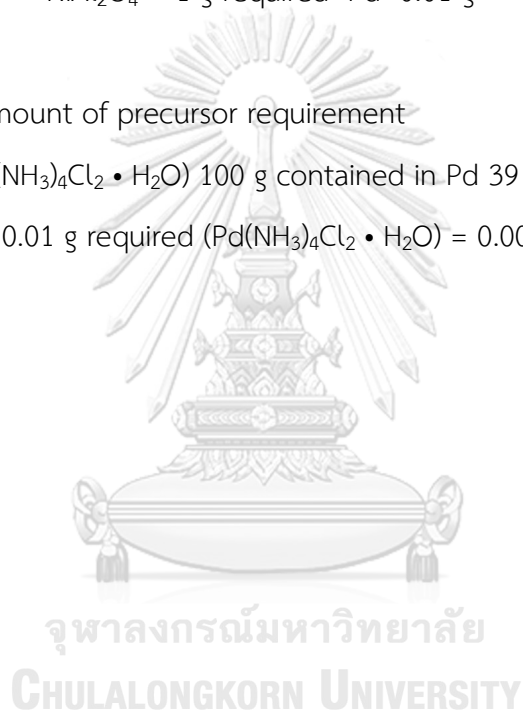
NiAl_2O_4 99 g required Pd 1 g

So, NiAl_2O_4 1 g required Pd 0.01 g

Find the amount of precursor requirement

$(\text{Pd}(\text{NH}_3)_4\text{Cl}_2 \cdot \text{H}_2\text{O})$ 100 g contained in Pd 39 g

So, Pd 0.01 g required $(\text{Pd}(\text{NH}_3)_4\text{Cl}_2 \cdot \text{H}_2\text{O}) = 0.0039$ g



APPENDIX B

CALCULATION OF THE CRYSTALLITE SIZE

Calculation of the crystallite size by Debye – Scherrer's equation

The crystallite size was calculated from the half – height width of the diffraction peak of XRD pattern using the Debye – Scherrer's equation.

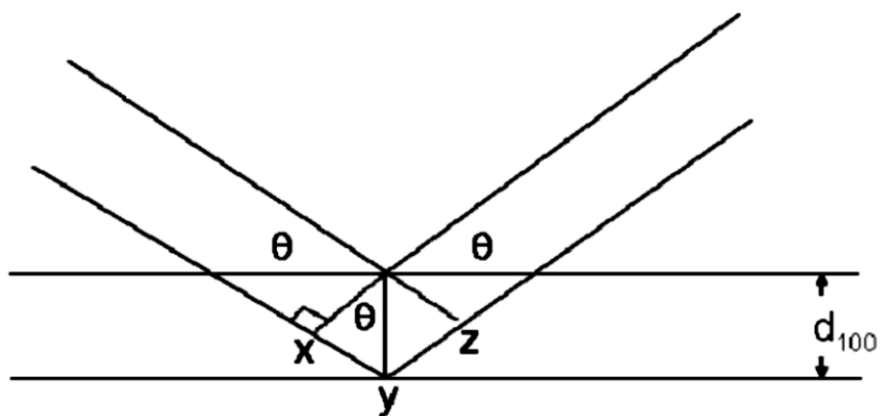


Figure B.1 Derivation of Bragg's Law for X-ray diffraction

$$xy = yz = d \sin \theta$$

$$xyz = 2d \sin \theta$$

Thus

But

$$xyz = n\lambda$$

Bragg's Law

So

$$d = \frac{n\lambda}{2\sin\theta}$$

The Bragg's Law was derived to B.1

From Scherrer's equation:

$$D = \frac{K\lambda}{\beta \cos\theta} \quad (\text{B.1})$$

Where	D	=	Crystallite size, Å
	K	=	Crystallite-shape factor = 0.9
	λ	=	X-ray wavelength, 1.5418 Å for CuK α
	θ	=	Observed peak angle, degree
	β	=	X-ray diffraction broadening, radian

The X-ray diffraction broadening (β) is the pure width of powder diffraction free from all broadening due to the experimental equipment. α -alumina is used as a standard sample to observe the instrumental broadening since its crystallite size is larger than 2000 Å. The X-ray diffraction broadening (β) can be obtained by using Warren's formula.

From Warren's formula:

$$\beta = \sqrt{B_M^2 - B_s^2} \quad (\text{B.2})$$

Where B_M = The measured peak width in radians at half peak height.
 B_s = The corresponding width of the standard material.

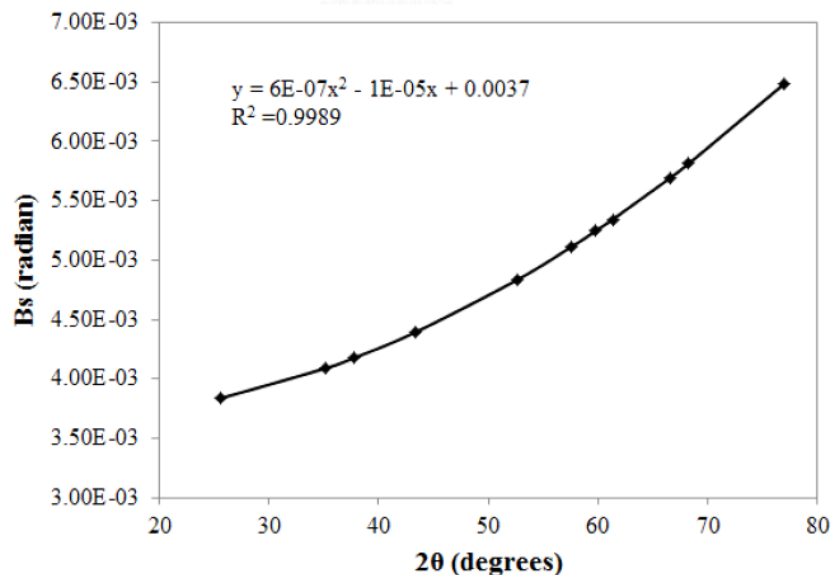


Figure B.2 The plot indicating the value of line broadening due to the equipment.

The data were obtained by using α -alumina as a standard.

APPENDIX C

CALCULATION OF CO₂ CONVERSION AND SELECTIVITY

The catalyst performance for the CO₂ methanation was evaluated in terms of activity for CO₂ conversion reaction rate and selectivity

Activity of the catalyst performed in term of CO₂ conversion which is defined as moles of CO₂ converted from feed inlet:

$$\text{CO}_2 \text{ conversion (\%)} = \frac{[\text{area of CO}_2 \text{ in feed} - \text{area of CO}_2 \text{ in product}]}{\text{area of CO}_2 \text{ in feed}} \times 100 \quad (\text{D.1})$$

Which area of CO₂ peak obtained from GC solution program based plot on TCD (GC-14B)

Selectivity is product is defined as weight of product (A) form with respect to total area of product:

$$\text{Selectivity of A (mol\%)} = \frac{\text{area of A product}}{\text{total area of all product}} \times 100 \quad (\text{D.2})$$

VITA

Miss Chanya Thamma was born in July 29th, 1994 in Bangkok, Thailand. She graduated high school from Udonpitthayanukoon School, Udonthani in 2011. She received the Bachelor's Degree of Chemical Engineering in Faculty of Engineering and Industrial Technology, Slipakorn University in May 2016. Subsequently, she entered the Master degree of Chemical Engineering in Faculty of Engineering at Chulalongkorn University since June 2016 and joined in center of excellence on catalysis and catalytic reaction engineering research group.





จุฬาลงกรณ์มหาวิทยาลัย
CHULALONGKORN UNIVERSITY